Examination of the Localization and Function of the Protein Leupaxin in Cytotoxic T Lymphocytes

by

Shugang Yao

A thesis submitted in partial fulfillment of the requirements for the degree of

Doctor of Philosophy

in

IMMUNOLOGY

Department of Medical Microbiology and Immunology

University of Alberta

ABSTRACT

Cytotoxic T lymphocytes (CTL) play an essential role in the immune surveillance of intracellular pathogen-infected cells and transformed tumor cells. Cytotoxic mechanisms include the direct killing of target cells and release of cytokines such as IFN-γ and TNF-α. One of the direct killing mechanisms is called degranulation, which is characterized by the directional release of lytic granules towards the target cells. Another mechanism is mediated by the interaction between FasL on the CTL and the Fas receptor on target cells, thereby inducing apoptosis. Both of these mechanisms are cell adhesion-dependent, and the adhesion between CTL and target cells is mediated by integrins, primarily LFA-1.

My research is to study the localization, molecular regulation and function of leupaxin in CTL. Leupaxin belongs to the paxillin family of proteins and is a cytoskeletal protein downstream of integrin signaling. I found that leupaxin was recruited to the contact surface, and regulated CTL spreading and migration on ICAM-1. At the contact surface, leupaxin was a component of focal adhesion-like structures and colocalized with paxillin, vinculin and talin. The focal adhesion-like structures were assembled at the leading edge and disassembled at the trailing edge. Although leupaxin was also recruited to the MTOC, it was more dynamic than paxillin at the MTOC.

I found that leupaxin was both tyrosine and serine phosphorylated upon TCR engagement, and the serine phosphorylation at Ser54 caused a leupaxin mobility shift. Both tyrosine and serine phosphorylation were dependent on the tyrosine kinase Pyk2. Corresponding to its involvement in the TCR signaling,

leupaxin was recruited to the immunological synapse during CTL conjugation. Separation of TCR signaling and LFA-1 signaling showed that this recruitment was mainly mediated by LFA-1.

To study the function of leupaxin in CTL, we generated leupaxin deficient mice. Deletion of leupaxin did not affect T cell development or animal viability. However, Pyk2 had reduced tyrosine phosphorylation at its activation sites when leupaxin was absent in CTL. Furthermore, leupaxin deficient CTL showed impaired MTOC reorientation during CTL conjugation with the target cells. These results suggested that leupaxin was required for optimal TCR signaling and MTOC reorientation in CTL.

ACKNOWLEDGMENTS

I would like to take this opportunity to thank everyone who has helped me finish this thesis. It would not be possible for me to complete my Ph.D. program without all your support. First and foremost, I would like to give my utmost thanks to my supervisor, Dr. Hanne Ostergaard for her accepting me as her student six years ago, and for her constant encouragement and support during my Ph.D. program. This will be definitely one of the most important events in my life. In addition, I would like to acknowledge my committee members, Dr. Marek Michalak and Dr. Robert Ingham for their suggestions and feedback on my project. I would also like to express my appreciation to Dr. Kevin Kane and Dr. Troy Baldwin, and everyone from the Ostergaard, Kane and Baldwin laboratories for their criticism and ideas during the lab meetings. In the end, I want to give my love and thanks to my wife, Qixing Ou and my family for their encouragement and support during my study.

CHAPTER 1: Introduction

1.1. The immune system…….....1

1.2. Biology of T lymphocytes…….…….4

1.2.1. T cell development…….…….4

1.2.2. Leukocytes trafficking…….……...6

1.2.3. T cell activation…….…….8

1.2.4. Signaling downstream of TCR/CD3 complex……...……...10

1.2.5. $CD8^+$ T cell cytotoxic mechanism…….15

1.2.6. The secretory mechanism of degranulation……...……...18

1.2.6.1. CTL killing cycles mediated by degranulation…….……..18

1.2.6.2. Structure of the immunological synapse……21

1.2.6.3. 'Inside-out' versus 'outside-in' signals……..23

1.2.6.4. Regulation of MTOC reorientation……25

1.3. Integrin-mediated cell adhesion and migration……27

1.3.1. Integrin……...……..27

1.3.2. Focal adhesions and cell migration in adherent cells…….……28

1.3.3. Leukocyte migration…….……31

1.4. Paxillin family proteins……32

1.4.1. Paxillin family members…….……..32

1.4.2. Paxillin family proteins structural domains…….…….35

1.4.3. Paxillin family proteins binding partners and function…….……37

1.4.4. Leupaxin in adherent cells……40

1.4.5. Leupaxin in leukocytes…….……40

1.5. Hypothesis and study objectives…….…….42

CHAPTER 2: Materials and Methods……..……..43

2.1. Mice……..……43

2.2. Cells…….……....43

2.3. Antibodies…….……..44

2.4. Reagents……..……45

2.5. Mutagenesis of leupaxin……..……46

2.5.1. Truncation mutagenesis of leupaxin……...……..46

2.5.2. Site-directed mutagenesis of leupaxin……..……49

2.6. Generation of polyclonal anti-leupaxin antibody……..…….…..51

2.6.1. GST-leupaxin-LD gene cloning……..…..…….51

2.6.2. GST-leupaxin-LD expression and protein purification…….51

2.6.3. Rabbit immunization, serum collection and IgG purification……..……52

2.7. Anti-CD3 antibody and anti-LFA-1 antibody immobilization……...…..52

2.8. CTL stimulation with immobilized anti-CD3 antibody or anti-LFA-1 antibody……..…53

2.9. CTL stimulation with PMA and ionomycin…….54

2.10. CTL nucleofection……...…..54

2.11. A20 cell transfection……...…...55

2.12. NIH 3T3 cell transfection……..…55

2.13. Cell lysis and immunoprecipitation……...……56

2.14. Immunoblots……..……57

2.15. Cell migration assay……...……58

2.16. Live cell imaging…….……..58

2.17. Fluorescence recovery after photobleaching (FRAP)……..…..60

2.18. Preparation of CTL for confocal microscopy……..…60

2.19. Generation of leupaxin KO mice…….……..63

2.20. Naïve $CD8^+$ T cells purification and activation……..……63

2.21. CD107a based degranulation assay……..…..64

2.22. LDH based killing assay……..……..65

2.23. Statistical analysis…….….66

CHAPTER 3: Characterization of leupaxin function in LFA-1 signaling and leupaxin localization during CTL migration……..……67

3.1. Introduction ……67

3.2. Results…….71

3.2.1. Generation of anti-leupaxin polyclonal antibodies……...……71

3.2.2. Leupaxin migrates as one band in naïve $CD8^+$ T cells and two bands after activation……..……..73

3.2.3. Leupaxin is tyrosine phosphorylated upon LFA-1 stimulation…….……75

3.2.4. Leupaxin phosphorylation upon LFA-1 stimulation is dependent on Pyk2 and Src family kinase activity……...……76

3.2.5. Leupaxin associates with Pyk2 in CTL and leupaxin-Pyk2 complex is distinct from the paxillin-Pyk2 complex……...……..80

3.2.6. Leupaxin shows variable colocalization with the MTOC compared to paxillin in CTL……82

3.2.7. Leupaxin is more dynamic than paxillin at the MTOC……..……84

3.2.8. Leupaxin is recruited to the focal adhesion-like structures during CTL migration on ICAM-1…….……86

3.2.9. Leupaxin is recruited to the focal adhesion-like structures at the contact zone by the LIM2-3 domains……..90

3.2.10. Overexpression of leupaxin in clone 11 reduces CTL migration velocity on ICAM-1……..92

3.2.11. Overexpression of paxillin or leupaxin in NIH 3T3 cells increases cell spreading on fibronectin…….94

3.3. Discussion……...……96

CHAPTER 4: Regulation of leupaxin phosphorylation in TCR signaling and the localization of leupaxin during CTL conjugation……..……102

4.1. Introduction…….……..102

4.2. Results…….……..105

4.2.1. Leupaxin is tyrosine phosphorylated and undergoes a mobility shift upon TCR stimulation…….……..105

4.2.2. Leupaxin tyrosine phosphorylation is dependent on Pyk2 and the mobility shift is dependent on Pyk2 and ERK…….108

4.2.3. Leupaxin mobility shift is mediated by the serine phosphorylation at Ser54……110

4.2.4. Leupaxin is recruited to the immunological synapse in CTL when conjugated with the target cells……...…113

4.2.5. Leupaxin is recruited to the synapse by LFA-1 engagement with ICAM-1.117

4.2.6. Leupaxin is recruited to the immunological synapse by the N-terminal LD domains……...…….120

4.2.7. Leupaxin LD domain shows redundancy in the recruitment of leupaxin to the immunological synapse……...….122

4.2.8. Leupaxin is recruited to the immunological synapse by the LD2-4 domains……...…….124

4.2.9. Leupaxin is recruited to the peripheral SMAC……..126

4.3. Discussion…….129

CHAPTER 5: Leupaxin contributes to MTOC reorientation during CTL conjugation with the target cell……135

5.1. Introduction……...……135

5.2. Results……...…138

5.2.1. Generation of leupaxin$^{-/-}$ mice……138

5.2.2. Thymocytes development is normal in leupaxin$^{-/-}$ mice……140

5.2.3. Leupaxin deficient CTL reduces tyrosine phosphorylation at specific phosphorylated band upon anti-CD3 stimulation……142

5.2.4. Pyk2 reduces tyrosine phosphorylation at Tyr579 and Tyr580 in leupaxin deficient CTL upon anti-CD3 stimulation……144

5.2.5. Leupaxin deletion does not affect MTOC reorientation, degranulation and killing when pulsed with the OVA N4 peptide……146

5.2.6. Leupaxin deficient OT-1 CTL shows impaired MTOC reorientation when pulsed with OVA T4 peptide……....149

5.2.7. Leupaxin deletion does not affect CTL degranulation and killing when pulsed with OVA T4 peptide……...…154

5.2.8. Leupaxin deletion does not affect CTL migration velocity on ICAM-1….156

5.3. Discussion……..…158

CHAPTER 6: General discussion…….……163

6.1. Summary of results……...….163

6.1.1. Leupaxin promotes TCR-stimulated Pyk2 activation…….163

6.1.2. Leupaxin regulates LFA-1 mediated CTL migration on ICAM-1…….....164

6.1.3. Leupaxin regulates MTOC reorientation during CTL conjugation with the target cell……..……168

6.2. Conclusions……...….168

6.2.1. Leupaxin is not a negative regulator of CTL activation……..168

6.2.2. Leupaxin has similar functions to paxillin in CTL……..170

6.3. Future directions……..…….172

REFERENCES……...….174

LIST OF FIGURES

Figure 1.1. The major TCR signaling events……12

Figure 1.2. CTL killing cycles……...19

Figure 1.3. Expression pattern of paxillin and leupaxin in different immune cells……...….34

Figure 1.4. Paxillin family protein structural domains……..36

Figure 3.1. Generation of anti-leupaxin polyclonal antibodies……..…72

Figure 3.2. Leupaxin migrates as one band in naïve $CD8^+$ T cells and two bands after activation……...…….74

Figure 3.3. Leupaxin is tyrosine phosphorylated upon LFA-1 stimulation……77

Figure 3.4. Leupaxin phosphorylation upon LFA-1 stimulation is dependent on Pyk2 and Src family kinase activity……...…….78

Figure 3.5. Leupaxin associates with Pyk2 in CTL and leupaxin-Pyk2 complex is distinct from the paxillin-Pyk2 complex……81

Figure 3.6. Leupaxin shows variable colocalization with the MTOC compared to paxillin in CTL……...83

Figure 3.7. Leupaxin is more dynamic than paxillin at the MTOC……85

Figure 3.8. Leupaxin is recruited to the focal adhesion-like structures during CTL migration on ICAM-1……87

Figure 3.9. Leupaxin is recruited to the focal adhesion-like structures at the contact zone by the LIM2-3 domains……..91

Figure 3.10. Overexpression of leupaxin in clone 11 reduces CTL migration velocity on ICAM-1……93

Figure 3.11. Overexpression of paxillin or leupaxin in NIH 3T3 cells increases cell spreading on fibronectin……95

Figure 4.1. Leupaxin is tyrosine phosphorylated and undergoes a mobility shift upon TCR stimulation……..106

Figure 4.2. Leupaxin tyrosine phosphorylation is dependent on Pyk2 and the mobility shift is dependent on Pyk2 and ERK…….……109

Figure 4.3. Leupaxin mobility shift is mediated by the serine phosphorylation at Ser54……112

Figure 4.4. Leupaxin is recruited to the immunological synapse in CTL when conjugated with the target cells……..……115

Figure 4.5. Leupaxin is recruited to the synapse by LFA-1 engagement with ICAM-1……119

Figure 4.6. Leupaxin is recruited to the immunological synapse by the N-terminal LD domains……..121

Figure 4.7. Leupaxin LD domain shows redundancy in the recruitment of leupaxin to the immunological synapse……..123

Figure 4.8. Leupaxin is recruited to the immunological synapse by the LD2-4 domains……125

Figure 4.9. Leupaxin is recruited to the peripheral SMAC……127

Figure 5.1. Generation of leupaxin$^{-/-}$ mice……...…139

Figure 5.2. Thymocytes development is normal in leupaxin$^{-/-}$ mice……141

Figure 5.3. Leupaxin deficient CTL reduces tyrosine phosphorylation at specific phosphorylated band upon anti-CD3 stimulation……..…143

Figure 5.4. Pyk2 reduces tyrosine phosphorylation at Tyr579 and Tyr580 in leupaxin deficient CTL upon anti-CD3 stimulation……...…145

Figure 5.5. Leupaxin deletion does not affect MTOC reorientation, degranulation and killing when pulsed with the OVA N4 peptide……...…147

Figure 5.6. Leupaxin deficient OT-1 CTL shows impaired MTOC reorientation when pulsed with OVA T4 peptide……...……152

Figure 5.7. Leupaxin deletion does not affect CTL degranulation and killing when pulsed with OVA T4 peptide……155

Figure 5.8. Leupaxin deletion does not affect CTL migration velocity on ICAM-1……..…..157

Figure 6.1. Proposed model for leupaxin function in the TCR signaling……..….165

Figure 6.2. Proposed model for leupaxin localization and function in CTL…...167

Figure 6.3. Proposed model of leupaxin in regulating MTOC reorientation…...169

LIST OF TABLES

Table 2.5.1. Primers used for truncation mutagenesis of leupaxin……49

Table 2.5.2. Primers used for Site-directed mutagenesis of leupaxin…….50

LIST OF ABBREVIATIONS

AA	amino acid
ADAP	adhesion and degranulation promoting adapter protein
APC	antigen presenting cell
Arp2/3	actin-related protein 2/3
BCR	B cell antigen receptor
BSA	bovine serum albumin
CLR	C-type lectin receptor
cSMAC	central supramolecular activation cluster
cTEC	cortical thymic epithelial cells
C-terminal	carboxyl-terminal
CTL	cytotoxic T lymphocytes
CTLA-4	cytotoxic T-lymphocyte-associated protein 4
DAG	diacylglycerol
DC	dendritic cell
dCS	defined calf serum
DMSO	dimethyl sulfoxide
DMEM	Dulbecco's modified Eagle's medium
DN	double negative
DP	double positive
dSMAC	distal supramolecular activation cluster
ECL	enhanced chemiluminescence
ECM	extracellular matrix
EDTA	ethylenediaminetetraacetic acid
ERK	extracellular signal-regulated kinase
ER	endoplasmic reticulum
ETP	early thymic progenitor
FA	focal adhesion
F-actin	filamentous actin
FADD	Fas-associated death domain
FAK	focal adhesion kinase
FAL	focal adhesion-like structure
FAT	focal adhesion targeting
FasL	Fas ligand
FBS	fetal bovine serum
FCA	complete Freund’s adjuvant
FERM	four-point-one ezrin, radixin, moesin
FIA	incomplete Freund’s adjuvant
FN	fibronectin
Fyn	fibroblast Src/Yes novel gene

GAPs	GTPase activating proteins
GAPDH	glyceraldehyde 3-phosphate dehydrogenase
Gads	Grb2-related adapter downstream of Shc
GEFs	guanine nucleotide exchange factors
GFP	green fluorescent protein
GDP	guanosine diphosphate
Grb2	growth factor receptor-bound protein 2
GST	glutathione S-transferase
GTP	guanosine triphosphate
HEV	high endothelial venule
Hic-5	hydrogen peroxide-inducible clone-5
HRP	horseradish peroxidase
ICAM-1	intercellular adhesion molecule 1
IFN	interferons
IL-2	interleukin-2
ILK	integrin-linked kinase
IP	immunoprecipitation
IP3	inositol 1,4,5-trisphosphate
IPTG	isopropyl β-D-1-thiogalactopyranoside
IRF	interferon regulatory factor
IS	immunological synapse
ITAM	immunoreceptor tyrosine-based activation motif
Itk	interleukin-2-inducible T-cell kinase
JNK	c-Jun N-terminal kinase
KDa	kilodalton
KO	knockout
LAT	linker for the activation of T cells
LB	lysogeny broth
Lck	lymphocyte-specific protein tyrosine kinase
LD	leucine-aspartic
LFA-1	lymphocyte function-associated antigen 1
LIM	Lin-1, Isl-1 and Mec-3
LPS	lipopolysaccharides
LPXN	leupaxin
MAPKK	MAPK kinase
MAPKKK	MAPK kinase kinase
MEK	MAP/ERK kinase
MHC	major histocompatibility complex
MLC	mixed lymphocyte cultures
mTEC	medullary thymic epithelial cells

MTOC	microtubule-organizing center
MW	molecular weight
NFAT	nuclear factor of activated T-cells
NF-κB	nuclear factor kappa B
NK	natural killer
NLR	nucleotide oligomerization domain (NOD)-like receptors
NP-40	nonidet P-40
N-terminal	amino-terminal
OVA	ovalbumin
PAMP	pathogen-associated molecular pattern
PBS	phosphate-buffered saline
PCR	polymerase chain reaction
PI3K	phosphoinositide 3-kinase
PIP2	phosphatidylinositol 4,5-bisphosphate
PKA	protein kinase A
PKC	protein kinase C
PLCγ	phospholipase C gamma
PMA	phorbol 12-myristate 13-acetate
PRR	pattern recognition receptor
pSMAC	peripheral supramolecular activation cluster
PTK	protein tyrosine kinase
PTP-PEST	protein tyrosine phosphatase-Pro/Glu/Ser/Thr
PVDF	polyvinylidene fluoride
PXN	paxillin
PY	phosphotyrosine
Pyk2	proline-rich tyrosine kinase 2
RasGRP1	Ras guanyl-releasing protein 1
RLR	retinoic acid inducible gene I (RIG-1)-like receptor
RPMI	Roswell Park Memorial Institute
S1P1	sphingosine-1-phosphate receptor 1
SDS-PAGE	sodium dodecyl sulfate-polyacrylamide gel electrophoresis
SH2	Src homology 2
SH3	Src homology 3
siRNA	small interfering RNA
SLOs	secondary lymphoid organs
SLP-76	SH2 domain-containing leukocyte protein 76
SMAC	supermolecular activation cluster
TCR	T cell antigen receptor
TLR	Toll-like receptors
TNF	tumor necrosis factor

Vav1	vav guanine nucleotide exchange factor 1
VCAM-1	vascular cell adhesion molecule 1
VLA	very late antigen
WASp	Wiskott-Aldrich syndrome protein
WB	western blot
WT	wild type
ZAP-70	Zeta-chain-associated protein kinase of 70 KDa

CHAPTER 1: Introduction

1.1. The immune system

Humans and other mammals have evolved a highly specific immune system to defend against various pathogenic microbes. The immune system is so exquisite that it allows the host to distinguish self from the non-self, even when a single epitope is altered due to infection or transformation. During the immune response, many immune cells with different functions are coordinated to work together in a spatial and temporal manner. The immune system has been broadly divided into two categories, the innate immune system and the adaptive immune system, based on the antigen specificity and immune memory.

Innate immunity, also known as 'non-specific' immunity, is able to recognize and respond to a particular type of pathogen more rapidly and efficiently than adaptive immunity. The innate immune system is predominately composed of various myeloid-lineage cells including monocytes, macrophages, dendritic cells (DCs), neutrophils, basophils, eosinophils and the lymphoid-lineage derived natural killer (NK) cells [1]. In addition to the cellular component, it also contains humoral components such as the C-reactive protein (CRP), complements and lipopolysaccharide (LPS) binding proteins to augment the immune response. One feature of the innate immunity is that it responds very rapidly upon exposure to pathogens. Within minutes of engagement with pathogens, the system is stimulated to generate the immune response. The second feature is that it recognizes the conserved microbial pathogen-associated molecular patterns (PAMPs) using germline-encoded pattern recognition receptors (PRRs) [2, 3].

The concept of PRRs was first proposed by Charles Janeway in 1989, that the innate immune system contains conserved receptors to recognize the invading microbes [4]. A number of PRRs were identified over the last twenty years, and are broadly divided into three categories: transmembrane, cytosolic and secreted classes [2]. This distinct cellular localization of PRRs represents two different models of antigen recognition: cell-extrinsic recognition and cell-intrinsic recognition [3]. Cell-intrinsic pattern relies on the recognition of microbial antigens in infected cells, whereas the cell-extrinsic pattern does not require the cells to be infected. A similar signaling pathway shared by the PRRs is that adaptor proteins are recruited to the receptors and connect to the downstream enzymatic signals. These PRRs signals lead to gene transcription, interferons (IFN) secretion, cell death [5, 6].

Among the innate immune cells, macrophages and DCs play a critical role in mounting the adaptive immune response, especially DCs which are the only cells to activate the naïve T cells [7, 8]. The cellular components of adaptive immunity are B lymphocytes and T lymphocytes. Unlike germline-encoded PRRs which recognize the conserved regions of pathogens, lymphocytes express antigen receptors that undergo gene rearrangement to generate millions of receptors with different antigen specificities [9]. Each cell only expresses one rearranged antigen receptor. Another key feature of the adaptive immune system is that both B lymphocytes and T lymphocytes generate long-lived memory cells after the immune response [9]. When the same pathogen enters the host, memory cells respond very quickly to eliminate the infection.

B cells mediate humoral immunity by producing antigen-specific antibodies after activation. In mammals, B lymphocytes develop from hematopoietic stem cells in bone marrow [10]. They undergo the random rearrangement of immunoglobulin segments, which creates a large pool of B cells expressing antigen receptors with diverse specificities [11]. This gives B cells the capability to recognize all pathological antigens. The naïve B lymphocytes circulate between blood and secondary lymphoid organs (SLOs) scanning for antigens, and it is the SLOs where B lymphocytes get activated. In the case of soluble low molecular weight antigens, B cells can be activated by diffusion of the antigens into the follicles independent of cell-mediated presentation [12, 13]. However, for most antigens, activation of B lymphocytes requires help from macrophages and DCs. It has been shown that there is a population of macrophages which localize beneath the subcapsular sinus [12]. These macrophages are able to present intact antigens on the surface to follicular B cells [14, 15].

One of the challenges faced by the adaptive immunity is the infection by intracellular pathogens, which reside in the cell to multiply. In this case, it is cell-mediated immunity, specifically $CD8^+$ T cells that are important for clearance by destroying the infected target cells. T lymphocytes are broadly categorized into $CD4^+$ T cells and $CD8^+$ T cells. Naïve $CD8^+$ T cells are activated by APC in the context of MHC I molecules and differentiate into cytotoxic T lymphocytes (CTL) which possess the capability to kill target cells directly. $CD4^+$ T cells, also called T helper cells (Th cells) secrete cytokines after activation and regulate the immune response. T helper cells are further divided into Th1, Th2, Th17 and other T cell

subsets based on their secreted cytokine profile [16]. Th1 cells mainly produce the cytokines IFN-γ, TNF-α and IL-2, which regulate the cell-mediated immunity. Th2 cells secrete cytokines such as IL-4, IL-6, IL-10, IL-13 and regulate the B cell-mediated humoral immune response [16, 17]. As this thesis mainly studies the regulation and function of CTL, I will only focus on the $CD8^+$ T cells in the following sections.

1.2. Biology of T lymphocytes

1.2.1. T cell development

The thymus is the place for T cell development and offers the microenvironment to generate a self-tolerant and MHC-restricted T cell repertoire [18]. Based on the function and localization of various thymocyte stages, the structure of thymus can be divided into four major areas: the subcapsular zone, cortex, medulla and the corticomedullary junction [19]. The cortex contains cortical thymic epithelial cells (cTEC), macrophages and fibroblast cells which are important for β-selection and positive selection. The medullary region contains stroma cells, DCs and medullary thymic epithelial cells (mTEC) and is site where negative selection happens to eliminate the recognition of autoantigens. After negative selection, single positive thymocytes leave the thymus through the corticomedullary junction in a chemokine-dependent manner [20].

The early thymic progenitors (ETPs), derived from bone marrow hematopoietic stem cells are the major progenitors to give rise to T cells. They first become the double-negative thymocytes (DN1-4) which lack CD4 and CD8 expression. The TCR receptor β chain rearrangement and β selection happen during

this stage [21, 22]. β selection only allows the DN3 cells that have a functional TCR for further development, whereas the cells that fail to pass β selection undergo apoptosis. The CD4 and CD8 molecules are upregulated for expression upon the initiation of pre-TCR signaling, eventually giving rise to the $CD4^+CD8^+$ thymocytes (DP) [18].

During T cell development, positive selection and negative selection are critical steps that enable mature T cells to be MHC-restricted and self-antigen tolerant. The positive selection takes place in the cortex, and cortical epithelial cells are crucial for presenting self-antigen-MHC molecules to DP cells [23]. DP thymocytes that fail to recognize self MHC molecules undergo apoptosis. The cells that have passed positive selection differentiate into either $CD4^+$ or $CD8^+$ single positive (SP) thymocytes. The mechanism of T cell lineage commitment to $CD4^+$ or $CD8^+$ SP T cells is still not fully clear. The evidence supports a model for T cell lineage commitment that is an instructive model. In this model, it is suggested that the coreceptor signaling received through either CD4 or CD8 molecule downregulates the other coreceptor, making it either $CD4^+$ or $CD8^+$ SP T cells [24]. SP thymocytes can then migrate into medulla for negative selection to eliminate autoreactive T cells. Those T cells with high-affinity to self-antigens are either clonally deleted or undergo further TCR editing. In addition, some high-affinity T cells can also differentiate into regulatory T cells to suppress the autoreactive T cells in the periphery [25]. After negative selection, thymocytes upregulate the chemokine receptor sphingosine-1-phosphate receptor 1 ($S1P_1$) and exit thymus for T cell trafficking.

1.2.2. Leukocytes trafficking

After development in the thymus, T lymphocytes and other leukocytes keep circulating between blood vessels and secondary lymphoid organs (SLOs) for activation. Upon engagement with APCs displaying foreign peptides, leukocytes are then recruited to the inflamed tissues for mounting an appropriate immune response. This coordination of leukocytes localization and trafficking is mainly mediated by a group of proteins called chemokines. Chemokines are small cytokines with molecular weight under 10 KDa. These proteins usually contain several cysteine residues which form disulfide bonds within the protein structure. Correspondingly, leukocytes express a combination of chemokine receptors on their surface. Chemokine receptors are G protein-coupled receptors that possess seven transmembrane domains and cytoplasmic signaling portion. Different leukocytes express distinct patterns of chemokine receptors. In this way, only the leukocytes that exhibit cognate chemokine receptors on the surface will be recruited to the specific sites for immune function.

Activation of naïve T lymphocytes occurs in the SLOs, and the T cells migrate into SLOs through crossing the specialized structures called high endothelial venules (HEVs). HEVs possess a single cell layer of unconventional endothelial cells that exhibit a plump morphology and express receptors specific for leukocytes [26]. Leukocyte rolling and extravasation are well-studied for neutrophils. The extravasation process starts from slowing down leukocytes by binding of selectins to their ligands. This allows the leukocytes to reduce the velocity and roll along the blood vessels [27]. In lymphocytes, the very late antigen-

4 (VLA-4) has been shown to be the major adhesion molecules mediating lymphocyte rolling [28]. The integrin lymphocyte function-associated antigen-1 (LFA-1) plays a critical role in leukocyte extravasation [29]. In its resting state, LFA-1 exhibits a closed conformation with low-affinity towards the ligand. Chemokines secreted from the lymph nodes, including CCL19 and CCL21, bind to receptors on the leukocyte surface. These 'inside-out' signals from chemokine receptors activate LFA-1, which changes into an extended conformation with increased affinity. The cells that produce chemokines CCL19 and CCL21 include follicular stromal cells, endothelial cells, and fibroblastic reticular cells [27]. Binding of LFA-1 to the ligand ICAM-1 on endothelial cells completely stops leukocyte migration, and allow them to extravasate into lymph nodes.

Once the naïve T cells have encountered antigens presented by professional APCs at the SLOs, they will form a stable adhesion with APCs for activation. Some activated T cells will stay in SLOs for effector functions, such as follicular T helper cells. Sphingosine-1-phosphate (S1P) signaling plays an essential role in regulating T cells exit of SLOs. When T cells are in the SLOs and search for antigens, they upregulate the receptor CD69. CD69 binds to the S1P receptor S1P1R and promotes S1P1R internalization [30, 31]. In addition, S1P is maintained in a low concentration through lysing the S1P by phosphatase. In this way, lymphocytes are trapped within SLOs for activation. After activation and differentiation, they upregulate various chemokine receptors and adhesion molecules, which are required for recruiting activated T lymphocytes to the specific inflamed sites.

Egress of the activated T cells and the rest of naïve T cells from the SLOs is similar to the process of T cells exit from the thymus.

1.2.3. T cell activation

It is now clear that naïve T cells are activated by the professional APC and this requires three signals [32, 33]. The first signal comes from the recognition of peptide-MHC complex by the T cell receptors (TCR). As there are two major types of T cells, $CD4^+$ T cells and $CD8^+$ T cells, the coreceptor CD4 or CD8 also binds to MHC II or MHC I molecules on DCs. The first signaling is essential for T cell activation, cells cannot be activated in the absence of TCR signaling. The second 'costimulation signals' is antigen-independent and triggered by the interaction between costimulatory molecules and their ligands on DCs. Without the second signals, T cell activation will lead to anergy and unresponsive to corresponding target cells. The ability of DCs to activate T cells by offering signal one and signal two is dependent on DC maturation. In brief, uptaken and process of pathogens by DCs lead to upregulation of MHC molecules and the costimulatory molecules for the activation.

It is well-established that the costimulatory signals modulate a number of T cell biological functions including activation, differentiation, effector function and T cell survival [34]. Numerous coreceptors have been identified for the past decades, such as CD28, ICOS and CD40L, among others. The most-characterized costimulatory molecules for T cell activation is the receptor CD28. CD28 is expressed on both naïve T cells and activated T cells and is the major costimulatory receptor. The professional APCs including DCs, macrophages and B cells express

CD28 ligand B7-1 (CD80) and B7-2 (CD86). Stimulation of CD28 by their ligands initiates the PI3K-Akt activity and activates the downstream NF-κB and NFAT transcriptional factors [34]. In this way, the signaling events promote cytokine production, T cell proliferation, survival and metabolism [35]. In addition to CD28, T cells also express the inhibitory receptor CTLA-4 (cytotoxic T-lymphocyte-associated protein 4). CTLA-4 is homologous to CD28 and has a higher affinity for B7 molecules than CD28 [36]. Different from CD28, the CTLA-4 expression is upregulated once T cells are activated. CTLA-4 negatively regulates the T cell response by competing with CD28 for its ligand. Recently, the mechanism of CTLA-4 function was utilized to suppress acute immune rejection and autoimmune response. CTLA-4-Ig molecule, a soluble protein which consists CTLA-4 extracellular domain and Fc portion of IgG, is used to block CD28-B7 interaction by competing with CD28. The therapeutic potential of CTLA-4-Ig has been shown in several animal models and is approved by the FDA for clinical use [35, 37]. The third signal for T cell activation comes from cytokines in the microenvironment. Recent studies have suggested that the cytokines type 1 IFN and IL-12 are the predominant sources of signal 3 for naïve $CD8^+$ T cell activation [32].

T cell activation can be induced *in vitro* by providing the above three signals. The first example is the activation of naïve $CD8^+$ T cells by immobilized anti-CD3 and anti-CD28 antibodies. These two antibodies will activate the first two signals. In addition, IL-2 is provided into the cell culture to promote cell survival. The second example of generating activated $CD8^+$ T cells *in vitro* is the mixed lymphocyte cultures (MLC), which is based on alloreactivity [38]. Alloreactivity is

defined as the recognition of alloantigen-MHC molecules which have not been encountered during T cell development. There are approximately 5-10% of peripheral T cells that are alloreactive towards different MHC haplotype [39]. The lymphocytes from one individual are irradiated and served as stimulators. Lymphocytes from another individual with different MHC haplotype are mixed with the stimulators for T cell activation. The first signal for T cell activation is provided by recognition of different MHC molecules. In addition, the costimulatory signals are provided from irradiated DCs. Cytokines are added to the cell culture to provide the third signal. In this way, the alloreactive T cells will be activated *in vitro* for functional assays.

1.2.4. Signaling downstream of TCR/CD3 complex

The T cell signaling is initiated by the binding of TCR/CD3 complex with the peptide-MHC molecules presented on either APC or target cells. The majority of T cells are αβ T cells expressing highly variable α and β chains. Besides that, a minority of T cells express the γδ TCRs which recognize the nonclassical MHC molecules. For both conventional αβ and nonconventional γδ TCRs, the variable region is rearranged by V, (D) and J gene segments and linked to the constant domain. In addition to the TCR subunits, it also associates with the CD3 signaling transduction components. The CD3 dimer consists of γε, δε and ζζ subunits [40]. The cytoplasmic portion of CD3 subunits contains the immunoreceptor tyrosine-based activation motif (ITAM) that can be tyrosine phosphorylated for signal transduction. Each of γ, ε and δ subunits possesses one ITAM and ζ contains three ITAM, with a total of ten ITAM in the CD3 component. Although it has been

known for many years that the TCR/CD3 complex coordinates the antigen recognition and signal transmission together, the mechanism of how antigen binding by TCR leads to signal initiation is still not fully clear. Current studies indicate that receptor aggregation and conformational change play critical roles in triggering the TCR signaling [41].

Some studies have suggested that lipid raft regulates the TCR signaling by separating important kinases from the antigen receptor [42, 43]. Lipid rafts are organized microdomains on the plasma membrane. They contain a high level of glycosphingolipids and cholesterol and are separated from the surrounding cell membrane [44]. Lck is the major Src family protein tyrosine kinase (PTK) that phosphorylates the ITAM of CD3 subunit. Lck is located to lipid raft by lipidation of its N-terminal membrane-anchoring motif, thus separating it from the TCR [44]. T cell stimulation by MHC molecules leads to the translocation of TCR to the lipid raft, followed by phosphorylation by Lck. In addition, TCR aggregation and crosslinking have also been shown to regulate the signal initiation. This is supported by the evidence that multimeric MHC molecules can activate TCR signaling, but not the monomeric molecule [41].

The earliest signaling events upon TCR engagement with MHC molecules is the activation and recruitment of Src family kinase Lck **(Figure 1.1)**. Lck is one of the earliest signaling molecules in the TCR signaling and is indispensable for T cell activation. Lck is an intracellular kinase associated with the cytoplasmic region of coreceptor CD4 and CD8 [45]. It contains a N-terminal plasma membrane

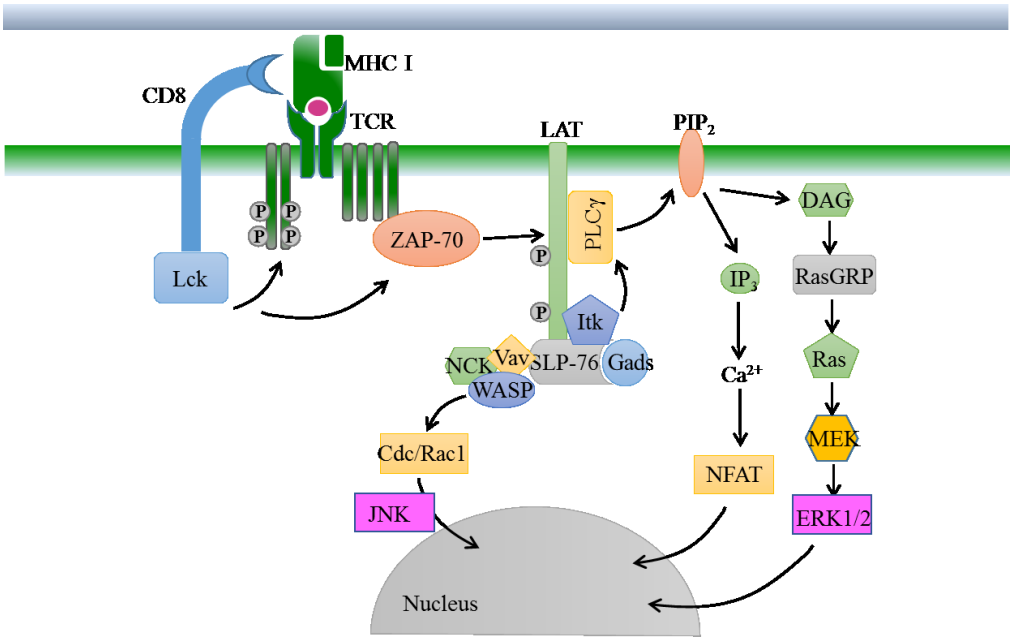

Figure 1.1. The major TCR signaling events. TCR engagement with cognate pMHC I molecules initiates the recruitment and activation of Lck. Lck phosphorylates the ITAMs on CD3 zeta chains which further recruit the kinase ZAP-70 to CD3 and activated by Lck. Activated ZAP-70 is able to phosphorylate the adaptor protein LAT at a number of tyrosine residues and propagate the downstream signaling events. Specifically, phospho-Y132 on LAT recruits PLCγ, which can be phosphorylated by the activated Itk. The activated PLCγ then hydrolyzes PIP_2 into IP_3 and DAG. IP_3 binds to receptors on the endoplasmic reticulum (ER) and releases Ca^{2+} from ER. This further induces the influx of extracellular Ca^{2+} and activates Ca^{2+} dependent pathways including NFAT. DAG stays in the membrane and activates PKC and RasGRP, which further activate the Ras-MEK-ERK signaling pathway.

anchoring domain, followed by SH3 and SH2 domains, and a tyrosine kinase domain at the C-terminus. Lck contains two major phosphorylation residues in the C-terminal kinase domain, Tyr 394 and Tyr 505. These two residues are critical sites for controlling Lck activity [33]. In resting T cells, Lck is constitutively inhibited due to phosphorylation of the negative regulating residue Tyr 505 by Csk and folding into a closed conformation by binding to the SH2 domain [46]. When T cells are stimulated, Lck is activated when the negative regulatory site Tyr 505 is dephosphorylated by CD45 [33]. The closed conformation is opened and available for further activation. This creates the docking site for the tyrosine kinase ZAP-70, which is recruited to the CD3 ζ chain. After phosphorylation by Lck, ZAP-70 is released from the TCR/CD3 complex, binds and phosphorylates LAT to activate a cascade of signaling events [40, 41].

Two of the most important signaling adaptor proteins downstream of ZAP-70 are linker for the activation of T cells (LAT) and Src homology 2 (SH2) domain-containing leukocyte phosphoprotein of 76 kDa (SLP-76) [41]. The essential roles of these two adaptor proteins have been confirmed as deletion of either of the proteins prevented TCR signaling transmission [47, 48]. LAT has a small extracellular domain, a transmembrane domain and a long cytoplasmic tail containing nine tyrosine residues [49]. Upon TCR stimulation, LAT is quickly phosphorylated, mainly by ZAP-70, and recruits numerous SH2 containing proteins, forming the signaling hub. These proteins include the PLCγ1, the adapters growth factor receptor-bound protein 2 (Grb2) and Grb2-related adapter downstream of Shc (Gads) [41]. SLP-76 is also recruited to the LAT signalosome by Grb2 and

Gads [50]. SLP-76 consists of three different domains: a N-terminal acidic domain, a central proline-rich region (PRR) and a C-terminal SH2 domain. It further recruits proteins such as Vav1, Nck, Itk and ADAP to the LAT complex and thus expands the signaling transduction [49]. It is noted that the recruitment and association of these signaling molecules are not mediated by a single binding partner but in a very complicated and mutual manner. Mass spectrometric analysis of the LAT signalosome suggested that there are over 90 signaling proteins associated with the complex [51].

The phospholipase PLCγ1 plays a critical role in initiating intracellular signal transduction after recruiting to LAT complex. PLCγ1 is activated by the Tec family tyrosine kinase Itk, whose function, in turn, is dependent on Lck, LAT, SLP-76 and Vav1 [52, 53]. Itk is recruited to the LAT complex at the membrane through its PH domain and phosphorylated for activation [41]. After activation by Itk, PLCγ1 hydrolyzes the phosphatidylinositol 4,5-bisphosphate (PIP_2) and produces two second messengers: diacylglycerol (DAG) and inositol 1,4,5-trisphosphate (IP_3) [54]. DAG plays an essential role in activating Ras signaling pathway by recruiting Ras guanyl-releasing protein 1 (RasGRP1) to the cell membrane [55]. Ras is a guanosine-nucleotide-binding protein and belongs to the small GTPase family. It becomes active when binding to the guanosine triphosphate (GTP), whereas inactive when binding to guanosine diphosphate (GDP). The process of exchanging GTP or GDP to Ras is regulated by guanine nucleotide exchange factors (GEFs) or GTPase activating proteins (GAPs). RasGRP1 is one of the GEFs that facilitated the binding of GTP to Ras. GTP-bound Ras initiates the activation of Raf, the

MAPK kinase kinase (MAPKKK), which further phosphorylates the MAPK kinase (MAPKK). Eventually, the MAP kinase ERK1/2 are activated and lead to transcriptional activation of Fos, Jun and STAT3 to regulate gene transcription [41, 56]. In addition to the Ras signaling pathway, another messenger regulated by DAG is the PKCθ. PKCθ signaling pathway leads to NF-κB activation and translocation from cytosol to the nucleus, initiating gene transcriptions that are important for T cell activation, function and survival [57].

Besides DAG, IP_3 is another signaling messenger produced by PLCγ1. IP_3 is a potent inducer of Ca^{2+} release from the endoplasmic reticulum (ER). It binds to the IP_3 receptor on ER membrane, opens the Ca^{2+} channel and triggers the release of Ca^{2+} to the cytosol [58]. Furthermore, loss of Ca^{2+} from ER opens Ca^{2+} channels in the plasma membrane and leads to a sustained influx of extracellular Ca^{2+} into the cytosol [41]. Increased Ca^{2+} induces the activation of downstream Ca^{2+} dependent signaling proteins and pathways including calmodulin and the NFAT transcription activity. NFAT translocates into the nucleus and initiates various gene transcriptions important for proliferation and function [41].

1.2.5. $CD8^+$ T cell cytotoxic mechanism

Naïve $CD8^+$ T cells do not possess cytotoxic activity until activated and differentiated into functional cytotoxic T lymphocytes (CTL). CTL utilize two direct primary killing mechanisms against the infected or transformed target cells: degranulation of cytotoxic granules to the target cells and recognition of Fas receptors by the Fas ligand (FasL) on CTL. In addition, CTL also secrete cytotoxic

cytokines such as interferon-γ (IFN-γ) and tumor necrosis factor-α (TNF-α) to facilitate the immune response.

CTL degranulation involves the directional movement and release of the secretory lytic granules against target cells. Presumably, in order to avoid bystander killing to the neighboring cells, the cytotoxic cargo is only released within a structure called immunological synapse [59]. The cytotoxic granules contain the membrane pore-forming protein perforin and a number of serine proteases granzymes [60]. Perforin has been shown to be an essential component for CTL cytotoxicity, as perforin-deficient CTL and NK cells lost the ability to induce target cell apoptosis [61, 62]. It was first thought that perforin oligomerized to form pores in the cell membrane and the process was dependent on Ca^{2+}. Indeed, purified perforin 1 can form pores on erythrocytes in the presence of Ca^{2+}, as shown by electron microscopy [63]. The original model is that perforin polymerizes and forms pores on the cell membrane, allowing the serine proteases granzymes to enter into the target cells [64]. However, ongoing studies demonstrated that granzyme B could enter into the target cells even in the absence of perforin, thus challenging the above model for perforin function [65]. The newest model for granzyme entry is that perforin formed pores lead to Ca^{2+} flux and cell membrane repair mechanism [66]. The granzymes are endocytosed into the target cells during the repair process. Granzymes are later released from the enlarged endosomes (gigantosomes) through perforin polymerized pores [66]. However, it is still possible that both of the models exist during degranulation.

Granzymes are a group of serine proteases that are stored in the same vesicles with perforin. Until now there are approximately 11 granzymes identified among human, rat and mice [64]. Granzyme A and granzyme B are the most studied enzymes. Granzyme B is the most potent factor of inducing target cell apoptosis as the target cleavage site for granzyme B is after the selected aspartate residues that mimics caspase cleavage [67]. Caspase-3 and Caspase-8 are both substrates of granzyme B in cells [64]. In addition to cleavage of pro-caspase, granzyme B can also initiate caspase-independent pathway for apoptosis, which is mediated mainly through mitochondria [68]. During the process of mitochondria-mediated apoptosis, mitochondria releases the pro-apoptosis proteins cytochrome *c*, which is dependent on granzyme B [64, 69]. Granzyme A is a tryptic protease and the cleavage sites are after lysine or arginine in the substrates [64].

Compared to degranulation, FasL-mediated killing is a Ca^{2+} independent cytotoxic activity. FasL-Fas interaction activates the caspase pathway and causes apoptosis of the target cells. It not only plays a critical role in the elimination of infected cells, but is also important in maintaining homeostasis, immune tolerance and contraction of T cell response [70]. Fas receptors (CD95) and FasL (CD95L) both belong to the TNF family receptors. Fas is a homotrimeric transmembrane protein with cytoplasmic signaling transduction domain. It is ubiquitously expressed on a variety of cells and tissues, thus the expression of FasL on CTL or NK cells is strictly regulated to avoid non-specific tissue damage [71]. A number of proteins have been identified that regulate FasL gene transcription and expression, such as interferon regulatory factor (IRF), NF-κB, NFAT and so on [70].

Normally the FasL is stored in cytosolic vesicles but distinct from the lytic lysosome [72]. When CTL are activated by the encountered target cells, stored FasL is quickly released to the cell membrane and binds to Fas on target cell surface. This interaction recruits the Fas-associated death domain protein (FADD) to the cytoplasmic portion of Fas receptor and subsequently activates the caspase-8. Caspase-8 is translocated to the cytosol and cleaves various proteins such as procaspase-3 and proapoptotic BCL2-family member BID, thus initiating target cell apoptosis [64, 73].

1.2.6. The secretory mechanism of degranulation

1.2.6.1. CTL killing cycles mediated by degranulation

One of the most important features of CTL is that they are serial killer cells. This means that they are capable of performing the killing cycles several times and killing more than one target cells. This feature makes them very effective killer cells to eliminate infected target cells. At the initial contact, CTL interact with the target cells with the actin-rich protrusions at the leading edge [74]. For every killing cycle, it starts from the recognition of antigens presented by MHC I molecules on target cells. Once TCR is activated, signaling event is initiated to activate the adhesion molecule LFA-1, followed by the formation of the immunological synapse between CTL and target cells. The F-actin flows away very quickly from the center of the immunological synapse, followed by the clustering of antigen receptors and cell polarization [74, 75].

A key event of degranulation is the directional polarization of microtubule cytoskeleton and MTOC towards the target cells **(Figure 1.2)**. Although this was

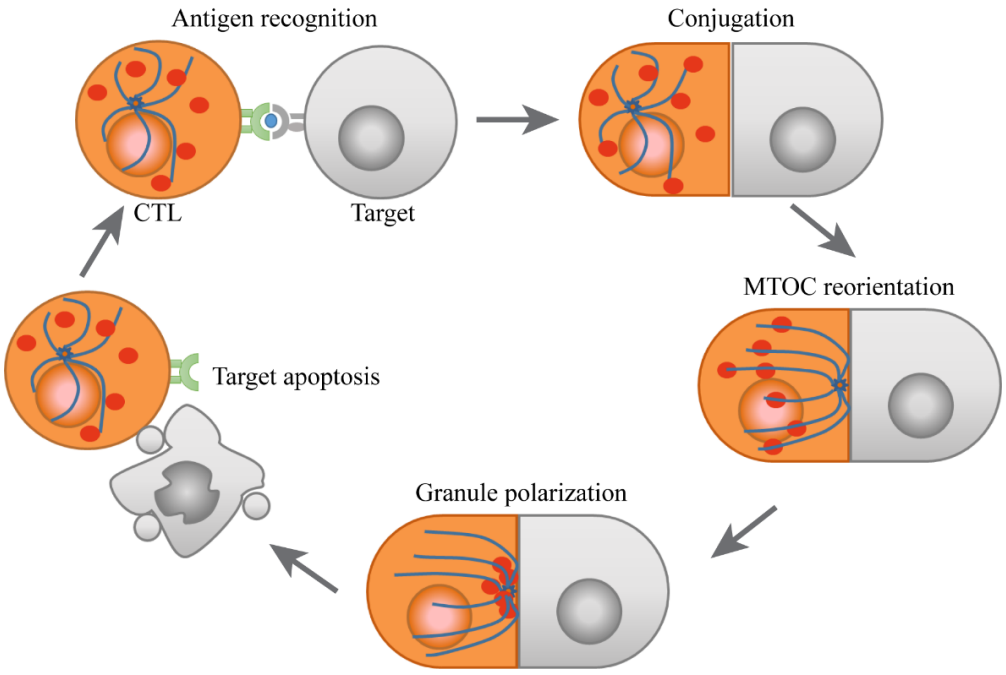

Figure 1.2. CTL killing cycles. CTL recognizes a target cell through the interaction between TCR and pMHC I molecule. Once the TCR is activated by the cognate antigen, this 'inside-out' signal from TCR triggers the activation of LFA-1 and results in the tight conjugation, forming the immunological synapse between CTL and target cell. CTL undergoes polarization of the MTOC and the following lytic granules along the microtubules. Granules are released into the target cell and induce apoptosis. Once the target cell is killed, CTL is disassociated from the target cell and moves to the next one.

observed in T cells and NK cells for a long time, the molecular regulation of this process is not fully clear. Recent studies suggested that the motor proteins dynein and its associated signaling molecules were involved in regulating cytoskeleton reorganization. The adaptor protein ADAP (adhesion-and degranulation-promoting adapter protein) was shown to recruit dynein to the plus end of the microtubules that were associated with the periphery of the immunological synapse [76]. Loss of ADAP resulted in decreased MTOC reorientation in T cells [76]. As the F-actin flows away from the immunological synapse during the MTOC reorientation, this may reflect a correlation between actin clearance and MTOC movement. Additionally, the cytoskeleton adaptor protein paxillin has been shown to regulate MTOC reorientation in CTL and NK cells [77]. A model was proposed that the plus ends of microtubules were connected to the F-actin via adaptor proteins. Actin depletion generates the mechanical forces that pull the MTOC towards the immunological synapse [75].

After MTOC reorientation, the lytic granules containing perforin and granzymes move along the microtubules, dock to the cell membrane and are released into the specialized cleft between the two cells. This process may finish within several minutes upon engagement with the target cells [74]. It is still controversial on the role of perforin during degranulation mediated killing. The earlier model suggested that perforin formed polymerized pores on the membrane of target cells, allowing the entry of granzymes [64, 78]. Later experiments suggested that the perforin formed pores triggered cell membrane damage and granules were endocytosed into the target cells [66]. After having killed the target

cells, CTL detach from the target cells and move to the next one. Although very little is known about the regulation of CTL detachment from the target cell, microscopy results showed that the MTOC and microtubule network were retracted from the target cells before it underwent apoptosis [75]. The whole killing process can finish within 30 minutes after CTL meet the target cells [74].

1.2.6.2. Structure of the immunological synapse

When T cells are activated by the pMHC from target cells or APCs, a highly organized interface is formed between the two cells with the rapid segregation of receptors and rearrangement of the actin cytoskeleton. This ring-structure interface is divided into three compartments: the central supermolecular activation cluster (cSMAC), peripheral supermolecular activation cluster (pSMAC) and the distal supermolecular activation cluster (dSMAC) [79]. The cSMAC contains TCRs, coreceptors CD28, CD8 and associated signaling molecules such as Lck, ZAP-70 and the LAT signalosome [80]. Visualization of TCR signaling by total internal reflection microscopy showed that the signals initiated from the TCR microclusters at the dSMAC [81]. Soon after TCR stimulation, the microclusters move to the cSMAC where TCR signaling is no longer stimulated [81]. Thus a model is proposed that the function of cSMAC is to downregulate TCR signaling through endocytosis and degradation of TCR. The ubiquitination machinery was found to be accumulated at the cSMAC [82]. The cSMAC is also docking site for MTOC reorientation. Once the MTOC is translocated and docked to the plasma membrane, cytotoxic granules move along the microtubules and are released within the cSMAC.

The cSMAC is surrounded by the pSMAC which consists of the adhesion molecules LFA-1 and its associated signaling proteins. It has been suggested that this pattern of the organization serves as a sealing ring to avoid cytotoxic release to the neighboring cells [83]. LFA-1 exhibits high-affinity conformation and forms a tight adhesion with target cells, facilitating CTL degranulation. In addition, studies suggest that LFA-1 also provides costimulatory signals by increasing T cell sensitivity, promoting IL-2 secretion, T cell proliferation [84]. LFA-1 is linked to the actin cytoskeleton via adaptor proteins including talin and vinculin and this physical connection is necessary to activate LFA-1 by the 'inside-out' signals. Upon interaction with the ligand, LFA-1 can also initiate the 'outside-in' signaling to regulate cytoskeleton rearrangement and granule reorientation during degranulation.

The dSMAC is abundant in polymerized F-actin, which is critical in maintaining the immunological synapse and degranulation. Specifically, F-actin formed ring has two major functions. First, it forms the physical barrier for degranulation and controls the dynamics of granule secretion. Second, the actin cytoskeleton exerts a mechanical force across the immunological synapse, promotes the perforin activity towards target cells [80]. Disruption of F-actin polymerization and signaling significantly impaired CTL cytotoxicity [80, 85]. Actin rearrangement is featured by its retrograde movement from cSMAC to dSMAC. When CTL first encounter the target cells, actin starts to polymerize and form a cortical actin layer around the surface of target cells to facilitate conjugation. Soon after the initial contact, the cortical actin layer begins to decrease and

retrogrades towards the dSMAC, accompanying with the TCR microclusters movement to the cSMAC [74]. The lytic granules are released at the area with depleted cortical F-actin.

1.2.6.3. 'Inside-out' versus 'outside-in' signals

'Inside-out' signaling refers to the intracellular signals initiated from other receptors that induce the activation and clustering of integrin [86]. In leukocytes, stimulation of chemokine receptors, TCR, BCR and selectins are able to activate the integrin, leading to conformational change and avidity increase [87]. There are at least two T cell activities that require 'inside-out' signaling for integrin activation: T cell conjugation with either APC or target cells and T cells extravasation through vascular endothelium into either lymphoid organs or inflamed tissues [29]. Although the intracellular signaling pathways triggered by TCR and chemokine receptors are slightly different, the key signaling events and components that lead to integrin activation are the same. In brief, there are four sequential signaling events in the 'inside-out' signaling: (1) TCR triggered assembly of LAT signalosome; (2) signal transduction from the LAT signalosome to integrin via PKC and ADAP; (3) activation and translocation of Rap1 and talin dependent separation of integrin subunits; (4) actin cytoskeleton rearrangement by WAVE2 signaling complex [88].

Rap1 is a member of small GTPase that plays a critical role in the 'inside-out' signaling for LFA-1 activation. Several GEFs that activate Rap1 have been identified, including C3G and CalDAG-GEF. TCR stimulation promotes the translocation of Rap1 to cell membrane and the immunological synapse. The

effectors identified for Rap1 are RapL, RAIM and Mst1 [88]. Rap1 recruits RapL and Mst1 to the membrane and then associate with the integrin LFA-1. Deletion of any of these signaling molecules will impact integrin activation, cell spreading and cell migration.

In addition to Rap1 and its effector proteins, talin is one of the essential proteins that regulate integrin activation [89, 90]. Talin has been suggested as the final step for integrin activation via a pull-push mechanism [91]. In resting state, talin forms a closed conformation through the association between its FERM domain and C-terminal rod domain. This closed conformation allows talin to hide the integrin β subunit binding domain [92]. After talin is activated, it associates and drags the β subunit from α subunit, thus leading to integrin activation [93].

'Outside-in' signaling is defined as the signals initiated by the binding of integrin to their ligands. 'Outside-in' signaling usually regulates integrin-mediated cellular responses such as cell spreading, cell migration, proliferation and degranulation. In T lymphocytes and B lymphocytes, Although integrin activation is usually dependent on the 'inside-out' signaling, there are studies showing that the treatment of lymphocytes with PMA or Mn^{2+} that bypass the 'inside-out' signaling can also trigger specific signaling pathways [86]. Similar to the 'inside-out' signaling, the earliest signaling events in the 'outside-in' pathway is the activation of Src family kinase and the following phosphorylation of adaptor protein ZAP-70. It is not unusual that many signaling proteins play dual roles in both 'inside-out' and 'outside-in' pathways.

One of the major cellular processes 'outside-in' signaling regulated is the reorganization of the actin cytoskeleton. This is mediated through modulating the Rho GTPases family proteins including Cdc42, Rac1 and RhoA. Most of the literature studying role of Rho GTPases are carried out in adherent cells such as fibroblasts. Each member has different distribution at the contact surface during cell migration. In lymphocytes, the major effector proteins of Rho GTPases identified is the Wiskott-Aldrich syndrome protein (WASp) [94]. Upon stimulation, activated WASp associates with Arp2/3 and together nucleate the actin polymerization process [86].

1.2.6.4. Regulation of MTOC reorientation

In $CD8^+$ T cells, MTOC reorientation appears to happen in two steps. MTOC first translocates from the distal side of nucleus to the immunological synapse [95]. The second step is that MTOC docks to the plasma membrane, which is dependent on the Lck signaling. In Lck^{off} CTL, although MTOC was able to move from the rear of CTL toward the target cell, it was unable to reach and dock to the membrane [95]. Another Src family kinase, Fyn, plays a role in MTOC polarization as Lck and Fyn doubly deficient CTL lost the ability of MTOC reorientation [95]. One explanation was that the actin cytoskeleton was unable to reorganize from the immunological synapse in Lck^{off} CTL [95]. This was consistent with the model that clearance of F-actin from the center of immunological synapse generated mechanical forces that pulled MTOC towards target cell [96]. In this model, the plus ends of microtubules are linked to the actin cytoskeleton such as adaptor protein IQGAP1 [96]. The actin reorganization from the synapse clears the plus

ends of microtubules and pulls MTOC towards membrane [96]. In addition, other models are also proposed mediated by the cytoskeletal motor protein dynein that drags MTOC towards synapse [97, 98].

A number of proteins have been identified to regulate MTOC reorientation. The scaffolding protein IQGAP1 has been demonstrated to regulate MTOC and granule polarization in NK cells [99]. In addition, IQGAP1 is also cleared away with actin cytoskeleton before MTOC reorientation in CTL [96]. IQGAP1 is an effector protein downstream of Cdc42 [100], which has also been shown to control MTOC polarization via regulating tethering plus ends of microtubules to the membrane [101]. As IQGAP1 can interact with both actin cytoskeleton and the microtubule network [102, 103], it is proposed that IQGAP1 serves as the linker between the cytoskeletons and coordinate the MTOC reorientation during actin reorganization [96].

The motor protein dynein and its related proteins have been implicated in regulating MTOC polarization. Dynein is recruited to the synapse through DAG and disruption of DAG accumulation at the synapse reduced MTOC reorientation [104]. Knockdown of dynein heavy chain expression impaired the MTOC polarization in Jurkat T cells [105]. The adaptor protein ADAP associated with dynein and loss of ADAP prevented dynein recruitment and MTOC polarization to the synapse in Jurkat T cells [76]. Confocal microscopy results suggest a role of dynein in the cortical sliding mechanism that anchored dynein at the cell cortex moves to the minus ends of microtubules, resulting in microtubule sliding [97]. In addition, another capture-shrinkage mechanism suggests that dynein drives the

depolymerization of microtubules at the plus ends and pulls the MTOC towards synapse through the end-on capture-shrinkage mechanism [98].

Paxillin, a cytoskeletal adaptor protein, has been shown to regulate MTOC reorientation in CTL and granule polarization in NK cells [77, 106]. Another paxillin family member, leupaxin also regulates MTOC reorientation during NK cell degranulation [107]. Paxillin family proteins mainly function as adaptor proteins at the focal adhesions that connect integrin to actin cytoskeleton [108]. Although it is unknown how paxillin family proteins are involved in MTOC polarization, they may participate in similar signaling events as IQGAP1. There is evidence that paxillin localizes to the microtubules and binds to tubulin directly [77, 109]. Paxillin has been shown to be recruited to the pSMAC at the immunological synapse in CTL [77], it will be interesting to determine the dynamic of paxillin during this process.

1.3. Integrin-mediated cell adhesion and migration

1.3.1. Integrin

Integrins are a large family of transmembrane receptors consisting of α and β subunits. There are a total of 18 α and 8 β subunits identified, forming 24 heterodimeric integrins. T cells mainly use the β1, β2 and β7 subunits to associate with the α subunits. The integrin identified on T cell surface includes αLβ2 (LFA-1), αMβ2, αXβ2, αDβ2, α4β7, αEβ7 and α1- α6β1 [110]. Each family of integrin has different binding ligands. The majority of studies are carried out around the integrin LFA-1 and VLA-4 (α4β1). T cells utilize LFA-1 and VLA-4 to mediate at least two activities. The first activity is T cell rolling and arrest along the vascular

endothelium during extravasation. The second activity is the formation of the immunological synapse with target cells or APCs [87].

Both α and β subunits contain the extracellular domain, transmembrane region and the cytoplasmic tail. The cytoplasmic tail is the signaling part which associates with other proteins during the 'inside-out' and 'outside-in' signaling events. It also connects actin cytoskeleton via the cytoskeletal proteins such as talin and vinculin. Integrin has three different states: closed, extended and opened conformation. Each conformation has distinct affinities towards their ligands. The low-affinity conformation shows a closed structure with the ligand binding headpiece hidden under the receptor. When β subunit is dragged from the α subunit by talin, it exposes the globular headpiece for ligand binding with intermediate-affinity. The high-affinity state is achieved when ligand binds to the extended conformation. Due to the conformational switch and exposure of distinct epitopes, these three conformations can be detected with antibodies recognizing distinct epitopes for human LFA-1.

1.3.2. Focal adhesions and cell migration in adherent cells

Focal adhesions are large adhesive structures that serve as mechanical links between extracellular matrix (ECM) and actin cytoskeleton. Cells utilize focal adhesions to mediate cellular processes such as adhesion, spreading, migration and mechanotransduction. The physical linkers are integrins or syndecans that interact with their ligands in the ECM. The intracellular part of the receptor recruits a number of signaling molecules that connect it to the actin cytoskeleton, thus regulating signal transduction and cytoskeleton reorganization. A number of

proteins are recruited to the adhesive complexes, including adaptor proteins, kinases, phosphatases, GTPase and proteases. It has been suggested that there are more than 160 distinct components recruited to the focal adhesions [111]. Based on the size, localization and composition of the adhesive complexes, they are divided into the small focal complexes, focal adhesions and fibrillar adhesions [112]. During cell migration, the leading edge protrudes forward by F-actin and forms the filopodia or lamellipodia and the nascent focal complexes are assembled at the periphery. This allows the cells to explore the microenvironment and adhere to the ECM.

The initial formation of focal complexes is regulated by small GTPase Rac1 and Cdc42 [113]. They both stimulate the assembly of focal complexes at the cell periphery. These nascent focal complexes are highly dynamic and short lived. However, some of them mature into the large focal adhesions and is dependent on RhoA activity [114]. It has been demonstrated that the initial integrin engagement with their ligands transiently inhibited RhoA activity by the negative regulator p90RhoGAP [115]. The RhoA activity was later upregulated by RhoA-specific GEFs at the focal adhesions [116]. One of the most important RhoA effector proteins is Rho kinase (ROCK), which is activated to phosphorylates the myosin light chain (MLC). Phosphorylation of MLC facilitates the interaction and assembly of myosin II into the actin filaments, increasing the bundling of actin filaments and actomyosin contractility [116]. The increased tension allows the formation of stress fibers and focal adhesion maturation.

In order to maintain migration, cells not only form the adhesive structures at the leading edge of the periphery, but also disassemble the focal adhesions at the trailing edge, which is termed focal adhesion turnover. Compared to focal adhesion formation, much less is known about how cells are released from the ECM. The Src-FAK signaling pathway has been demonstrated to play important roles in focal adhesion disassembly [117]. FAK regulates both focal adhesion formation and turnover, although FAK deficiency seems to affect more on focal adhesion disassembly [118]. In FAK-null fibroblasts, the rate of focal adhesion assembly at the leading edge was similar to that of WT cells, whereas focal adhesion disassembly at the rear was much slower [117]. Similarly, Src kinase inhibition resulted in a decreased rate of focal adhesion disassembly, as Src kinase has been shown to phosphorylate FAK for activation [117].

In addition to the above signaling molecules, proteolytic cleavage of focal adhesion proteins by calpain shows an important role in regulating focal adhesion turnover. This was supported by the experiments of inhibiting calpain activity or knockdown which resulted in the failure of focal adhesion turnover and cell migration [119, 120]. A number of focal adhesion components have been identified as cleavage substrates of calpain, including talin, FAK, Src, paxillin, integrins, vinculin and so on [116]. The cleavage sites of these substrates were mapped, and expression of the cleavage-resistant mutants resulted in decreased focal adhesion turnover and cell migration [121-123].

Although focal adhesions have been intensively studied in adherent cells, it should be noted that the majority of studies are carried out in tissue culture in a 2D

environment. In the artificial environment, the matrix is coated with homogeneous with the integrin ligands. Whereas *in vivo* the cells are surrounded by multicellular conditions, raising the question of whether focal adhesions observed *in vitro* are artificial structures. Indeed, the stress fibers and focal adhesions are very rarely detected in physiological conditions *in vivo* [124, 125]. There are several reasons that explain the abundance of focal adhesions in tissue culture. First, the serum for tissue culture may contain components that can activate the RhoA and promote actin contractility and focal adhesion assembly [116]. In addition, many studies have shown that the stiffness of the underlying surface is a critical factor regulating focal adhesion formation [116]. Indeed, equivalent structures are observed in endothelial cells and tissue staining *in vivo*, thus suggesting a relevance between the adhesive structures and cell behavior in physiological condition [126, 127].

1.3.3. Leukocyte migration

Compared to adherent cells which migrate with less than 1 um/min, leukocytes can migrate with the speed of up to 30 um/min [128, 129]. In addition, they lack the strong interactions with the ECM and do not form the conventional focal adhesions and stress fibers [130]. These differences suggest that leukocytes use a distinct migration mode, called amoeboid mode, to achieve such high motility. The advantage of amoeboid mode is that it allows leukocytes to migrate efficiently and sense the signals from microenvironment very quickly [130]. During leukocyte migration, the leading edge protrudes out and sense the environment. The leading edge is very sensitive to the receptor signaling such as signals from the chemokine receptors and antigen receptors [131].

T cell migration is extensively studied on the substrate ICAM-1 in a 2D environment. The integrin protein LFA-1 is not evenly distributed at the contact surface during T cell migration [132]. LFA-1 is expressed with the highest level at the trailing edge and lowest level at the leading edge [132]. The intermediate-affinity LFA-1 is mainly localized at the leading edge and associates with α-actinin-1, which links LFA-1 to actin cytoskeleton [133]. α-actinin -1 was also required for T cell migration as knockdown of α-actinin impaired T cell migration [133]. The possible explanation was that the F-actin at the leading edge was unable to protrude out for migration. Compared to the leading edge, the focal zone, or the central region, was distributed with high-affinity LFA-1 which associated with the adaptor protein talin [132]. This high-affinity LFA-1 bound to the substrate and generated actomyosin-based stiffness, thus stabilizing the cell contact with the extracellular matrix [130]. Although there was abundant of LFA-1 at the trailing edge, the conformational state was unknown and LFA-1 was believed to be recycled at the trailing edge for migration [134].

1.4. Paxillin family proteins

1.4.1. Paxillin family members

Paxillin family proteins are multidomain cytoskeletal adaptor proteins that provide protein binding modules for signaling transmission at the focal adhesions [108]. Integrin activation or clustering leads to the recruitment of paxillin family proteins to the focal adhesions and through which, the actin cytoskeleton is linked to the extracellular matrix, thus mediating cell adhesion, migration and environment sensing [135]. All of these proteins have been used as markers for focal adhesions

in adherent cells. This family contains three members: paxillin (PXN), Hic-5 (hydrogen peroxide-inducible clone-5) and leupaxin (LPXN).

Paxillin is the first characterized protein in this family and is ubiquitously expressed, with the least expressed in the nervous system [135]. Paxillin is required for normal development in the mouse as paxillin knockout is embryo lethal [136]. This also suggests that the other two members cannot compensate for paxillin function during embryo development. In addition to the canonical paxillin, another three paxillin isoforms, β, γ and δ have been identified [137]. These isoforms have more restricted expression pattern. Compared to paxillin, less is known about the other two family members. Hic-5 shows restricted expression and is abundant in smooth muscle cells [138]. Hic-5 KO mice have been generated and the mice are healthy and viable [139]. Leupaxin was initially thought to be preferably expressed in leukocytes **(Figure 1.3)**. More recently it has been demonstrated that leupaxin has a broader expression pattern, which is expressed in smooth muscle cells, prostate cancer cells and other cancer cells [140, 141]. While the function of paxillin is extensively explored, the function of Hic-5 and leupaxin is less studied.

Interestingly, all of the paxillin family members have been linked to cancer development and malignancy. Aberrant expression, hyperphosphorylation and mutations are found in a number of invasive cancers such as lung cancer, prostate cancer and breast cancer. Hic-5 was recently shown to promote breast cancer progression and a major indicator of tumor cell invasive behavior [139, 142]. In addition, leupaxin is overexpressed in prostate cancer cells and the expression level correlated with the progression of the tumor [140]. Thus, paxillin family proteins

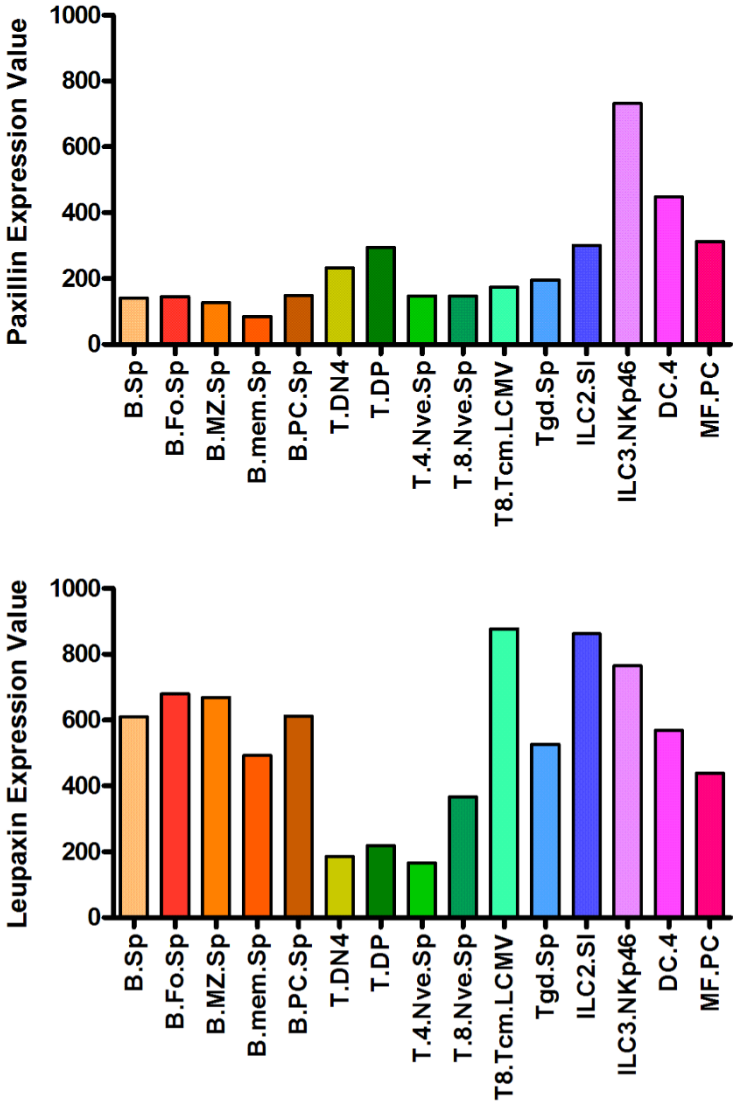

Figure 1.3. Expression pattern of paxillin and leupaxin in different immune cells. The RNA-seq data was collected from the website of Immunological Genome Project. The figures were created by GraphPad Prism6. B.Fo.Sp represents splenic follicular B cells. B.MZ.Sp represents splenic marginal zone B cells. B.mem.Sp represents splenic memory B cells. B.PC.Sp represents splenic plasma cells. MF.PC represents peritoneal macrophages.

are extensively studied in different tumors as potential diagnostic and therapeutic targets [143]. On the other hand, the majority of studies on paxillin family were carried out in tumor cell lines. As paxillin family proteins are usually overexpressed and hyperphosphorylated in tumor cells, these studies may not represent the real functions in physiological conditions. Therefore, experiments need to be performed in primary cells to confirm their functions.

1.4.2. Paxillin family proteins structural domains

Paxillin family proteins do not possess enzymatic activity and rely on their multiple structural domains to mediate their roles in signaling transmission [135]. All three family members share similar structures, with N-terminal LD domains and C-terminal LIM domains [137] **(Figure 1.4)**. In addition, they also have the proline-rich region which binds to SH-3 containing proteins and a number of tyrosine and serine phosphorylation residues [137].

The LD domains contain several leucine-aspartic (LD) motifs. These motifs are variations of the consensus sequence, LDXLLXXL, where X can be any amino acid. The N-terminal LD domains are less conserved among the three members, as paxillin contains five LD domains whereas the other two members only have four LD domains. Protein structures showed that the LD motifs formed an amphipathic helices structure with the leucine residues aligned on the helix, thereby forming the hydrophobic interface [144]. These motifs serve as docking sites for the majority of proteins that have been shown to associate with paxillin [137].

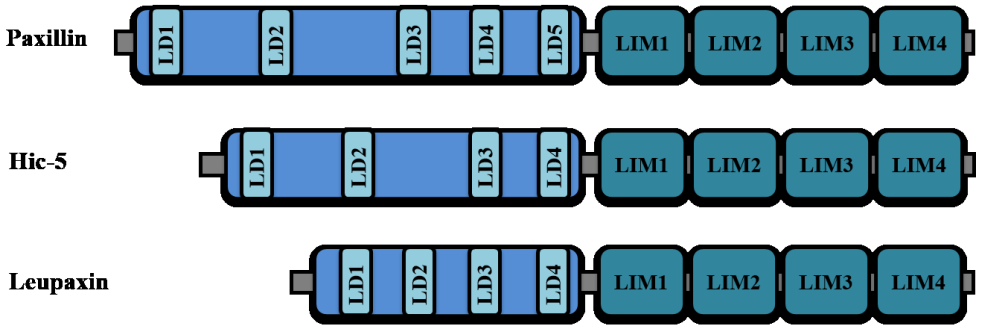

Figure 1.4. Paxillin family protein structural domains. Paxillin and its family members Hic-5 and leupaxin contain N-terminal LD domains and C-terminal LIM domains. Each LD domain contains a leucine-rich LD motif (LDXLLXXL). The LIM domains contain double-zinc finger motifs and are highly conserved among family members.

The C-terminal LIM domains are more conserved among all paxillin family proteins and all contain four LIM domains. Each LIM domain has a double-zinc finger, cysteine-rich motif. This motif was first identified in transcription factors Lin-1, Isl-1 and Mec-3, thus later termed LIM motif [145]. Structure analysis of LIM domain suggests that the every double zinc finger motif contains two antiparallel β-sheets [137, 146]. Although it was proposed that the LIM domains could bind to DNA, a number of studies suggested that they mainly function as protein binding modules. LIM domains are necessary for targeting of paxillin and leupaxin to the focal adhesions [147, 148].

In addition to the LD domains and LIM domains, paxillin family proteins also contain multiple tyrosine and serine phosphorylation sites that are phosphorylated upon stimulation. The cellular distribution and function of paxillin family proteins are tightly regulated by phosphorylation. The major tyrosine phosphorylation sites for paxillin are Tyr31 and Tyr118, which are phosphorylated by FAK [149, 150]. One example is that paxillin is required for focal adhesion assembly and maintenance at the leading edge, whereas paxillin tyrosine phosphorylation by FAK promotes the focal adhesion disassembly and cell migration [117]. Serine phosphorylation of paxillin is also important for proteasome-dependent degradation and the following regulation of cell migration [151]. Until now, no studies have examined serine or threonine phosphorylation of Hic-5 or leupaxin.

1.4.3. Paxillin family proteins binding partners and function

The N-terminal LD domains of paxillin family proteins account for the association of the majority of identified binding partners. Two of the most important proteins that regulate paxillin family protein phosphorylation are FAK and Pyk2. FAK and Pyk2 are non-receptor tyrosine kinases that share similar domain structures and bind to the LD2 and LD4 motifs of both paxillin and leupaxin [152, 153]. FAK is ubiquitously expressed in various cells whereas Pyk2 is preferentially expressed in hematopoietic lineage cells. Both of them contain a N-terminal FERM domain, a central kinase domain and a C-terminal FAT (focal adhesion targeting) domain. FAK and paxillin together play important roles in cell adhesion and migration. FAK is recruited to the focal adhesions by paxillin, and via phosphorylation of paxillin, promoting focal adhesion turnover and cell migration [117]. The importance of Pyk2 in regulating $CD8^+$ T cell migration was confirmed by our lab that inhibition of Pyk2 kinase activity reduced the cell migration on ICAM-1 by inhibiting the detachment of trailing edge from the substrate [154]. As leupaxin is also preferentially expressed in hematopoietic lineage cells, it would be interesting to explore the role of leupaxin in regulating leukocyte adhesion and migration.

Although both paxillin and leupaxin bind to Pyk2, the binding affinity between Pyk2 and leupaxin is three-fold higher than that of paxillin [152]. In addition, protein structures show that leupaxin forms a more stable complex with Pyk2 whereas paxillin-Pyk2 complex is unstable and the 1:1 complex is a mixture of two different conformations [153]. Therefore, it was proposed that leupaxin

served as the native binding partner of Pyk2 in leukocytes and played major roles in regulating cell adhesion and migration, instead of the paxillin-FAK complex.

In addition to tyrosine phosphorylation, serine phosphorylation of paxillin plays important roles in protein degradation, cell migration and protein translocation. Serine phosphorylation of paxillin at Ser178 by JNK regulates cell adhesion and migration [151, 155]. Paxillin associated with ERK at the focal adhesions via N-terminal LD domains [156]. The FAK-Src signaling pathway led to activation of MAP kinase and promoted focal adhesion turnover [117, 157]. Treatment of murine fibroblasts with MEK inhibitor U0126 significantly reduced the rate of focal adhesion turnover. Whether leupaxin is also serine phosphorylated is unknown.

As expected, dephosphorylation of paxillin family proteins is also important in cell adhesion and migration. One of the phosphatases that have been identified to associate with paxillin family proteins is PTP-PEST. PTP-PEST has been shown to associate with paxillin via C-terminal LIM2 and LIM3 domains [158]. Leupaxin is also a binding partner of PTP-PEST in prostate cancer cells [159]. In macrophages, PTP-PEST deletion resulted in hyperphosphorylation of Pyk2 and paxillin, and resulted in defective polarization, migration and macrophage fusion [160]. PTP-PEST regulated cell adhesion and migration by modulating Rac1 activity, and paxillin association with PTP-PEST was required for the regulation [161]. The underlying mechanism is probably through GIT2, as GIT2 was identified as a substrate of PTP-PEST [161]. Dephosphorylation of GIT2 by PTP-

PEST reduced the formation of GIT2-PIX-PAK complex and association with paxillin, thereby decreasing Rac1 activation [108].

1.4.4. Leupaxin in adherent cells

Unlike paxillin which is extensively studied, the function of leupaxin is largely unknown and the majority of studies have been carried out in adherent cells and tumor cells. Similar to paxillin, leupaxin is recruited to the focal adhesions during cell adhesion and spreading, and this recruitment was mainly mediated by the LIM3 domains [148, 162]. Leupaxin was also tyrosine phosphorylated upon integrin stimulation [162]. As paxillin and leupaxin both associated with Pyk2 and leupaxin suppressed tyrosine phosphorylation of paxillin [148, 152], it was proposed that leupaxin may antagonize paxillin during integrin signaling.

While paxillin and leupaxin are structurally similar, they seem to have different functions in regulating cell adhesion and migration. Glenn *et al* showed that knockdown of leupaxin expression in breast cancer cells stimulated cell adhesion, whereas knockdown of paxillin expression inhibited cell adhesion [162]. However, contradictory results have been shown in leupaxin regulating cell spreading on the substrate. Knockdown of leupaxin expression in breast cancer cells reduced cell spreading on the substrate collagen I [162], whereas overexpression of leupaxin in NIH 3T3 cells reduced the cell spreading on fibronectin [148]. One explanation is that cancer cells and tumor cell lines usually have aberrant integrin signaling and protein expression. The role of leupaxin in cell adhesion and spreading needs to be examined in primary cells.

1.4.5. Leupaxin in leukocytes

Although leupaxin is preferentially expressed in the leukocytes, very little is known about its contribution to cell adhesion and migration in these cells. Until now, there are only two papers published focusing on the function of leupaxin in leukocytes [107, 163]. Chew et al demonstrated that leupaxin was tyrosine phosphorylated in B cells upon BCR engagement, and the phosphorylation site was identified at Tyr72. Furthermore, overexpression of leupaxin in A20 cells inhibited JNK, MAPK and Akt signaling, and suppressed IL-2 production upon BCR stimulation, thus suggesting a negative regulating function in B cells. However, all of the experiments were performed in the A20 lymphoblastic B cell line and they did not confirm the role of leupaxin in primary B cells, raising the question of whether it can represent leupaxin function in *ex vivo* B cells.

The most convincing evidence that showed an important role of leupaxin in leukocytes came from studies of leupaxin in NK cells. Dr. Long's group identified a signaling complex centered on ILK-Pyk2-leupaxin which were phosphorylated downstream of LFA-1 signaling in NK cells. In addition, knockdown of leupaxin in NK cells reduced MTOC reorientation and granule polarization during NK cell conjugation with the target cells. This suggests that leupaxin is required for optimal NK cell degranulation. As both CTL and NK cells utilize degranulation for the clearance of target cells, it would be interesting to determine whether leupaxin has a similar function in CTL.

1.5. Hypothesis and study objectives

The underlying hypothesis is that leupaxin is required for optimal TCR signaling and migration and contributes to the MTOC reorientation during CTL conjugation.

Specifically, the following questions will be addressed in my thesis.

1. Is leupaxin phosphorylated as part of the TCR signaling cascade? How is the phosphorylation modulated during the TCR signaling?

2. What is the subcellular distribution of leupaxin in CTL? What structural domains are required for the localization?

3. Does leupaxin function as a negative regulator in TCR signaling?

4. Does leupaxin regulate CTL adhesion, migration and spreading?

5. Does leupaxin regulate the MTOC reorientation, granule polarization and CTL degranulation?

CHAPTER 2: Materials and Methods

2.1. Mice

The C57BL/6 mice, OT-1 transgenic mice and the B6.C-Tg (CMV-cre) 1Cgn/J mice were purchased from the Jackson Laboratory. The leupaxin floxed mice (C57BL/6N-A^{tm1Brd} Lpxn$^{tm1a(EUCOMM)Hmgu}$/WtsiPh) were purchased from the Sanger Institute in the UK. The leupaxin knockout (KO) mice were generated by breeding leupaxin floxed mice with CMV-Cre mice. The OT-1 transgenic leupaxin KO mice were generated by breeding leupaxin KO mice with OT-1 transgenic mice. The C57BL/6 mice were housed in conventional housing facility (Health Sciences Laboratory Animal Service, University of Alberta). Leupaxin floxed mice and leupaxin KO mice were maintained virus antigen free facility. All animal studies were approved by the University Animal Policy and Welfare Committee at the University of Alberta and adhered to the guidelines put forward by the Canadian Council on Animal Care (protocol number AUP305).

2.2. Cells

The alloreactive murine CD8$^+$ T cell clone AB.1 (H-2^d) and clone 11 (H-2^k) are non-transformed CTL that are dependent on antigen and IL-2, as described previously [164, 165]. Both clone AB.1 and clone 11 are alloreactive against MHC class I H-2K^b. They were stimulated weekly by irradiated (2500 rad) C57BL/6 splenocytes [164, 166]. OT-1 CD8$^+$ T cells were obtained from the OT-1 transgenic mice by stimulating the splenocytes with OVA$_{257-264}$ peptide (SIINFEKL) for 3-4 days in the presence of IL-2. All CTL were used for experiments 4-6 days after stimulation. The B cell line A20 cells were cultured in RPMI 1640 supplemented

with 8% dCS and penicillin/streptomycin. The target cells L1210 and L1210 K^b/D^d lymphoma cell lines were gifts from Dr. K.P. Kane (University of Alberta) and described before [167].

2.3. Antibodies

The polyclonal Pyk2 antibodies F245 and F298 were generated by immunizing New Zealand white rabbit with the Pyk2 fragment peptide 2-12 and peptide 720-862, respectively [168]. Anti-Pyk2 monoclonal antibody, anti-Lck antibody and anti-paxillin antibody were purchased from BD Biosciences (Mississauga, ON). Anti-GFP monoclonal antibody, anti-ERK antibody and anti-GFP polyclonal antibody were purchased from Life Technologies (Carlsbad, California, USA). Anti-phosphotyrosine antibody PY72.10.5 was purified from the hybridoma which was obtained from Dr. B, Sefton at the Salk Institute [169]. Anti-CD3ε antibody (clone 145-2C11) and anti-LFA-1 antibody (clone M17/5.2) were purified from hybridomas, as described previously [170]. The phospho-Pyk2 polyclonal antibodies pY402, pY579 and pY580 were purchased from Biosource International (Camarillo, CA). Anti-α-tubulin antibody was purchased from Abcam Inc (Cambridge, MA). Anti-GAPDH antibody was purchased from Meridian Life Science (Saco, ME). Anti-actin antibody was purchased from Sigma-Aldrich (Mississauga, ON). Anti-mouse-Alexa Fluor 488, anti-rabbit-Alexa Fluor 594, anti-rabbit-Alexa-Fluor 488 and anti-rat-Alexa Fluor 594 were purchased from Molecular Probes (Eugene, OR). Anti-IQGAP1 antibody was purchased from Santa Cruz Biotechnology (Santa Cruz, California, USA). HRP-conjugated goat anti-mouse IgG and mouse anti-rabbit IgG were purchased from Jackson

ImmunoResearch Laboratories (West Grove, PA). BV421-conjugated anti-CD3 antibody, PE-conjugated anti-CD8 antibody, FITC-conjugated anti-CD4 antibody, APC-conjugated anti-CD107a antibody, APC-conjugated anti-TCRβ antibody and the corresponding isotype control antibodies were purchased from BD Biosciences (Mississauga, ON).

2.4. Reagents

Phorbol 12-myristate 13-acetate (PMA), Histopaque-1077, EGTA, bovine serum albumin (BSA), IPTG, ampicillin, kanamycin, dimethyl sulfoxide (DMSO), poly-D-lysine, complete Freund's adjuvant (FCA), incomplete Freund's adjuvant (FIA), MEK inhibitor U0126, INT (2-p- iodophenyl-3- p-nitrophenyl- 5-phenyl tetrazolium chloride), PMS (N-methylphenazonium methyl sulfate), NAD (nicotinamide adenine dinucleotide), lactic acid, acetic acid, Src kinase inhibitor PP2 and the control PP3 were purchased from Sigma-Aldrich (Mississauga, ON). Econo-Pac serum IgG purification kit and PVDF membrane were purchased from Bio-rad (Hercules, USA). The protease inhibitor was purchased from Roche (Indianapolis, Indiana, USA). The ECL detection buffer, fetal bovine serum (FBS), calf serum (dCS), fetalclone I serum, L-glutamine, protein A-coupled sepharose were purchased from GE Healthcare (Piscataway, USA). Ionomycin and saponin were purchased from Calbiochem (San Diego, USA). Fibronectin and vitronectin were purchased from EMD Millipore (Billerica, MA). The surfactant-free white sulfate latex was purchased from Interfacial Dynamics Corp (Portland, USA). The Micam-1/Fc chimera was purchased from R&D Systems (Minneapolis, USA). The Pyk2 inhibitor PF431396 was purchased from Symansis (Auckland, New Zealand).

The fluorescence dye CellTracker blue, CellTracker violet, CellTracker green and Prolong Gold Antifade Mountant were purchased from Life Technologies (Burlington, ON). The eight well-chambered coverglass and coverslip were purchased from Fisher Scientific (Ottawa, ON). The $CD8^+$ T cell purification kit was purchased from StemCell (Vancouver, BC). The mouse primary T cell nucleofector kit (Lonza) was purchased from ESBE Scientific (Markham, ON). The OVA N4 peptide (SIINFEKL), T4 peptide (SIITFEKL) and G4 peptide (SIIGFEKL) were purchased from Sigma-Genosys (Canada). The Endofree plasmid maxi kit, Gel extraction kit and QIAprep spin miniprep kit were purchased from QIAGEN (Toronto, ON). The restriction enzymes *EcoRI*, *SalI*, and Q5 site-directed mutagenesis kit were purchased from New England Biolabs (Carlow Court, ON). The competent cells DH5α *E.coli* and BL21(DE3) *E.coli* and high-fidelity DNA polymerase were purchased from Thermo Fisher Scientific (Canada). The plasmids mCherry-talin, GFP-vinculin and mCherry lifeact were purchased from Addgene (Cambridge, MA).

2.5. Mutagenesis of leupaxin

2.5.1. Truncation mutagenesis of leupaxin

Truncations of leupaxin LD domains were performed by a step-wise PCR method. The full-length leupaxin with *EcoRI* and *SalI* on N-terminus and C-terminus was used as the template for PCR amplification. A forward primer on the C-terminus of the deletion part was used with the reverse *SalI* primer to amplify the C-terminal fragment. The reverse primer on the N-terminus of the deletion part, containing an 11bp bridge sequence complementary to the C-terminus of the

deletion part, was used with the forward *EcoRI* primer to amplify the N-terminal fragment. After PCR, the DNA products were separated by electrophoresis in 0.85% agarose gel and the DNA bands corresponding to the correct size were excised and purified with the PCR purification kit. After that, the N-terminal fragment and the C-terminal fragment were mixed as the template for a third PCR reaction by using the *EcoRI* primer and *SalI* primer. The PCR products were separated by electrophoresis, purified and digested with *EcoRI* and *SalI*. After purification of the digested PCR products, DNA segments were inserted into EGFP-C1 plasmid for ligation at 16 ºC. Next, the ligation mix was transformed into DH5α. Single colonies were picked from the LB plates and cultured in LB medium. Plasmids were extracted from the cultured bacteria and followed by sequencing to ensure the correct truncation. The bacteria were cultured in one liter of LB medium, and the Endofree plasmids were extracted by Endofree plasmid maxi kit. All the primers used for leupaxin truncation were shown in **Table 2.5.1**.

Construct	Primer	Sequence (5'-3')
ΔLD2	Forward-N	CCGGAATTCGAAGAGCTGGATGCCTTATTGG
	Reverse-N	GCTCATCCAACTGAGCCTTGCTCTCCTCTGTGGATTG
	Forward-C	CACAGAGGAGAGCAAGGCTCAGTTGGATGAGCTCATG
	Reverse-C	GCGGTCGACCTACTGTGAAAAGAGCTTAGTGAAGC
ΔLD3	Forward-N	CCGGAATTCTGAAGAGCTGGATGCCTTATTGG

	Reverse-N	GCATTGAGTCCAGAGAAGCAGCTGCTGAGGTTTTGGG
	Forward-C	AACCTCAGCAGCTGCTTCTCTGGACTCAATGCTGGGG
	Reverse-C	GCGGTCGACCTACTGTGAAAAGAGCTTAGTGAAGC
ΔLD4	Forward-N	CCGGAATTCTGAAGAGCTGGATGCCTTATTGG
	Reverse-N	AGTAGCCCTTGGGGACTGCCTTGTGATCCTGCTGGT
	Forward-C	GCAGGATCACAAGGCAGTCCCCAAGGGCTACTGTGC
	Reverse-C	GCGGTCGACCTACTGTGAAAAGAGCTTAGTGAAGC
ΔLD2-3	Forward-N	CCGGAATTCTGAAGAGCTGGATGCCTTATTGG
	Reverse-N	TGAGTCCAGAGACTTGCTCTCCTCTGTGGATTGC
	Forward-C	GAGGAGAGCAAGTCTCTGGACTCAATGCTGG
	Reverse-C	GCGGTCGACCTACTGTGAAAAGAGCTTAGTGAAGC
ΔLD2-4	Forward-N	CCGGAATTCTGAAGAGCTGGATGCCTTATTGG
	Reverse-N	GCCCTTGGGGACCTTGCTCTCCTCTGTGGATTGC
	Forward-C	GAGGAGAGCAAGGTCCCCAAGGGCTACTGTGCTTC
	Reverse-C	GCGGTCGACCTACTGTGAAAAGAGCTTAGTGAAGC
ΔLD3-4	Forward-N	CCGGAATTCTGAAGAGCTGGATGCCTTATTGG
	Reverse-N	GCCCTTGGGGACAGCAGCTGCTGAGGTTTTGGGAG
	Forward-C	TCAGCAGCTGCTGTCCCCAAGGGCTACTGTG

	Reverse-C	GCGGTCGACCTACTGTGAAAAGAGCTTAGTGAAGC
NT-LD	Forward	CCGGAATTCTGAAGAGCTGGATGCCTTATTGG
	Reverse	GCGGTCGACCTAGTAGCCCTTGGGGACTGTGGCAA
CT-LIM	Forward	CCGGAATTCTGTCCCCAAGGGCTACTGTGCTTC
	Reverse	GCGGTCGACCTACTGTGAAAAGAGCTTAGTGAAGC
ΔLD1	Forward	CCGGAATTCTTCTTGTCACCTGGATCAGCAATC
	Reverse	GCGGTCGACCTACTGTGAAAAGAGCTTAGTGAAGC
ΔLIM4	Forward	CCGGAATTCTGAAGAGCTGGATGCCTTATTGG
	Reverse	GCGGTCGACCTAGAGGGTCCCTCGGCGGTGATGG
ΔLIM3-4	Forward	CCGGAATTCTGAAGAGCTGGATGCCTTATTGG
	Reverse	GCGGTCGACCTATTTGGGTGAGAACATGGCTAAG
ΔLIM2-4	Forward	CCGGAATTCTGAAGAGCTGGATGCCTTATTGG
	Reverse	GCGGTCGACCTAGCGTGGAGAGAACAGGCGGTGGTAG

Table 2.5.1. Primers used for truncation mutagenesis of leupaxin

2.5.2. Site-directed mutagenesis of leupaxin

In order to find the potential Ser or Thr phosphorylation sites, I mutated several Ser and Thr residues into Ala. First, the potential Ser and Thr phosphorylation residues within LD1 and LD2 domains were predicted on NetPhos 3.1 server. The results suggested that Ser19, Ser34, Ser49, Ser54 and Ser73 had

high values of phosphorylation. Next, these residues were mutated into Ala by Q5 site-directed mutagenesis kit. After exponential amplification, the PCR products were treated with DpnI restriction enzyme for 5 minutes at room temperature, followed by transformation into DH5α. Single colonies were picked from the LB plates and cultured in LB medium. Plasmids were extracted from the cultured bacteria, followed by sequencing to ensure the correct mutation. The bacteria were cultured in one liter of LB medium, and the Endofree plasmids were extracted by Endofree plasmid maxi kit.

The primers used for the mutagenesis were shown in **Table 2.5.2.**

Construct	Primer	Sequence (5'-3')
S19A	Forward	CTTTCAGGACGCTGAGGAATATTCAAATCC AGTTTC
	Reverse	GTGCAGCGTTCCAATTCC
S34A	Forward	GGATCAGCAAGCCACAGAGGA
	Reverse	AGGTGACAAGAAACTGGATTTG
S49A	Forward	GACCTTGTCAGCGCAGGGTAA
	Reverse	TTTGGAGTTTGGGGAATCTTG
S54A	Forward	GGGTAACACAGCTCCCTTGAAGGTGC
	Reverse	TGCGATGACAAGGTCTTTG
S73A	Forward	CAATGTCTACGCTGAGGTCCAAGAGCC AAAG
	Reverse	GGCTCCTGGATATTGGTTG

Table 2.5.2. Primers used for site-directed mutagenesis of leupaxin

2.6. Generation of polyclonal anti-leupaxin antibody

2.6.1. GST-leupaxin-LD gene cloning

As leupaxin C-terminal LIM domains showed high similarity with paxillin LIM domains in amino acid sequence, I only used leupaxin-LD domains for antibody generation. First, leupaxin LD domains (amino acid 1-151) were amplified from the full-length leupaxin, with restriction enzymes *EcoRI* and *SalI* added on 5' end and 3' end. The PCR product of leupaxin-LD fragment was digested with *EcoRI* and *SalI* at 37 ^{o}C overnight, followed by purification with PCR product purification kit. The digested leupaxin-LD fragment was ligated into pGEX vector which was already digested with *EcoRI* and *SalI* restriction enzymes. The ligation reaction was transformed into DH5α. Twenty-four hours later, single colonies were picked and seeded into LB medium for bacteria growth. The plasmids were extracted from bacteria and sequenced to ensure the correct DNA sequence.

2.6.2. GST-leupaxin-LD expression and protein purification

The pGEX plasmids containing leupaxin-LD domains were transformed into BL21 (DE3), followed by picking single colonies and seeding in the LB growth medium. Liquid cultures containing the transformed BL21 (DE3) were transferred to 1 liter of LB medium for bacteria growth with vigorous agitation. Once the A_{600} reached 0.6 to 0.8, IPTG was added to the LB medium with final concentration to 100 mM to induce the GST fusion protein expression. Three hours later, the cell pellet was collected by centrifugation, resuspended in PBS and lysed by sonication. Triton X-100 was added to the cell lysates to a final concentration of 1% to facilitate

protein solubilization. In the end, the cell lysates were centrifuged and the supernatant was transferred to a new container.

In order to purify GST fusion protein, the glutathione sepharose 4B was added to cell lysates and incubated with gentle agitation for 30 minutes. The beads were collected by centrifugation, washed with PBS for 3 times. The fusion protein was eluted from the beads by glutathione elution buffer, followed by centrifugation. The supernatant was collected in a fresh tube.

2.6.3. Rabbit immunization, serum collection and IgG purification

The solution containing GST fusion proteins was concentrated with centrifugal concentrator by centrifugation. The final concentration of the protein was determined by BCA protein assay kit. Antigen emulsion was performed by mixing protein solution with either complete Freund's adjuvant (FCA) or incomplete Freund's adjuvant (FIA). For the first immunization, the New Zealand white rabbits were injected with antigens in FCA. The next three immunizations were performed every two weeks with antigen in FIA. The rabbit underwent pre-immunization bleeding before every injection.

The rabbit was sacrificed two weeks after the fourth immunization, followed by blood collection. The serum was separated from red blood cells by centrifugation with the speed of 800 rcf. The serum was collected after centrifugation and IgG was purified from the serum according to the protocol of Econo-Pac serum IgG purification kit. The concentration of IgG after purification was measured by BCA protein assay kit.

2.7. Anti-CD3 antibody and anti-LFA-1 antibody immobilization

For antibody immobilization, either anti-CD3 antibody or anti-LFA-1 antibody was diluted to 10 μg/ml in PBS and added to 60 mm petri dish. The antibody was incubated for immobilization at 4 ºC overnight. Before stimulation, the dish was washed three times with D-PBS, followed by blocking with 2% BSA for 45 minutes at 37 ºC. The dish was washed three times with D-PBS before being used for stimulation.

2.8. CTL stimulation with immobilized anti-CD3 antibody or anti-LFA-1 antibody

For immobilized anti-CD3 antibody stimulation, CTL clone 11, clone AB.1 or OT-1 T cells were collected, washed with D-PBS and resuspended in RPMI 1640 at a concentration of 1×10^7 cells per 600 μl. 1×10^7 cells were added to the anti-CD3 antibody-coated dish and incubated at 37 ºC for various times. An equal volume (600 μl) of 2% NP-40 lysis buffer was added to the dish and incubated at 4 ºC for 25 minutes. Cell lysates were collected from the dish and centrifuged at 13000 rpm to remove the nuclei. The supernatant was used for immunoprecipitation. Immobilized anti-LFA-1 antibody stimulation was performed similarly, except that the dish was coated with anti-LFA-1 antibody.

For Pyk2 inhibition experiments, clone AB.1 were first treated with either PF431396 (5 μM) or DMSO control for 1 hour at 37ºC. Cells were washed twice and resuspended in RPMI 1640 containing either 5 μM PF431396 or DMSO control before stimulation. For Src kinase inhibition experiments, clone AB.1 were pre-treated with either control PP3 (10 μM) or Src kinase inhibitor PP2 (10 μM) on ice for 15 minutes. Cells were washed twice and resuspended in RPMI 1640 containing

either control PP3 or PP2 before stimulation. For U0126 treatment experiments, clone AB.1 were pre-treated with MEK inhibitor U0126 (10 μM) at 37ºC for 30 minutes. Cells were washed twice and resuspended in RPMI 1640 before stimulation.

2.9. CTL stimulation with PMA and ionomycin

CTL were collected, washed with D-PBS and resuspended in RPMI 1640 at 1×10^7 cells/ml. PMA and ionomycin were added to the cell solution at the final concentration of 100 ng/ml and 2 μM. Cells were incubated at 37 ºC and stimulated for various times prior to lysis.

2.10. CTL nucleofection

CTL were transfected with Lonza primary cell nucleofector kits according to the manufacturer's protocol. Clone 11 cells were stimulated with irradiated splenocytes from C57BL/6 mice in the presence of IL-2. Four days after stimulation, cells were collected from the 24-well plates. The dead cells were removed by density centrifugation. Histopaque-1077 was gently added to the bottom of the cell solution, followed by centrifugation at 800 rcf for 15 minutes at room temperature. When centrifugation was finished, the cell layer between histopaque and medium was gently collected and transferred to complete medium containing 10% FCS, 0.1 nM non-essential amino acids, 1 mM sodium pyruvate, 2 mM L-glutamine, 100 μg/ml penicillin/streptomycin and 53 nM 2-mercaptoethanol. The enriched cells were washed once with D-PBS and resuspended in D-PBS at 5×10^6 per 100 μl. Five million CTL were used for each transfection. The cells were centrifuged at the lowest speed at 4 ºC for 10 minutes. After centrifugation, the supernatant was

removed and cell pellets were gently resuspended in 50 µl of the nucleofector solution. The cell solution was mixed with 50 µl of nucleofector solution containing 2 µg of the endofree plasmid. The mixed cell solution was transferred to the electroporation cuvette, followed by nucleofection using the program X-01 of the Alexa nucleofector. Cells were then transferred to the complete medium which was supplemented with component B and IL-2 and pre-warmed at 37 ^{o}C incubator. Cells were cultured for 24 hours 37 ^{o}C before confocal analysis.

2.11. A20 cell transfection

A20 cells were cultured in RPMI 1640 containing 8% dCS and 100 µg/ml penicillin/streptomycin. Cells were fed with fresh medium 24 hours before transfection. A20 cells were collected, washed once with pre-warmed RPMI. Cells were resuspended in ice-cold RPMI at a concentration of 25×10^{6}/ml. 10 million cells were transferred to the electroporation cuvette, mixed with 10 µg of endofree plasmid (5-10 µl) and incubated on ice for 5 minutes. The electroporator was set up for the following parameters: 330 v, 3 msec and 5 pulses with the interval of 1 second. After electroporation, the cuvette was incubated on ice for another 10 minutes. Cell solution was then transferred to the ice-cold complete medium containing 8% dCS and cultured at 37 ^{o}C incubator for 24 hours before PMA stimulation.

2.12. NIH 3T3 cell transfection

NIH 3T3 cells were cultured in DMEM containing 10% FCS and 1% L-glutamine and transfected by the Effectene kit from QIAGEN. 6×10^{5} cells were seeded into 60 mm treated dish wish fresh medium twenty-four hours before

transfection. Briefly, 2 μg of plasmid was mixed with 16 μl of Enhancer and 300 μl of Enhancer buffer provided by the kit. The mixed reagent was incubated for 5 minutes at room temperature, followed by the addition of 60 μl of Effectene transfection reagent. The mixture was incubated for another 10 minutes at room temperature. During the incubation time, NIH 3T3 cells were washed once with pre-warmed D-PBS and 7 ml of the complete medium was added to the dish. 10 minutes later, 3 ml of the complete medium was added to the plasmid solution, which was transferred in drops to the dish. The NIH 3T3 cell culture dish was mixed gently by shaking so that the plasmid was distributed uniformly. Cells were cultured for 48 hours before confocal analysis.

2.13. Cell lysis and immunoprecipitation

For CTL stimulation experiments, 0.6 ml of 1% NP-40 lysis buffer (1% NP-40, 1 mM sodium orthovanadate, 150 mM NaCl, 5 mM EDTA, 10 mM Tris and protease inhibitor cocktail, Roche) was added to the stimulated cells and incubated for 25 minutes at 4 ^{o}C. If no cell stimulation was required, 10 million cells were resuspended in 1 ml of 1% NP-40 lysis buffer and incubated for 25 minutes at 4 ^{o}C. Cell lysates were collected and centrifuged at 13200 rpm for 10 minutes at 4 ^{o}C. The supernatant was collected and transferred to new tubes. 40 μl of cell lysates corresponding to 4×10^5 cells were transferred to new tubes and used for lysate control.

For leupaxin immunoprecipitation, 2 μg of anti-leupaxin antibody was added to the cell lysate. Lysate was rotated at 4 ^{o}C for 1 hour before adding 30 μl of protein A sepharose beads. Samples were incubated for another 1 hour at 4 ^{o}C,

followed by centrifugation at 4000 rpm for 10 minutes at 4 ºC. The bead pellet was washed 3 times with 1 % NP-40 lysis buffer. After washing, the beads were resuspended in 70 µl of 1×Laemmli reducing sampling buffer, boiled for 5 minutes and centrifuged at 13000 rpm before loading to SDS-PAGE.

For Pyk2 F245 or F298 immunoprecipitation, 6 µl of the serum was added to the cell lysate, followed by immunoprecipitation as above. For paxillin immunoprecipitation, 4 µl of anti-paxillin antibody was added to the cell lysate. After incubation for 1 hour at 4 ºC, 4 µl of rabbit anti-mouse IgG was added to the lysate and incubated at 4 ºC for another 1 hour. Protein A sepharose beads were added to the lysates for immunoprecipitation as above.

2.14. Immunoblots

Protein samples were denatured in 1× reducing sampling buffer and boiled for 5 minutes, followed by centrifugation at 13000rpm for 5 minutes. The supernatant was loaded to 8.5% SDS-PAGE that was run at 9 mA overnight. Proteins were then transferred to the PVDF membrane at 250 mA for 4 hours. After transfer, the PVDF membrane was blocked with 4% BSA in ECL buffer for 1 hour at room temperature. Immunoblots were probed with appropriate primary antibodies and HRP-conjugated secondary antibodies with washes 3 times in between. Signals were detected by GE healthcare western blot detection reagent (RPN2106). When multiple blots were required, the PVDF membrane was stripped with stripping buffer (62.5 mM Tris-HCI pH 6.7, 2% SDS and 100 mM 2-mercaptoethanol), followed by blocking and immunoblots. The anti-phosphotyrosine blots including 4G10 and PY72 blot were always performed first

to detect the strongest signal, whereas the loading control GAPDH blot was performed last.

2.15. Cell migration assay

The 8-well chambered coverglass was coated with 3ug/ml of ICAM-1 overnight at 4 ^{o}C. The coated coverglass was washed 3 times with D-PBS before use. The transfected CTL clone 11 were collected, washed once with D-PBS. Histopaque-1077 was gently added to the bottom of the cell solution and dead cells were removed by density centrifugation as above. The live cells were washed once with RPMI 1640 containing 2% serum. 1.5×10^5 cells were transferred to each well and incubated for 45 minutes at 37 ^{o}C incubator before imaging. The chambered coverglass was placed onto an Olympus IX-81 spinning disk confocal microscopy stage and the temperature was maintained at 37 ^{o}C. The cell migration was tracked for 10 minutes with the time interval of 30 seconds.

For non-transfected OT-1 T cells, cells were first resuspended in D-PBS and labeled with CellTracker green (5 μM) for 20 minutes. Cells were washed two times with RPMI 1640 containing 2% serum before transferring to the chambered coverglass for imaging.

2.16. Live cell imaging

To determine the localization of leupaxin at the MTOC, clone 11 were co-transfected with plasmids of either GFP-paxillin and mCherry-tubulin or GFP-leupaxin and mCherry-tubulin, as described above. Twenty-four hours after transfection, cells were collected and dead cells were removed by density centrifugation. 1.5×10^5 cells were transferred to chambered coverglass which was

pre-treated with 3 μg/ml of ICAM-1. Images were captured at 37 ºC by Olympus IX-81 spinning disk confocal microscopy supplemented with 5% CO_2. For colocalization of paxillin or leupaxin with the MTOC, 491 nm laser and 561 nm laser were acquired sequentially at the MTOC and images were merged for colocalization analysis. A total of 60 cells from three independent experiments were collected for statistic analysis.

To determine whether leupaxin was recruited to the immunological synapse by live cell imaging, clone 11 were transfected with either GFP, GFP-paxillin or GFP-leupaxin by nucleofection, as described above. The target cells L1210 K^b/D^d were collected, washed once with D-PBS and then labeled with CellTracker blue (5uM) for 20 minutes at 37 ºC. The labeled L1210 K^b/D^d cells were washed twice with RPMI 1640 containing 2% serum. 0.5×10^5 transfected clone 11 were mixed with 1×10^5 L1210 K^b/D^d target cells and centrifuged at 100 g for 3 minutes at 4 ºC. The cell pellet was vortexed gently and transferred to chambered coverglass. The coverglass was incubated at 37 ºC for 20 minutes, allowing the cells to adhere to the bottom. The coverglass was placed into the live cell chamber of Olympus IX-81 spinning disk confocal microscopy provided with 5% CO_2 and humidifier. The 405 nm laser and 491 nm laser were opened at the same time to look for the conjugates formed between clone 11 and L1210 K^b/D^d target cells. Once the conjugates were focused, the two channels were acquired sequentially by Z-stack and images were merged for analysis.

Total internal reflection fluorescence microscopy (TIRF) was used to capture the contact surface during CTL migration on the ICAM-1. 1.5×10^5

transfected clone 11 cells were seeded into chambered coverglass which was coated with ICAM-1, as described above. The coverglass was placed into the live cell chamber of OMX structured illumination microscopy. 60× TIRF objective was used and a small drop of oil was placed on the lens. Epi-fluorescence mode was used to find the cells. Once the cells were found and in focus, epi mode was switched to TIRF mode. The lens was adjusted up and down until the contact zone was in focus. Different channels were acquired sequentially, and the images were merged by ImageJ.

2.17. Fluorescence recovery after photobleaching (FRAP)

Clone 11 cells were transfected with either GFP-paxillin or GFP-leupaxin. Twenty-four hours after transfection, cells were collected, washed and transferred to chambered coverglass which was pre-coated with ICAM-1 (3 μg/ml), followed by incubation at 37 ^{o}C for 45 minutes. The coverglass was placed into the live cell chamber of OMX structured illumination microscopy provided with 5% CO_2 and humidifier. Epi-fluorescence mode was used at the beginning to find the cells and the MTOC. One MTOC was focused, the microscopy was switched to the TIRF mode by increasing the angle of penetrating laser. MTOC was bleached with 488 nm laser and the fluorescence recovery at the MTOC was tracked every second. F3, F4, F5 represents the fluorescence before, during and 1 second after photobleaching. The percentage of fluorescence recovery 1 second after photobleaching was calculated by (F5-F4)/F3.

2.18. Preparation of CTL for confocal microscopy

The target cells L1210 or L1210 K^b/D^d were cultured in fresh DMEM containing 8% dCS twenty-four hours before the experiment. Cells were collected, washed once with D-PBS and labeled with CellTracker blue (5uM) for 20 minutes at 37 ^oC, as described above. The labeled cells were washed twice in DMEM and resuspended in RPMI 1640 containing 2% dCS with a concentration of 10 million cells/ml.

For the transfected CTL, cells were collected, washed with D-PBS and resuspended in RPMI 1640 containing 2% dCS with a concentration of 10 million cells/ml. 5×10^5 CTL (50 μl) were mixed with 1×10^6 target cells L1210 or L1210 K^b/D^d (100 μl) and pelleted at 100 g for 3 minutes at 4 ^oC. The cell pellet was incubated at 37 ^oC for 4 minutes to facilitate the conjugate formation between CTL and target cells. The cell pellet was gently vortexed, transferred to a coverslip which was pre-coated with poly-L-lysine and incubated for another 7 minutes at room temperature. Cells were then fixed with 4% paraformaldehyde for 10 minutes, followed by permeabilization with 0.2% NP-40 for 5 minutes, with three washes in between. After that, cells were blocked with 2% BSA for 30 minutes at room temperature. The primary antibody was diluted with 1/100 in blocking buffer (2% BSA in D-PBS) and stained for 45 minutes at room temperature. The appropriate secondary antibody was diluted with 1/400 in blocking buffer and stained for 30 minutes at room temperature. If two colors staining was required, each color staining was performed separately with three washes in between. All staining steps were performed in the dark place. After staining, the prolong gold antifade

mounting media (Molecular Probes, P36930) was used to preserve the stained cells on the coverslip.

In the case of untransfected CTL, CTL cells were first labeled with CellTracker green (5 μM) for 20 minutes at 37 ^{o}C, as described above. The target cells L1210 or L1210 K^{b}/D^{d} were labeled with CellTracker blue (5uM) for 20 minutes. After washing with D-PBS, CTL were mixed with the labeled target cells for an E:T ratio of 1:2 and pelleted at 100 g for 3 minutes at 4 ^{o}C. Cells were fixed, permeabilized and stained as described above.

In the case of conjugate between CTL and latex beads, the beads were first diluted in D-PBS to 10 million/ml and coated with ICAM-1 (3ug/ml) overnight at 4 ^{o}C. Beads were blocked with 2% BSA and washed 3 times before use. CTL were mixed with the latex beads at a ratio of 1:2, pelleted at 100 g for 3 minutes at 4 ^{o}C. The pellet was incubated at 37 ^{o}C for 4 minutes, followed by transferring to the coverslip which was pre-coated with poly-L-lysine. After incubating at room temperature for 7 minutes, cells were fixed, permeabilized and stained for the endogenous leupaxin as above.

All images were collected with the Zeiss LSM710 laser scanning confocal microscopy at the Cross Cancer Institute. For data collection, CellTracker blue was excited by 351 UV laser. Alexa488 and Alexa 594 were excited by 488 nm argon and 543 nm HeNe lasers, respectively. The 60×/1.4 oil DIC objective lens was used and Z-stack images were acquired with the interval of 0.3 um between images. For LFA-1 staining, the three-dimensional immunological synapse was created by

Imaris software. All Z-stack images were performed Z-stack into one image by ImageJ software.

2.19. Generation of leupaxin KO mice

The sperm from leupaxin floxed mice were purchased from the Sanger Institute in the UK. The sperm were used to generate offspring as a fee for service contract with Charles Rivers, US. The leupaxin floxed mice were first breed with FLP mice in order to delete the first *loxp* site which locates between the two *FRT* sites. Once the homologous mice were obtained, the mice were breed with CMV-Cre mice in order to delete the second exon which was between the two *loxp* sites. Mice were kept breeding until the homologous leupaxin KO mice were obtained. The leupaxin KO mice were also bred with OT-1 transgenic mice to get the OT-1 background leupaxin KO mice.

2.20. Naïve $CD8^+$ T cells purification and activation

Naïve $CD8^+$ T cells were purified through negative selection from splenocytes of C57BL/6 mice by EasySep mouse naïve $CD8^+$ T cell isolation kit from Stemcell. In brief, spleens were isolated from 4-6 week old C57BL/6 mice, homogenized and resuspended in D-PBS containing 2% FCS at a concentration of 100 million cells/ml. Rat serum and isolation cocktail were added to the cell solution, followed by incubation at room temperature for 10 minutes. The streptavidin rapidspheres were added to the cells and incubated at room temperature for 5 minutes. The cell solution D-PBS containing 2% FCS was topped to a final volume of 2.5 ml and placed into the magnet for 2.5 minutes. Cells were then

poured to complete medium. Cells were washed twice with RPMI containing 2% FCS before transferred to 24-well plates for activation.

For naïve $CD8^+$ T cell activation, 24-well plates were first coated with 10 μg/ml anti-CD3 antibody and 3 μg/ml anti-CD28 antibody at 4 ^oC overnight. The coated plates were washed three times with sterile D-PBS, followed by blocking with 2% BSA for 30 minutes at 37 ^oC. Plates were washed three times again before T cell activation. 4×10^5 of the purified naïve $CD8^+$ T cells (1 ml) were seeded into each well and cultured for 48 hours in the absence of IL-2. Forty-eight hours later, the activated cells were collected, washed twice, split one well into four wells and cultured in the presence of IL-2.

For OT-1 T cell activation, spleens were isolated from 4-6 week old OT-1 transgenic mice and homogenized in RPMI 1640 containing 2% FCS. The splenocytes were washed twice and resuspended in complete medium at 2.5 million cells/ml. Cells were cultured in 24-well plates, with each well containing 5 million splenocytes, IL-2 (10 U/ml) and OVA N4 peptide (SIINFEKL). 48 hours later, cells were collected, washed twice and split one well into four wells and continue to culture in complete medium in the presence of IL-2.

2.21. CD107a based degranulation assay

Target cells L1210 K^b/D^d were collected, washed once with D-PBS and resuspended in D-PBS at 10 million cells/ml. Cells were labeled with CellTracker violet (10 μM) for 20 minutes at 37 ^oC. After labeling, cells were washed once and resuspended in plain RPMI. Target cells were then pulsed with OVA N4 peptide (SIINFEKL) or T4 peptide (SIITFEKL) at the indicated concentration for 1 hour at

37 ºC. After peptide pulsing, cells were washed twice and resuspended in RPMI containing 2% FCS at 10 million cells/ml before use.

OT-1 T cells were collected at day 6 post-activation. Cells were washed, labeled with CellTracker green (10 μM) described as above. Cells were washed and resuspended in RPMI containing 2% serum at 10 million cells/ml before mixing with the target cells.

100 μl of labeled OT-1 T cells were mixed with 200 μl of labeled L1210 K^b/D^d (at the ratio of 1:2) and 1 μl of APC-conjugated anti-CD107a antibody. Cells were pelleted at 100 g for 3 minutes at 4 ºC. Once the spin was done, cells were transferred to 37 ºC waterbath and incubated for the indicated times. When incubation was complete, cells were washed three times with ice-cold D-PBS containing 5 mM EDTA and then fixed with 4% paraformaldehyde. Samples were analyzed by flow cytometry. The level of degranulation was determined by calculating the percentage of APC positive cells in CellTracker green positive and CellTracker violet negative T cells.

2.22. LDH based killing assay

Target cells L1210 K^b/D^d were collected, washed once with D-PBS and resuspended in plain RPMI at 10 million cells/ml. Cells were pulsed with OVA N4 peptide (SIINFEKL) or T4 peptide (SIITFEKL) at the indicated concentration for 1 hour at 37 ºC. After peptide pulsing, cells were washed twice and resuspended in RPMI containing 2% FCS at 2 million cells/ml before use. OT-1 T cells were collected at day 6 post-activation. Cells were washed and resuspended in RPMI containing 2% FCS at 10 million cells/ml.

100 µl of T cells were mixed with 100 µl of L1210 K^b/D^d target cells (at the ratio of 5:1) in the V-bottom 96-well plate. The plate was centrifuged at 100 g for 3 minutes at 4 ºC. Cells were then incubated at 37 ºC incubator for various times. At the indicated time, 50 µl of supernatant was gently transferred to a new 96-well plate, mixed with 50 µl of 2× LDH buffer and incubated for 10 minutes at room temperature. The reaction was stopped by adding 50 µl of stopping buffer (1 M acetic acid). Plates were read by the plate reader at 490 nm.

2.23. Statistical analysis

Statistical analysis was performed with the software GraphPad Prism6. The statistical analysis used for specific experiment is shown in the legend below each figure.

CHAPTER 3: Characterization of leupaxin function in LFA-1 signaling and leupaxin localization during CTL migration

3.1. Introduction

Paxillin family members are multi-domain scaffold proteins which recruit other signaling molecules to the focal adhesions [135]. Their scaffolding role is mediated by the protein binding modules including LD motifs, LIM domains, proline-rich region and multiple phosphorylation sites [137]. The majority of studies have been focused on paxillin family members in cell migration. Paxillin is recruited to the cell protrusion for the assembly of adhesive complexes at the leading edge [117, 171]. Additionally, paxillin is also recruited to the trailing edge to promote focal adhesion turnover [117, 172, 173]. Thus, paxillin may play dual roles during cell migration. Although leupaxin shares similar domain structure with paxillin, studies have demonstrated that it might have different roles in cell adhesion and migration in adherent cells [148, 162]. The goal of this chapter is to characterize the contribution of leupaxin in LFA-1 signaling and CTL migration.

The mechanism of cell migration is well established in adherent cells, which is coordinated by the assembly and disassembly of focal adhesions [174]. Focal adhesions are integrin-dependent adhesive structures that connect the extracellular matrix to the actin cytoskeleton [111]. They function as both signaling transmission centers and traction points for mechanical forces during migration. The outside part is integrin which binds to the extracellular matrix, and their cytoplasmic portion associates with a number of kinases and adaptor proteins such as FAK, paxillin and talin [175, 176]. There are more than 160 distinct signaling proteins participating

in the focal adhesion signaling network [111]. In resting condition, integrin exhibits a closed conformation with low-affinity for the ligand. It can be activated by the signaling events from other receptors, such as chemokine receptors, that leads to the extended conformation with intermediate-affinity for the ligand [87]. In addition, binding of integrins to the multivalent ligands also promotes integrin clustering and activation, which is termed the 'outside-in' signals [177]. The nascent adhesive complexes smaller than 0.25 um are first assembled at the leading edge of protruding cells [178]. These complexes undergo either disassembly or mature into focal adhesions and focal adhesion proteins are recruited to the integrin cytoplasmic tail. The paxillin family proteins have all been shown to be recruited to the focal adhesions [117, 148, 179]. While focal adhesions are assembled at the cell protrusion, these adhesive structures need to be disassembled at the trailing edge so that cells can release the contraction forces for migration. The calpain-mediated cleavage of focal adhesion proteins plays an important role in the turnover of focal adhesions [180]. A number of focal adhesion proteins, such as FAK, integrin, talin and paxillin, have all been shown to be cleaved by calpain and promote de-adhesion [121, 181, 182]. Therefore, the formation and turnover of focal adhesions allow cells to undergo migration.

LFA-1 consists of the α_L and β_2 subunits. The importance of LFA-1 in leukocytes migration and function has been illustrated in β_2 subunit-deficient mice and leukocyte adhesion deficiency (LAD) disorders [183, 184]. Compared to adherent cells, leukocytes lack stress fibers and classical focal adhesions [29]. The high-speed motility of leukocytes requires T cells to utilize very dynamic adhesive

complexes with frequent turnover of adhesive complexes. The model of LFA-1 mediated T cell migration on ICAM-1 has been extensively investigated *in vitro* on 2D model [29, 185]. The distribution of LFA-1 at the contact surface varies during T cell migration. The leading edge has a relatively low level of LFA-1 localization, whereas the trailing edge has the most amount of LFA-1 [132]. In addition, distinct contact regions have different conformational states. The extended LFA-1 with intermediate-affinity was organized at the leading edge [133]. The focal zone contained LFA-1 with high-affinity to ICAM-1 [132]. This area may provide firm adhesion to stabilize the contact with the substrate.

The contribution of leupaxin to adhesion and migration in adherent cells and tumor cells has been studied in several papers [140, 148, 162, 186]. Knockdown of leupaxin expression in breast cancer cells promoted cell adhesion to collagen [162]. In addition, overexpression of leupaxin in NIH 3T3 cells inhibited cell spreading on fibronectin [148]. These papers proposed that leupaxin may antagonize paxillin and inhibit cell adhesion and migration. However, opposite result has been shown in prostate cancer cells, as knockdown of leupaxin in these cells decreased cell adhesion and cell spreading on collagen and fibronectin [140]. The conflicting data may result from using different tumor cells, as paxillin family protein expression level varies in distinct tumor cells [143].

Leupaxin is preferentially expressed in the leukocytes. However, the contribution of leupaxin to leukocyte adhesion and migration is completely unknown. As LFA-1 plays an essential role in T cell migration and leupaxin serves as a cytoskeletal adaptor protein in integrin signaling, I propose that leupaxin is

involved in LFA-1 signaling and regulates LFA-1 mediated adhesion, spreading and migration in CTL. In this chapter, I first investigated the regulation of leupaxin downstream of LFA-1 signaling and leupaxin localization during CTL migration on ICAM-1. Leupaxin was tyrosine phosphorylated when stimulated with anti-LFA-1 antibody, and was recruited to the dynamic focal adhesion-like structures at the contact zone. I overexpressed leupaxin in NIH 3T3 cells, which resulted in increased cell spreading on fibronectin. Dr. Samuel Cheung overexpressed leupaxin in *ex vivo* activated OT-1 CTL and it also increased CTL spreading on ICAM-1. In addition, I overexpressed leupaxin in CTL and found that it decreased cell motility on ICAM-1. These results suggest that leupaxin promotes CTL adhesion and spreading.

3.2. Results

3.2.1. Generation of anti-leupaxin polyclonal antibodies

Since the first leupaxin paper was published in 1998, there have been several papers focusing on the role of leupaxin in integrin signaling through biochemistry techniques. All of these studies used an anti-leupaxin monoclonal antibody provided by Dr. Brian Lipsky, the author of the first leupaxin paper [187]. No current source for this monoclonal antibody could be identified. In order to study the role of leupaxin in CTL, I generated a leupaxin-specific polyclonal antiserum. As the leupaxin C-terminal domain shows over 70% similarity to paxillin in amino acid sequence, only the N-terminal region containing LD domains (amino acid 1-151) alone was amplified and inserted into the pGEX plasmid. The plasmid was transformed into BL21 (DE3) competent *E. coli* for protein expression. GST-tagged proteins were purified with glutathione sepharose 4B. Two New Zealand white rabbits were immunized four times, following the immunization procedure **(Figure 3.1A)**. Serum was separated from the clotted rabbit blood by centrifugation and IgG was purified from the serum using an Econo-Pac serum IgG purification kit.

In order to test the polyclonal antibody, the B lymphoma cell line, A20 cell, was transfected with either GFP-leupaxin or GFP-leupaxin-LD constructs. Cell lysates of the transfected cells were immunoprecipitated with either anti-GFP antibody or anti-leupaxin antibody. After SDS-PAGE and transfer, immunoblots were performed with anti-GFP antibody, followed by stripping and reprobing with

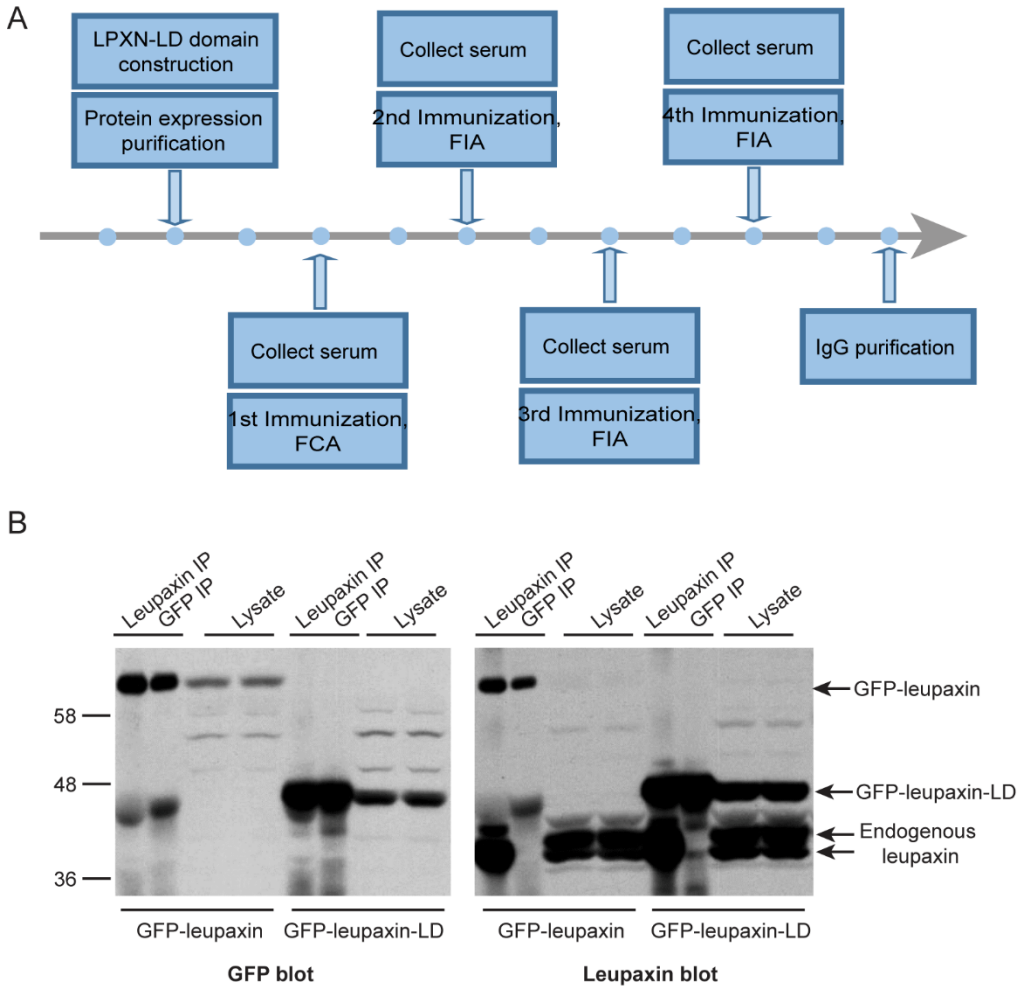

Figure 3.1. Generation of anti-leupaxin polyclonal antibodies. (A) Anti-leupaxin polyclonal antibodies were generated following the protocol. In brief, leupaxin N-terminal LD domains were amplified and inserted into pGEX plasmid. The proteins were expressed in BL21 (DE3) and purified with glutathione sepharose 4B. The purified GST fusion proteins were emulsified with Freund's adjuvant before injecting into New Zealand white rabbits. After four immunizations, serum was obtained and IgG was purified from the serum by IgG purification kit. (B) A20 cells were transfected with either GFP-leupaxin or GFP-leupaxin-LD constructs. Twenty-four hours after transfection, cells were lysed by 1% NP-40 lysis buffer and proteins were immunoprecipitated with either leupaxin or GFP antibodies. Proteins were separated by SDS-PAGE. Immunoblots were probed with the indicated antibodies.

the anti-leupaxin antibody. GFP blot showed that GFP-leupaxin was immunoprecipitated by both anti-GFP and anti-leupaxin antibodies, suggesting that the antibody I generated works for protein immunoprecipitation. The membrane was stripped, followed by leupaxin blot. As shown in **Figure 3.1B**, the GFP-leupaxin band was detected by anti-leupaxin antibody, implying that it also detects leupaxin by western blot. In addition, there were also two bands at around 45 KDa detected by the leupaxin antibody. These two bands, which were very close to each other, migrated at the predicted molecular weight of endogenous leupaxin. Interestingly, this is the first leupaxin blot revealing that leupaxin migrates as two, or perhaps more bands. Although it is suggested that leupaxin has alternative splicing (Immunological Genome Project Database), different leupaxin isoforms should not contribute to such little molecular weight difference. One of the explanations might be the result of post-translational modification, as paxillin has been shown to be serine phosphorylated, leading to the mobility shift [169, 188], which will be addressed in more detail in the next chapter.

3.2.2. Leupaxin migrates as one band in naïve $CD8^+$ T cells and two bands after activation

As I detected two bands of the endogenous leupaxin in A20 cells **(Figure 3.1B)**, I wondered whether this pattern would also be detected in naïve and activated $CD8^+$ T cells. To address this question, I purified the naïve $CD8^+$ T cells from splenocytes of C57BL/6 mice and activated them with immobilized anti-CD3 and anti-CD28 antibodies. Cells were collected 24 hours and 48 hours after activation and lysed in 1% NP-40 lysis buffer. After SDS-PAGE and transfer, immunoblots

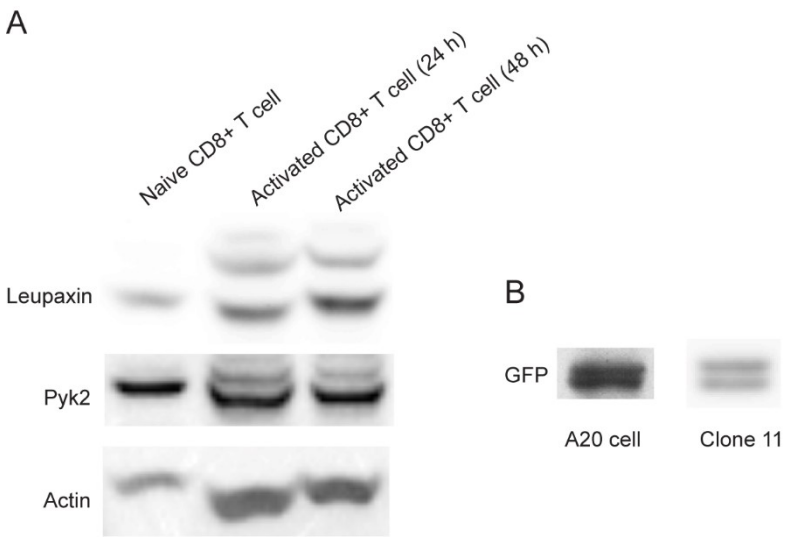

Figure 3.2. Leupaxin migrates as one band in naïve CD8$^+$ T cells and two bands after activation. (A) The naïve CD8$^+$ T cells were isolated from splenocytes of C57BL/6 mice by negative selection, followed by activation with immobilized anti-CD3 and anti-CD28 antibodies. The cell lysates corresponding to 4×10^5 cells were separated by SDS-PAGE, followed by transferring to PVDF membrane. Proteins were detected with the indicated antibodies. (B) A20 cells or clone 11 cells were transfected with GFP-leupaxin. Twenty-four hours after transfection, cell lysates corresponding to 4×10^5 cells were separated by SDS-PAGE and transferred as above. Proteins were detected with anti-GFP antibody. All experiments were performed three times, and representative data are shown.

were performed with anti-leupaxin antibody. As shown in **Figure 3.2A**, I only detected one major leupaxin band in the naïve $CD8^+$ T cells. However, once $CD8^+$ T cells were activated, two leupaxin bands were detected by the polyclonal anti-leupaxin antibodies. This data strongly suggested that the newly appeared leupaxin band was the result of post-translational modification after T cell activation. Although I used the same number of $CD8^+$ T cells for each lane, the loading control actin blot showed fewer proteins loaded in the lane of naïve $CD8^+$ T cells. The reason was that the naïve $CD8^+$ T cells differentiated into larger CTL after activation.

I also transfected the A20 cells and clone 11 cells with GFP-leupaxin and the fusion protein was detected with anti-GFP antibody. Interestingly, two GFP-leupaxin bands were detected in the cell lysates **(Figure 3.2B)**. This result suggested that the two leupaxin bands were not a product of alternative splicing, since expression by a cDNA also resulted in the presence of a doublet.

3.2.3. Leupaxin is tyrosine phosphorylated upon LFA-1 stimulation

Leupaxin is tyrosine phosphorylated upon LFA-1 engagement in adherent cells [162]. However, this has not been examined for leupaxin in CTL. In order to determine the effect of LFA-1 signaling upon leupaxin in CTL, the CTL clone AB.1 was stimulated with immobilized anti-LFA-1 antibody to mimic integrin engagement. Cells were lysed in 1% NP-40 lysis buffer after stimulation, followed by SDS-PAGE and immunoblot. As shown in **Figure 3.3A**, LFA-1 stimulation led to tyrosine phosphorylation of various proteins in CTL, with most phosphorylation peaking at around 20 minutes after stimulation. Specifically, I detected two robust

tyrosine phosphorylated bands at ~110 and 65 KDa. These two bands are most likely Pyk2 and paxillin, as both of them have been shown to be tyrosine phosphorylated upon LFA-1 engagement in CTL [154, 189].

To determine if leupaxin is tyrosine phosphorylated, clone AB.1 were stimulated as above, and leupaxin was immunoprecipitated from the cell lysates, followed by SDS-PAGE and immunoblot. As shown by 4G10 blot in **Figure 3.3B**, leupaxin was tyrosine phosphorylated upon LFA-1 stimulation. The phosphorylation was observed as early as 5 minutes after stimulation and reached the maximal level at 20 minutes after stimulation. It was previously demonstrated that leupaxin was tyrosine phosphorylated upon activation of the 'inside-out' signals in fibroblasts, osteoclasts and B cells [162, 163, 190]. CTL stimulation with the immobilized anti-LFA-1 antibody may induce integrin clustering on the surface or conformational switch, thus driving LFA-1 activation and leupaxin phosphorylation. Similar to A20 cells, I also detected two leupaxin bands in resting and LFA-1 stimulated CTL. These two bands overlapped with the two tyrosine phosphorylated proteins, suggesting that they were both tyrosine phosphorylated upon LFA-1 stimulation **(Figure 3.3B)**.

3.2.4. Leupaxin phosphorylation upon LFA-1 stimulation is dependent on Pyk2 and Src family kinase activity

In adherent cells, paxillin has been shown to be a substrate of focal adhesion kinase (FAK) [147]. Paxillin was phosphorylated by FAK at tyrosine 31 and tyrosine 118, which created two binding sites for SH2-containing Crk family proteins [149, 150, 191, 192]. In order to determine whether leupaxin tyrosine

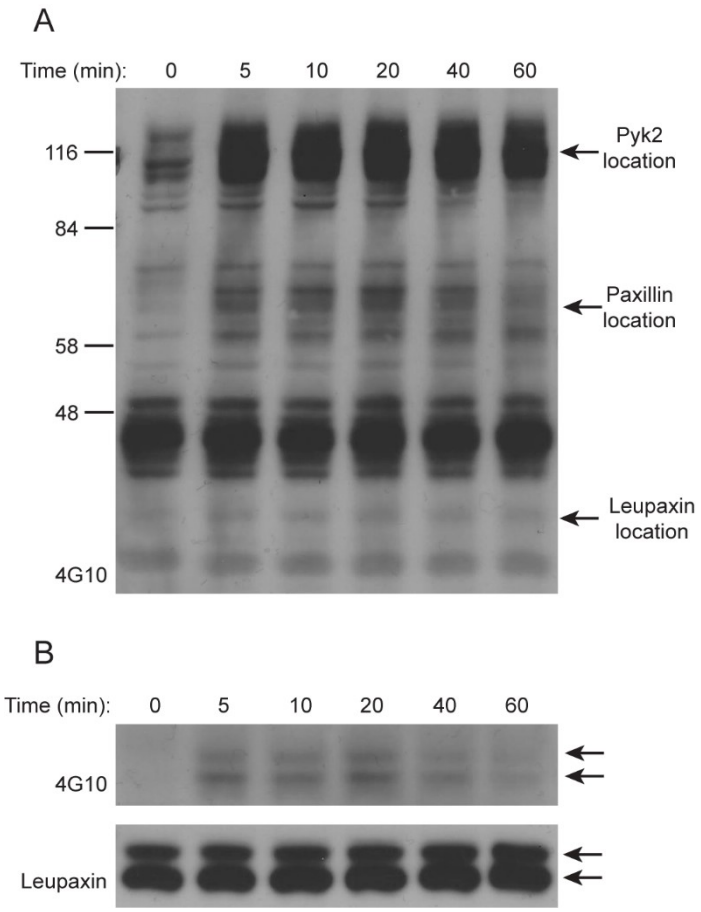

Figure 3.3. Leupaxin is tyrosine phosphorylated upon LFA-1 stimulation. (A) CTL clone AB.1 were stimulated with anti-LFA-1 antibody for various times. Cells were lysed in 1% NP-40 lysis buffer after stimulation. The cell lysates corresponding to 4×10^5 cells were separated by SDS-PAGE, followed by transferring to PVDF membrane. Proteins were detected with anti-phosphotyrosine antibody (clone 4G10). (B) Clone AB.1 were stimulated as above for the indicated time points. Leupaxin was immunoprecipitated from cell lysates of 10 million cells and then separated by SDS-PAGE. The proteins were probed with clone 4G10 antibody followed by stripping and reprobed with the anti-leupaxin antibody. The leupaxin bands and phosphorylated bands were pointed by arrows. All experiments were performed three times, and representative data are shown.

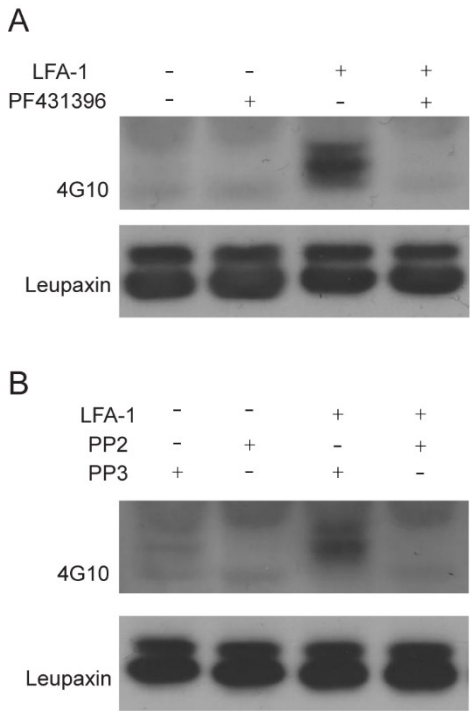

Figure 3.4. Leupaxin phosphorylation upon LFA-1 stimulation is dependent on Pyk2 and Src family kinase activity. (A) CTL clone AB.1 were pre-treated with either carrier control or Pyk2 inhibitor PF431396 (5 μM) for 1 hour at 37ºC. Cells were stimulated with plate-bound anti-LFA-1 antibody for 20 minutes. Cell lysates of 10 million cells were immunoprecipitated with anti-leupaxin antibody, followed by SDS-PAGE and transferring to PVDF membrane. Proteins were detected with anti-tyrosine phosphorylation antibody 4G10 and anti-leupaxin antibody. (B) Clone AB.1 cells were pre-treated with either control PP3 or Src kinase inhibitor PP2 (10 μM) on ice for 15 minutes, followed by LFA-1 stimulation as above. Immunoblots were probed with 4G10, followed by stripping and reprobed with anti-leupaxin antibody. All experiments were performed three times, and representative data are shown.

phosphorylation was dependent on Pyk2 activity in CTL, I treated the CTL clone AB.1 with Pyk2/FAK inhibitor, PF431396, followed by stimulating clone AB.1 with the immobilized anti-LFA-1 antibody for 20 minutes. 4G10 blot showed that leupaxin was no longer tyrosine phosphorylated when Pyk2 activity was inhibited, suggesting that anti-LFA-1 stimulated leupaxin phosphorylation was dependent on Pyk2 activity in CTL **(Figure 3.4A)**.

It has been shown that Src family kinases play a key role in Pyk2 activation and phosphorylation of the paxillin family proteins by Pyk2 [193, 194]. Pyk2 undergoes autophosphorylation at Y402, which allows Pyk2 to recruit Src family kinase [193]. The recruited Src kinase then phosphorylates Pyk2 at Y579/Y580 [193]. Paxillin has been shown to associate with Src kinases Lck and Fyn in T cells [91]. Leupaxin from other species has been shown to associate with Src family kinases in different cell types [163, 195]. For example, human leupaxin was demonstrated to associate with Lyn kinase through its LD3 domain [163], whereas rabbit leupaxin binds to Src through its LD2 domain in osteoclasts [195]. I found that leupaxin phosphorylation upon LFA-1 stimulation was dependent on Src family kinase activity in CTL. As shown in **Figure 3.4B**, when clone AB.1 was treated with Src kinase inhibitor PP2, leupaxin was no longer phosphorylated upon LFA-1 stimulation, but was still tyrosine phosphorylated in the presence of the inhibitor control, PP3. This effect may be through Pyk2, which is not activated when the Src kinase activity is inhibited.

3.2.5. Leupaxin associates with Pyk2 in CTL and leupaxin-Pyk2 complex is distinct from the paxillin-Pyk2 complex

Paxillin has been shown to associate with Pyk2 and was tyrosine phosphorylated by Pyk2 in hematopoietic lineage cells [169]. Although leupaxin associates with Pyk2 in human cancer cells [187], the association between leupaxin and Pyk2 in CTL has not been established. As leupaxin molecular weight is very close to the IgG heavy chain, I am unable to detect the endogenous leupaxin after Pyk2 immunoprecipitation. The reason is that Pyk2 F245 and F295 antiserum contains lots of immunoglobulins. In order to address the question, I performed immunoprecipitation experiment using CTL clone 11 which were first transfected with GFP-leupaxin. Our lab has previously demonstrated that Pyk2 antibodies clone F245 and clone F298 recognized different Pyk2 populations [196]. As a control, I confirmed that paxillin only associated with the Pyk2 recognized by F245 **(Figure 3.5A)**. Interestingly, the GFP blot indicated that leupaxin associated equally with the two Pyk2 populations. It has been demonstrated that the binding affinity of leupaxin to Pyk2 is 3-fold higher than to paxillin [152]. Furthermore, leupaxin forms a more stable complex with Pyk2 compared to the highly dynamic paxillin-Pyk2 complex [152, 153]. My data suggested that both populations of Pyk2 complexed with leupaxin which suggested less restricted binding relative to paxillin.

Structural investigation has demonstrated that Pyk2 focal adhesion targeting (FAT) domain forms a four-helix bundle structure, which contains two paxillin family protein binding sites [153]. As both paxillin and leupaxin associate with Pyk2 in CTL, this raised the question of whether they could bind to Pyk2 in the same complex. Sequential immunoprecipitation was performed in cell lysates of clone AB.1 cells. I performed immunodepletion with either leupaxin antibody or

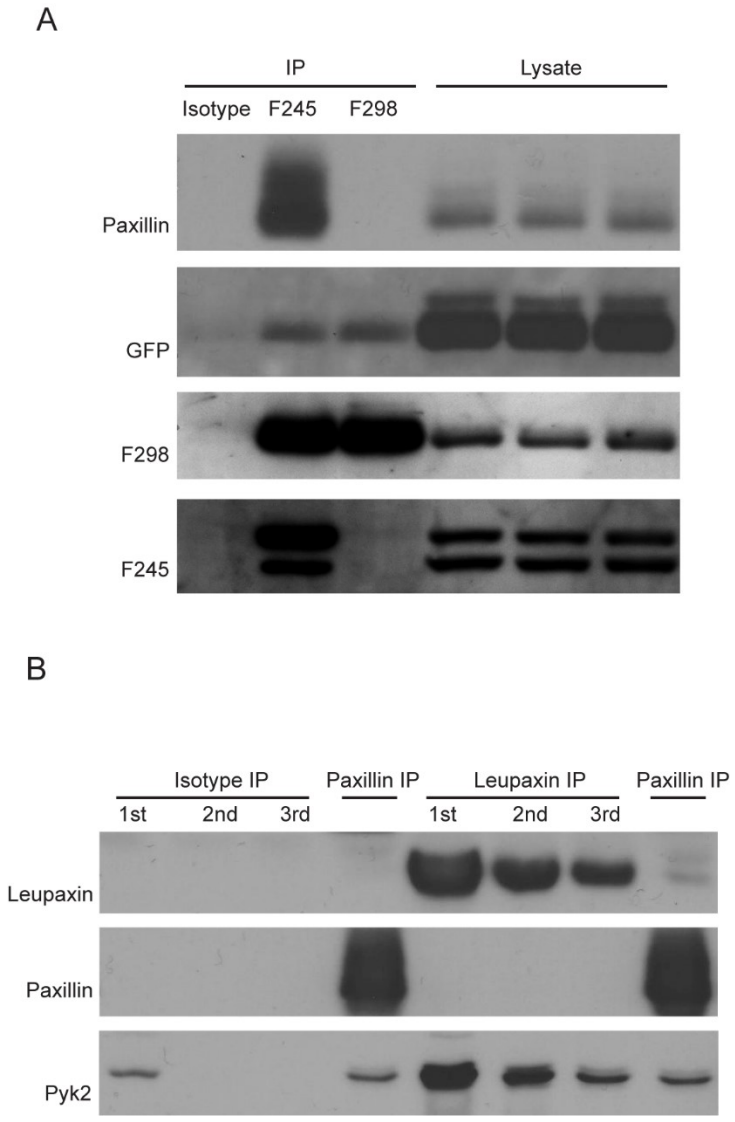

Figure 3.5. Leupaxin associates with Pyk2 in CTL and leupaxin-Pyk2 complex is distinct from the paxillin-Pyk2 complex. (A) CTL clone 11 were transfected with GFP-leupaxin. Cells were lysed in 1% NP-40 lysis buffer 24 hours after transfection. Cell lysates were immunoprecipitated with the indicated Pyk2 antibodies or isotype control. Proteins were separated by SDS-PAGE and the immunoblots were probed with the indicated antibodies. Cell lysates on the right were shown to confirm the protein expression. (B) Sequential immunoprecipitation was performed with the indicated antibodies from AB.1 cell lysates of 10 million cells. After immunoprecipitation for three times, paxillin was immunoprecipitated from the final cell lysates, followed by SDS-PAGE and transfer. Immunoblots were performed with the indicated antibodies. All experiments were performed two times, and representative data are shown.

isotype IgG, followed by immunoprecipitation with paxillin antibody. As shown in **Figure 3.5B**, the first three leupaxin immunoprecipitations removed the majority of the leupaxin-Pyk2 complexes. Paxillin was not detected in leupaxin immunoprecipitates. After leupaxin immunodepletion, paxillin was immunoprecipitated from the remaining cell lysates. As expected, Pyk2 was detected to associate with paxillin upon paxillin immunoprecipitation. However, the Pyk2 that associated with paxillin was not decreased compared to isotype control. These results both suggested that although both paxillin and leupaxin associated with Pyk2 in CTL, the leupaxin-Pyk2 complex appeared to be distinct from the paxillin-Pyk2 complex.

3.2.6. Leupaxin shows variable colocalization with the MTOC compared to paxillin in CTL

Previous studies from our lab indicated that clone F245 and F298 recognized Pyk2 populations exhibited different localization in T cells and macrophages [196]. The F245 recognized Pyk2 associated with paxillin and colocalized with the MTOC, whereas the F298 recognized Pyk2 did not associate with paxillin and did not go to the MTOC [196]. As leupaxin associated with both F245 and F298 recognized Pyk2 populations, I wondered whether leupaxin showed different localization from paxillin in CTL. In order to answer the question, CTL clone 11 cells were co-transfected with either GFP-paxillin and mCherry-tubulin or GFP-leupaxin and mCherry-tubulin. Twenty-four hours later, the cells were transferred to ICAM-1 coated coverglass and live cell imaging was acquired by spinning disk confocal microscopy. As shown in **Figure 3.6A**, GFP-paxillin

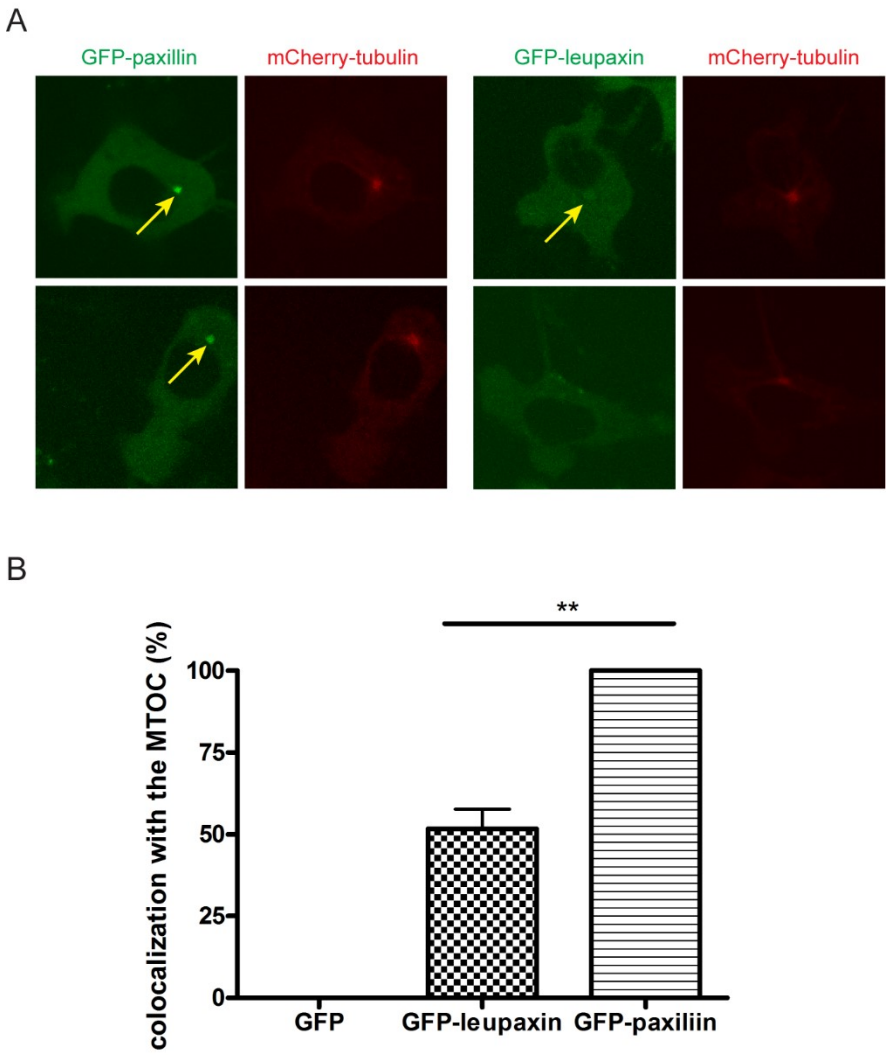

Figure 3.6. Leupaxin shows variable colocalization with the MTOC compared to paxillin in CTL. (A) CTL clone 11 were transfected with either GFP-paxillin and mCherry-tubulin or GFP-leupaxin and mCherry-tubulin. Twenty-four hours after transfection, cells were transferred to chambered coverglass which was coated with ICAM-1. The migrating cells were imaged by spinning disk confocal microscopy and a projection of the merged optical sections is shown. The arrows point to the MTOC. (B) Quantification of the transfected cells which showed colocalization of GFP proteins with the MTOC. At least 60 cells were captured for each group from three independent transfections. All experiments were performed three times, and representative data are shown. The unpaired student *t*-test was used with 95% confidence intervals where ** indicates $p < 0.01$. The error bar represents standard error of the mean.

showed very strong colocalization with the MTOC. However, for the GFP-leupaxin transfected clone 11, not all the cells exhibited colocalization with the MTOC. Quantification of the transfected cells showed that only 50% of GFP-leupaxin transfected cells showed colocalization with the MTOC, whereas all GFP-paxillin transfected cells showed the colocalization **(Figure 3.6)**. This showed that paxillin and leupaxin did not have different localization at the MTOC. My biochemistry result **(Figure 3.5)** shows that leupaxin associates with both F245 and F298 recognized Pyk2 species, whereas paxillin only associates F245 recognized Pyk2. In addition, our lab has previously shown that F245 recognized Pyk2 goes to MTOC whereas F298 recognized Pyk2 does not go to MTOC [196]. Based on these results, I proposed that leupaxin had at least two populations in CTL: one population associated with F298 recognized Pyk2 which did not go to the MTOC; the other leupaxin population associated with F245 recognized Pyk2 which colocalized with the MTOC. It is possible that these two leupaxin populations could translocate to each other, making it more dynamic than paxillin at the MTOC.

3.2.7. Leupaxin is more dynamic than paxillin at the MTOC

In order to determine whether leupaxin localization is more dynamic than paxillin at the MTOC, I performed fluorescence recovery after photobleaching (FRAP). Clone 11 cells were transfected with either GFP-paxillin or GFP-leupaxin. Twenty-four hours after transfection, cells were transferred to coverglass, which was coated with ICAM-1. As shown in **Figure 3.7A**, both paxillin and leupaxin accumulated at the MTOC. The MTOC was photobleached by the laser, followed by capturing images at every second to measure the fluorescence recovery. After

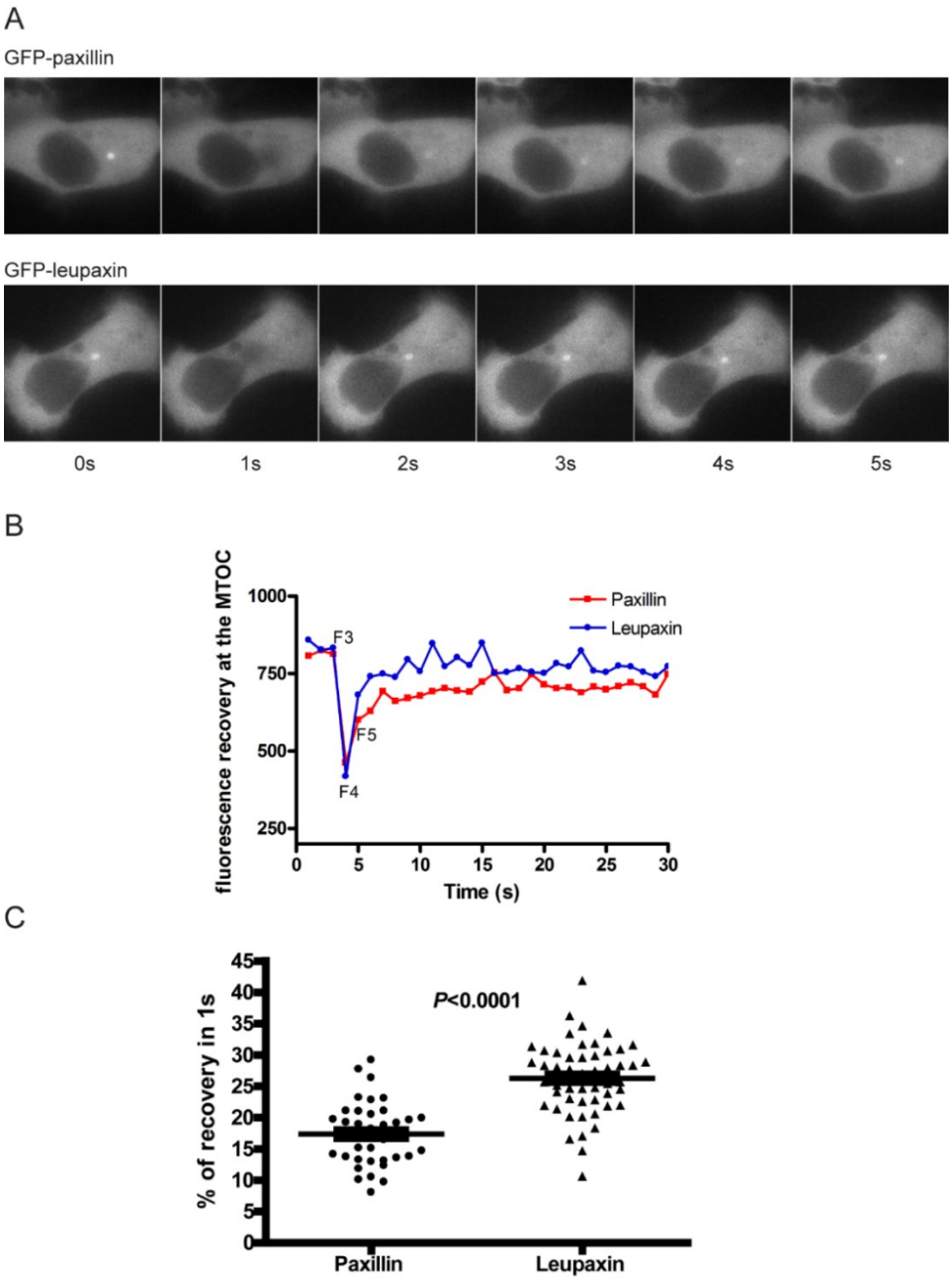

Figure 3.7. Leupaxin is more dynamic than paxillin at the MTOC. (A) CTL clone 11 were transfected with either GFP-paxillin or GFP-leupaxin. The MTOC was photobleached by the laser, followed by measuring fluorescence recovery at the MTOC. Images were captured every second. (B) Fluorescence recovery was tracked at the MTOC before and after photobleaching. F3, F4, F5 represents the fluorescence before, during and 1 second after photobleaching. (C) The percentage of fluorescence recovery 1 second after photobleaching was calculated by (F5-F4)/F3. At least 60 cells were analyzed for each group. All experiments were performed three times, and representative data are shown. The unpaired student *t*-test was used with 95% confidence intervals. The error bar represents standard error of the mean.

photobleaching, the fluorescence intensity at the MTOC recovered gradually. However, GFP-leupaxin recovery was faster than GFP-paxillin. To quantify the degree of fluorescence recovery, I measured the percentage of fluorescence recovery one second after photobleaching **(Figure 3.7B)**. Compared to paxillin which only recovered around 17% of fluorescence intensity within one second, leupaxin recovered approximately 27% of fluorescence intensity **(Figure 3.7C)**. Therefore, these FRAP data confirmed our hypothesis that leupaxin was more dynamic than paxillin at the MTOC.

3.2.8. Leupaxin is recruited to focal adhesion-like structures during CTL migration on ICAM-1

Leupaxin is recruited to focal adhesions in adherent cells [148, 162]. Leupaxin domain truncations indicated that LIM3 domain is essential for targeting leupaxin to the focal adhesions and this is consistent with paxillin [147, 148, 197]. I first confirmed that both paxillin and leupaxin were recruited to focal adhesions. Fibroblast cell line NIH 3T3 cells were co-transfected with GFP-paxillin and DsRed-leupaxin and imaged by spinning disk confocal microscopy. Leupaxin colocalized with paxillin at the focal adhesions **(Figure 3.8A)**. Compared to fibroblasts which migrate very slowly, the leukocytes can migrate up to 30 um/min [29, 128, 130]. Although leukocytes do not form the traditional focal adhesions and lack the actin stress fibers, both GFP-paxillin and mCherry-leupaxin were recruited to the contact zone **(Figure 3.8A)**. The contact surface was captured by total internal reflection fluorescence microscopy (TIRF) when CTL clone 11 were migrating on ICAM-1. The focal adhesion-like structures were assembled at the

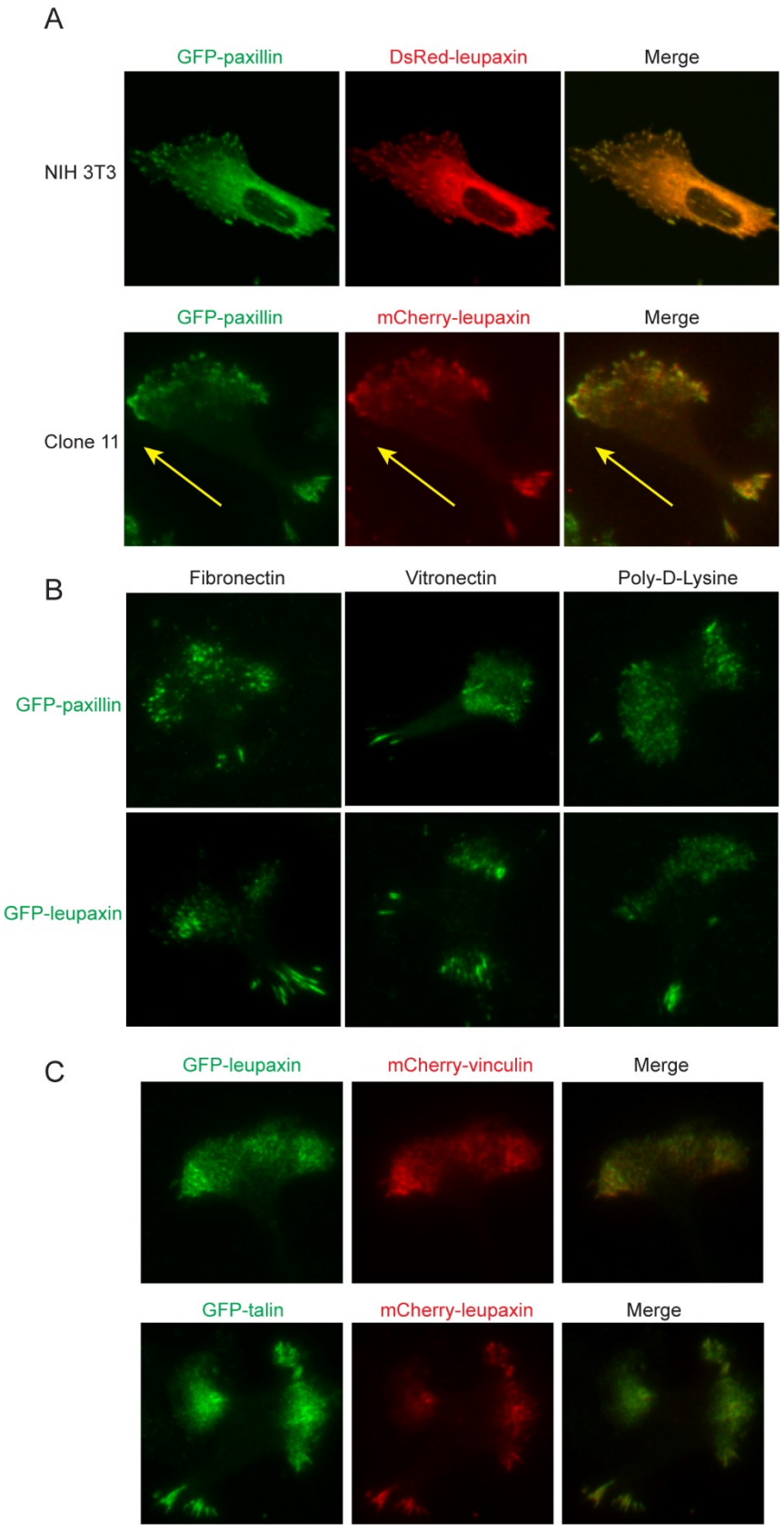
A
GFP-paxillin
DsRed-leupaxin
Merge
NIH 3T3
GFP-paxillin
mCherry-leupaxin
Merge
Clone 11
B
Fibronectin
Vitronectin
Poly-D-Lysine
GFP-paxillin
GFP-leupaxin
C
GFP-leupaxin
mCherry-vinculin
Merge
GFP-talin
mCherry-leupaxin
Merge

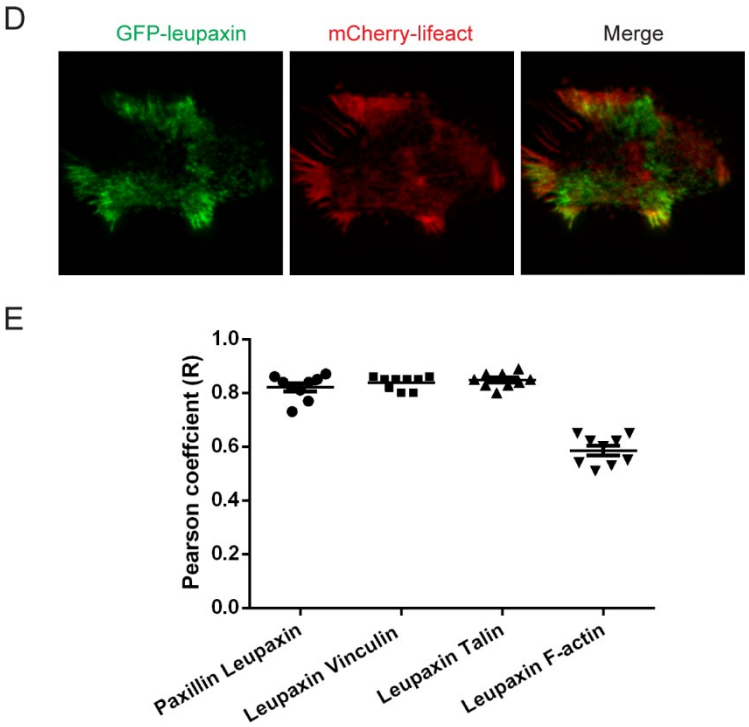

Figure 3.8. Leupaxin is recruited to the focal adhesion-like structures during CTL migration on ICAM-1. (A) NIH 3T3 cells were transfected with GFP-paxillin and DsRed-leupaxin. Twenty-four hours after transfection, cells were transferred to coverglass coated with fibronectin. Cells were then fixed with 4% paraformaldehyde and imaged by spinning disk confocal microscopy. Similarly, CTL clone 11 were transfected with GFP-paxillin and mCherry-leupaxin. Cells were harvested 24 hours after transfection, and transferred to chambered coverglass coated with ICAM-1. Live cells migrating on ICAM-1 were imaged by total internal reflection microscopy (TIRF). (B) CTL clone 11 were transfected with either GFP-paxillin or GFP-leupaxin. Cells were seeded in chambered coverglass which was coated with the indicated substrates. The contact surface was captured by TIRF during CTL migration. (C) Clone 11 cells were transfected with either GFP-leupaxin and mCherry-vinculin or GFP-talin and mCherry-leupaxin. Cells were transferred to chambered coverglass coated with ICAM-1. (D) Clone 11 cells were transfected with GFP-leupaxin and mCherry-lifeact and live cells migrating on ICAM-1 were imaged by TIRF. (E) Pearson coefficient corresponding to cells taken in three independent experiments was calculated by Fiji imageJ. A total of 60 cells were captured from three independent experiments, and representative images are shown.

leading edge, then disassembled at the trailing edge during CTL migration. Interestingly, previous studies suggested that the intermediate affinity LFA-1 localized at the leading edge, and the high-affinity LFA-1 localized at the central focal zone in T cells [132, 133]. This is different from the classical focal adhesions, in which paxillin and leupaxin connect the high-affinity integrin to the actin cytoskeleton at this area [108, 192, 198]. As the focal adhesion-like structures are only assembled at the leading edge and absent at the focal zone, this suggests CTL use intermediate-affinity LFA-1 to form the adhesive complexes and to maintain the high motility. Although paxillin and leupaxin colocalized with each other at the focal adhesion-like structures, our biochemistry data **(Figure 3.5B)** showed that they did not associate with each other.

Besides LFA-1, CTL also express integrins αVβ3 which are able to recognize fibronectin and vitronectin [199]. When CTL migrated on immobilized fibronectin or vitronectin, they also formed focal adhesion-like structures at the leading edge, whereas they were absent at the focal zone **(Figure 3.8B)**. These data suggested that CTL formed focal adhesion-like structures at the leading edge while migrating on fibronectin and vitronectin.

In addition to paxillin family proteins, vinculin and talin are focal adhesion proteins which connect the integrin to the actin network. Binding of talin to the integrin cytoplasmic tail leads to integrin clustering and activation [200-202]. As shown in **Figure 3.8C**, both vinculin and talin were also recruited to focal adhesion-like structures and colocalized with leupaxin. Hogg lab has demonstrated that talin colocalized with the high-affinity LFA-1 at the focal zone, the center of the contact

surface during T cell migration on ICAM-1 [132]. My data suggested that instead of localizing at the focal zone, talin was distributed at the leading edge, which was also consistent with a recent paper [203]. Compared to vinculin and talin, F-actin only showed partial colocalization with leupaxin **(Figure 3.8D)**. This suggests that the focal adhesion-likes structures are different from the classical focal adhesions that connect the filamentous actin.

3.2.9. Leupaxin is recruited to the focal adhesion-like structures at the contact zone by the LIM2-3 domains

Paxillin LIM3 domain is critical for the recruitment to focal adhesions in fibroblasts [147]. Consistent with paxillin, leupaxin LIM3 was identified as the major determinant for focal adhesion targeting in NIH 3T3 cells [148]. I mapped the leupaxin domains required for focal adhesion-like structure targeting in CTL. Leupaxin N-terminal LD domains and C-terminal LIM domains alone were first constructed and transfected into clone 11 cells **(Figure 3.9A)**. When LIM domains were deleted from the full-length leupaxin, the adhesive structures were no longer detected by TIRF, suggesting that C-terminal LIM domains were required for focal adhesion-like structure targeting. Next, LIM domains were deleted sequentially from the full-length leupaxin. When LIM2-3 domains were truncated, leupaxin failed to accumulate at the focal adhesion-like structures **(Figure 3.9B&C)**. Thus, consistent with previous studies in adherent cells, the LIM2-3 domains were critical for targeting leupaxin to the focal adhesion-like structures.

Since I deleted the leupaxin LIM2-4 segment, this domain deletion could also disrupt the leupaxin protein structure making it unable to bind to its

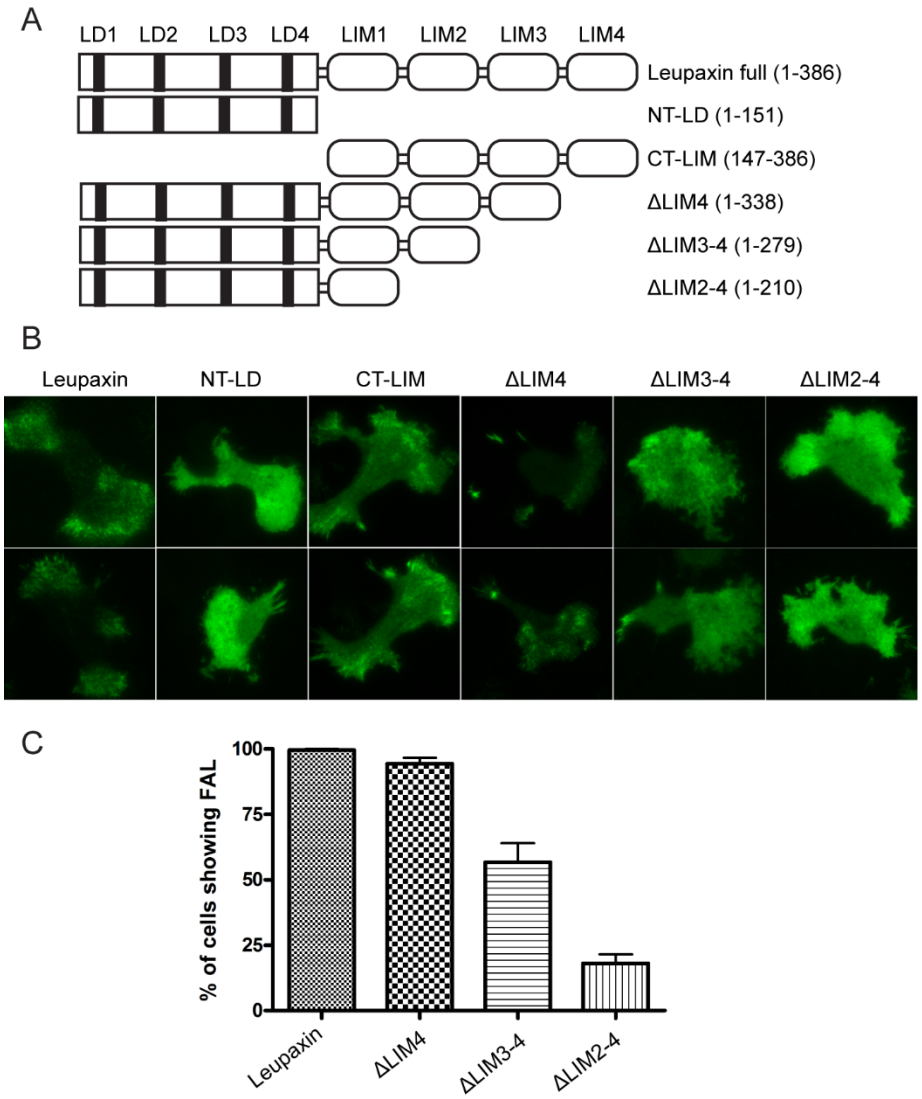

Figure 3.9. Leupaxin is recruited to the focal adhesion-like structures at the contact zone by the LIM2-3 domains. (A) Various leupaxin truncations were constructed into EGFP-C1 plasmids. (B) The indicated leupaxin constructs were transfected into CTL clone 11. The transfected cells were transferred to chambered coverglass coated with ICAM-1. The contact surface was captured by TIRF during CTL migration. (C) The transfected cells which still formed the dynamic focal adhesion-like structures were quantified. A total of 60 cells were captured from three independent experiments, and representative images are shown. The error bar represents standard error of the mean.

partner responsible for recruiting leupaxin to the focal adhesion-like structures. One way to confirm the role of LIM2-3 domain is to generate the leupaxin LIM 2-3 domain segment and determine whether it is sufficient for the recruitment of leupaxin to the focal adhesion-like structures. Since my results were consistent with a previous publication [162], I conclude that the leupaxin LIM2-3 domains are important for focal adhesion-like structure targeting.

3.2.10. Overexpression of leupaxin in clone 11 reduces CTL migration velocity on ICAM-1

The contribution of leupaxin in cell adhesion and migration has been studied in several literature in adherent cells. Knockdown of leupaxin expression by siRNA in prostate cancer cell lines PC-3 and DU 154 cells decreased cell adhesion and spreading on fibronectin [140, 159], suggesting a role of leupaxin in stimulating cell adhesion and migration. On the contrary, overexpression of leupaxin in a fibroblast cell line, NIH 3T3 cells, inhibited cell spreading on fibronectin, suggesting a role of leupaxin in suppressing adhesion and spreading [148]. Paxillin family proteins, especially leupaxin, have been shown to be upregulated, hyperphosphorylated and linked to malignant progression in a variety of cancers, including breast cancer and prostate cancer [143, 204-209]. Thus, the studies mentioned above may not accurately represent the physiological condition in primary cells.

To determine whether leupaxin regulates CTL migration, I overexpressed GFP-leupaxin in CTL clone 11 via nucleofection. Twenty-four hours after transfection, cells were placed on ICAM-1 and the non-directional CTL migration

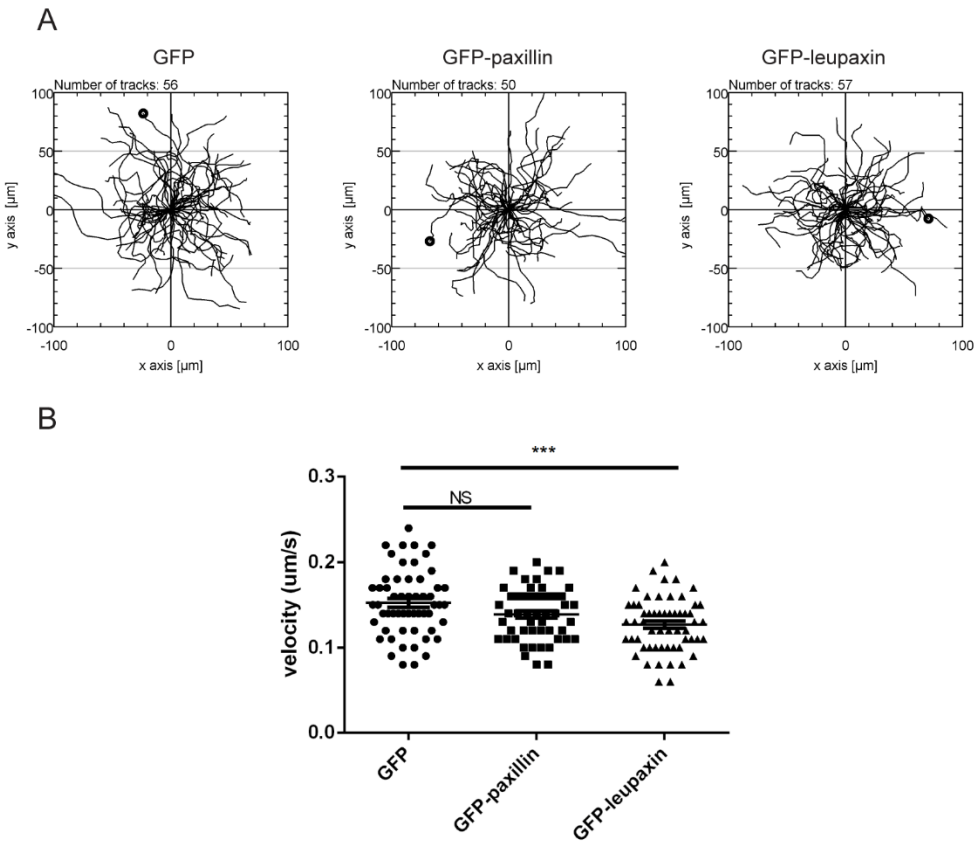

Figure 3.10. Overexpression of leupaxin in clone 11 reduces CTL migration velocity on ICAM-1. (A) CTL clone 11 were transfected with GFP, GFP-paxillin or GFP-leupaxin. Twenty-four hours after transfection, cells were collected and transferred to chambered coverglass coated with ICAM-1. The migrating cells were tracked for 10 minutes with the time interval of 30 seconds between images. The migration patterns of the transfected cells were analyzed by ImageJ. (B) The velocity of migrating cells above were measured by ImageJ. At least 50 cells were analyzed for each group. All experiments were repeated three times. One-way ANOVA was used for statistical analysis with Dunnett's multiple comparisons test result shown. NS and *** represent no significant difference and $p < 0.001$. The error bar represents standard error of the mean.

was captured by spinning disk confocal microscopy. The cell migration video was a duration of 10 minutes and cell migration was analyzed by manual tracking function of ImageJ. As shown in **Figure 3.10A**, all the analyzed cells were pooled together, and the average migration velocity was calculated. Overexpression of paxillin or leupaxin reduced cell migration velocity on ICAM-1.

3.2.11. Overexpression of paxillin or leupaxin in NIH 3T3 cells increases cell spreading on fibronectin

Dr. Samuel Cheung overexpressed leupaxin in *ex vivo* activated OT-1 CTL and it increased CTL spreading on ICAM-1, suggesting that leupaxin promoting cell adhesion and spreading. This is contradictory to previous studies in NIH 3T3 cells. To verify the role of leupaxin in adherent cells, I overexpressed paxillin or leupaxin in NIH 3T3 cells. After overexpression, cells were plated on fibronectin and the cell area was measured by ImageJ. As shown in **Figure 3.11**, GFP-paxillin or GFP-leupaxin was expressed in NIH 3T3 cells. Both paxillin and leupaxin were exported from the nucleus, which was consistent with a previous study that the LD domains contained the nuclear export sequence [186]. Overexpression of either paxillin or leupaxin increased NIH 3T3 cell spreading on fibronectin, indicating that both paxillin and leupaxin promoted cell spreading in adherent cells.

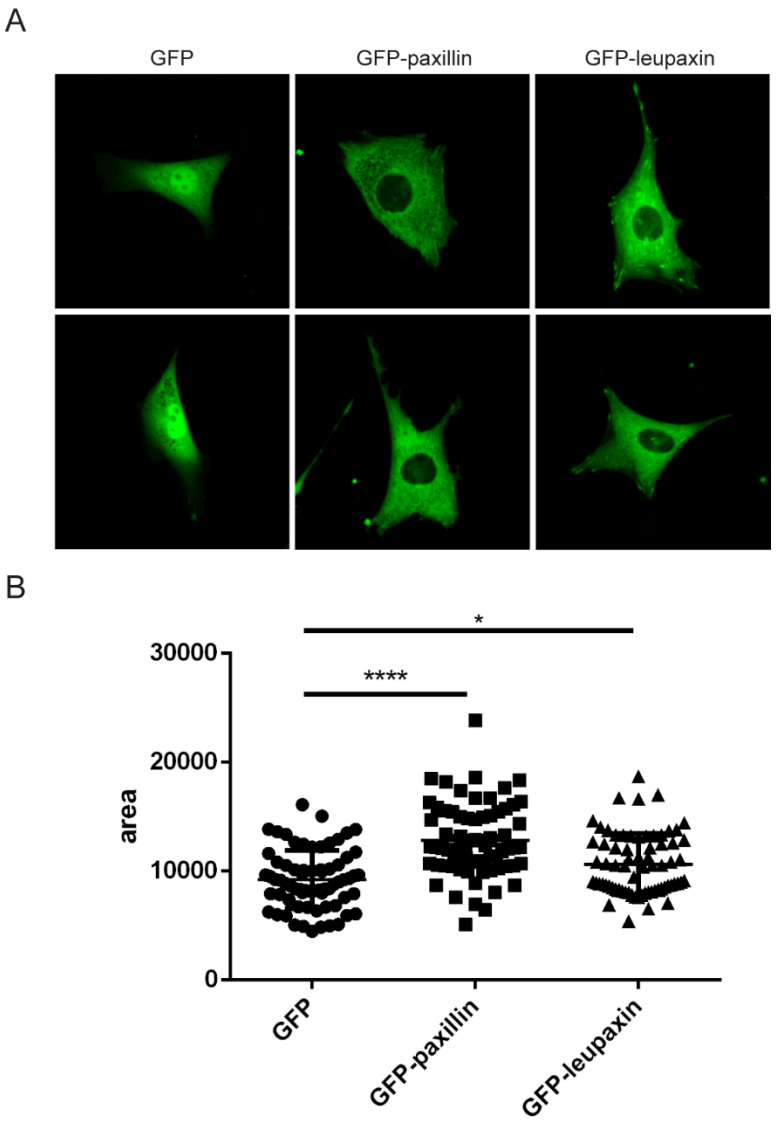

Figure 3.11. Overexpression of paxillin or leupaxin in NIH 3T3 cells increases cell spreading on fibronectin. (A) NIH 3T3 cells were transfected with either GFP, GFP-paxillin or GFP-leupaxin. Twenty-four hours after transfection, cells were collected and seeded in chambered coverglass which was coated with fibronectin. After incubation in 37^{o}C for 30 minutes, cells were fixed with 4% paraformaldehyde. Images were collected by spinning disk confocal microscopy. (B) The area of NIH 3T3 cells collected above was measured by ImageJ. At least 60 cells were selected and analyzed for each group from three independent transfections. All experiments were performed three times independently, and representative images are shown. One-way ANOVA was used for statistical analysis with Dunnett's multiple comparisons test result shown. * and **** represent $p < 0.05$ and $p < 0.0001$. The error bar represents standard error of the mean.

3.3. Discussion

In this chapter, I studied the molecular regulation of leupaxin in the LFA-1 signaling in CTL and the distribution of leupaxin during CTL migration. I have demonstrated that leupaxin showed tyrosine phosphorylation in response to integrin stimulation by anti-LFA-1 antibody **(Figure 3.3)**. The tyrosine phosphorylation was dependent on the FAK family kinase Pyk2 **(Figure 3.4)**. I found that leupaxin associated equally with both F245 recognized Pyk2 and F298 recognized Pyk2 whereas paxillin only associated with F245 recognized Pyk2 **(Figure 3.5)**. In addition, I showed that leupaxin was more dynamic than paxillin at the MTOC **(Figure 3.6)**. Although leukocytes do not have actin stress fibers and focal adhesions, I found that the focal adhesion proteins, such as paxillin, leupaxin, vinculin and talin were recruited to the contact zone during CTL migration on the ICAM-1. These focal adhesion-like structures were assembled at the leading edge, and disassembled at the trailing edge, to maintain the high motility of CTL. When I overexpressed leupaxin in clone 11, CTL reduced cell migration, suggesting that it may promote cell adhesion to ICAM-1.

Compared to the other two paxillin family members, the study of leupaxin has been progressed very slowly. One reason is the lack of available commercial anti-leupaxin antibodies. Dr. Lipsky, the author of the first leupaxin paper, has generated the anti-leupaxin monoclonal antibody and has been used in the following studies [159, 163, 190, 195]. All of the studies which used the anti-leupaxin monoclonal antibody can only detect a single leupaxin band, no matter in adherent cells, osteoclasts, B cell line A20 cells and BJAB cells [162, 163, 186, 187,

190]. However, two leupaxin bands were detected in both resting CTL and A20 cells with the polyclonal anti-leupaxin antibody I developed. More interestingly, only the lower leupaxin band was detected in naïve $CD8^+$ T cells. This suggested that leupaxin may undergo post-translational modification after naïve $CD8^+$ T cell activation. In addition, it also indicated that my leupaxin antibody and Dr. Lipsky's leupaxin antibody might recognize different leupaxin species.

Although leupaxin has been shown to have alternative splicing (Immunological Genome Project), this shift is not predicted to be due to different leupaxin isoforms based on available data. Confirmation of this is that when I transfected GFP-leupaxin into A20 cells and clone 11, two leupaxin bands were also detected by GFP blot. I predicted the potential SUMOylation sites in leupaxin by GPS-SUMO software [210]. The result showed that leupaxin had a very low possibility of being sumoylated. Paxillin blot has also been shown to have two bands [211]. When integrin signaling was stimulated, it shifted further, which was caused by serine/threonine phosphorylation [212]. One explanation for the existence of two leupaxin bands in resting CTL is that leupaxin undergoes a basal level of serine/threonine phosphorylation. This will be determined by phosp-tag SDS-PAGE in the future experiment.

Consistent with previous studies, I found that leupaxin associated with Pyk2 in CTL [152, 187]. The molecular weight of leupaxin is very close to the IgG heavy chain, which makes it impossible to detect the endogenous leupaxin after Pyk2 immunoprecipitation as the anti-Pyk2 serum contains lots of immunoglobulins. To circumvent this problem, I transfected the clone 11 with GFP-leupaxin which would

allow us to separate it from IgG heavy chain. In addition to transfection, I also performed leupaxin immunoprecipitation in clone 11 and clone AB.1 cell lysates, and the endogenous Pyk2 was detected to associate with leupaxin **(Figure 3.5B)**. Compared to paxillin which mainly associated with F245 recognized Pyk2, I found that leupaxin associated with both F245 and F298 recognized Pyk2 populations **(Figure 3.5A)**. The reason for the different association pattern of paxillin and leupaxin with Pyk2 was unknown. Another difference between the two Pyk2 species was that F298 recognized Pyk2 exhibited hyperphosphorylation [196]. Consistent with a previous study showing that the binding affinity of leupaxin to Pyk2 was three-fold higher than that of paxillin [152, 153]. Although the specific phosphorylated sites on Pyk2 were not identified, this may reduce the binding affinity between the two proteins, and paxillin could not bind to Pyk2 anymore as the binding affinity is much lower than leupaxin. Previous studies suggested that leupaxin might compete with paxillin for binding to Pyk2 [148, 162]. Pyk2 FAT domain contains two binding sites for LD motif, which made me question whether paxillin and leupaxin could bind to Pyk2 in one complex. My results suggested that leupaxin-Pyk2 complex was distinct from the paxillin-Pyk2 complex **(Figure 3.5B)**. However, I cannot rule out the possibility that paxillin and leupaxin may compete with each other for binding to Pyk2.

Compared with paxillin which always colocalized with the MTOC, leupaxin showed variable colocalization at the MTOC by live cell imaging **(Figure 3.6A)**. Indeed, the FRAP analysis demonstrated that leupaxin was more dynamic than paxillin at the MTOC. Pyk2 may contribute to the higher redistribution rate of

leupaxin at the MTOC. I proposed that there were at least two populations of leupaxin-Pyk2 complexes: one associated with F245 recognized Pyk2 and localized at the MTOC; another associated with F298 recognized Pyk2 and localized in the cytosol. This may allow leupaxin to transcolate between cytosol and the MTOC, thus making it more dynamic than paxillin [196].

The majority of studies about focal adhesions come from adherent cells which have actin stress fibers and produce very strong mechanical forces [213-215]. Compared to adherent cells which migrate very slow, leukocytes do not have stress fibers and traditional focal adhesions [29]. The weak traction forces in leukocytes may allow them to move with high speed. Interestingly, I observed that focal adhesion-like structures were formed when CTL were migrating on various substrates **(Figure 3.8)**, which were also recently identified in T cells [203]. Paxillin family proteins are used as markers for labeling focal adhesions. My data implies that these focal adhesion-like structures are assembled at the leading edge when T cells move forward and disassembled at the trailing edge. The canonical focal adhesion proteins, such as paxillin, vinculin and talin, were colocalized at the focal adhesion-like structures **(Figure 3.8)**. My results were supported by a recently published paper which showed a similar pattern of protein localization in T cells that the intermediate-affinity LFA-1 was enriched at the protrusions and paxillin colocalized with vinculin and talin at these adhesive structures [203]. It has been shown that the intermediate-affinity LFA-1 was distributed at the leading edge, whereas the high-affinity LFA-1 localized at the focal zone [132, 133]. As the focal adhesion-like structures were only formed at the leading edge, whereas absent at

the focal zone, the center of the contact surface. This was in contrast to the classical focal adhesions, which was characterized by the high-affinity integrin at the leading edge [216]. I speculate that the intermediate-affinity LFA-1 allows T cells to form faster and more dynamic adhesions, in order to obtain the fast migration.

Similar to the classical focal adhesions, I showed that leupaxin LIM 2-3 domains were required for leupaxin targeting to the focal adhesion-like structures **(Figure 3.9)** [162]. The majority of paxillin and leupaxin binding partners associated with them through N-terminal LD domain, so the proteins that bound to leupaxin LIM domains and recruited it to the focal adhesion-like structures were still unknown [137]. I performed a number of experiments to determine whether leupaxin was found in a complex with LFA-1 in CTL. However, no association was detected between leupaxin and LFA-1.

The majority of previous studies on leupaxin function were performed in tumor cells and lymphoma cell lines. However, the paxillin family members have all be linked to the malignancy of tumors, including breast cancer, prostate cancer, lung cancer and leukemia [143]. A previous study showed that overexpression of leupaxin in prostate cancer cells increased cell motility [209]. However, it was shown that MAPK, FAK and Pyk2 were significantly activated by RhoC in prostate cancer cells [217]. Furthermore, paxillin was overexpressed and promoted androgen receptor (AR)-mediated gene transcription by binding to AR in prostate cancer cells [218]. Abnormal expression of any paxillin family members or Pyk2 in tumor cells will change the downstream signaling pathway and affect tumor malignancy. Thus, previous studies carried out in tumor cells may not accurately

represent the physiological condition in primary cells. Our overexpression experiment showed that overexpression of leupaxin or paxillin reduced cell migration velocity on ICAM-1. Dr. Samuel Cheung overexpressed leupaxin in *ex vivo* activated OT-1 CTL and it increased CTL spreading on ICAM-1, suggesting that leupaxin promoting cell adhesion and spreading. This reduced migration was different from Pyk2 inhibition, in which the CTL cannot detach from the substrate at the trailing edge [154]. I speculate that T cells formed these adhesive structures to facilitate T cell adhesion and migration. Engagement of the intermediate-affinity LFA-1 recruited the focal adhesion proteins such as paxillin, leupaxin, vinculin, talin and Pyk2.

CHAPTER 4: Regulation of leupaxin phosphorylation in TCR signaling and the localization of leupaxin during CTL conjugation

4.1. Introduction

Activated $CD8^+$ T cells, or CTL, are critical in the elimination of intracellular pathogen-infected cells and transformed tumor cells. Engagement of TCR on CTL with the cognate MHC class I molecules on target cells triggers downstream signaling cascades which eventually lead to the killing of antigen-bearing target cells. Signals are initiated from the recognition of MHC I molecules, which induces a conformational change of CD3 subunits and then phosphorylation by the Src family kinase Lck [219]. Next, ZAP-70 is recruited to the phosphorylated ITAMs on the zeta chain via its SH2 binding domains [220, 221]. A number of kinases are sequentially recruited and activated, such as PLC-γ1, protein kinase C (PKC) and PI3K [222].

In addition to kinases, another group of signaling proteins that play important roles in TCR signaling are the adaptor proteins [223]. The majority of adaptor proteins do not possess enzymatic activities. Instead, they are involved in the TCR signaling by the recruitment and formation of multiple protein complexes, thus facilitating protein interaction and signal transmission. One of the essential adaptor proteins that is well-explored in T cell signaling is LAT (linker for activation of T cells) that forms a signalosome at the membrane during the early stage of TCR signaling. LAT contains a short extracellular region and cytoplasmic tail, which possesses ITAMs that are rapidly phosphorylated upon TCR stimulation [49]. The phosphorylated motifs further recruit and bind multiple SH2 containing

proteins, such as PLC-γ1, Grb2 and Gads, thus facilitating protein interaction and signal transduction [50, 224].

Paxillin family proteins are also a group of adaptor proteins that play important roles in integrin signaling. The function of paxillin family proteins has been intensively explored in adherent cells. However, their contribution in non-adherent cells, such as $CD8^+$ T cells is less studied. Our lab has previously demonstrated that paxillin was tyrosine phosphorylated in response to TCR stimulation and the phosphorylation was dependent on Src family kinase and Pyk2 kinase activity [169]. Paxillin localizes to the microtubule cytoskeleton and MTOC, and is recruited to the immunological synapse during CTL conjugation with the target cells [77]. In addition, paxillin has been shown to be involved in the degranulation process by promoting the MTOC reorientation in both CTL and NK cells [77, 106].

Compared to paxillin, leupaxin is preferentially expressed in the leukocytes [187]. Studies of adherent cells and certain cancer cells suggested that leupaxin may antagonize paxillin in integrin signaling [148, 162]. There have been two studies which examined the function of leupaxin in leukocytes. The first study showed that leupaxin was a negative regulator of the B cell receptor signaling [163]. They found that leupaxin was tyrosine phosphorylated upon BCR engagement, and leupaxin overexpression suppressed the phosphorylation of JNK, p38 and Akt in A20 cells [163]. Whether leupaxin performed the negative regulating function by antagonizing paxillin is unknown. In another study of leupaxin function performed

in NK cells, leupaxin has been shown to promote the MTOC reorientation and granule retention and this was similar to the role of paxillin in NK cells [106, 107].

Despite the fact that leupaxin is preferentially expressed in hematopoietic lineage cells [187], its function in CTL is completely unknown. In this chapter, I wanted to address the question of whether leupaxin was involved in TCR signaling, and if leupaxin was recruited to the immunological synapse during CTL conjugation with the target cells. I found that leupaxin was both tyrosine and serine phosphorylated upon TCR engagement. It was also recruited to the synapse when conjugating with the target cells, but the recruitment was mainly mediated by the LFA-1 signaling before activation of TCR signaling.

4.2. Results

4.2.1. Leupaxin is tyrosine phosphorylated and undergoes a mobility shift upon TCR stimulation

The Immunological Genome Project (http://www.immgen.org/) shows that leupaxin is strongly expressed in hematopoietic lineage cells, including $CD8^+$ T cells **(Figure 1.3)**. However, nothing is known about the contribution of leupaxin in $CD8^+$ T cells. As paxillin is both tyrosine and serine phosphorylated in TCR signaling [77, 169], I first examined whether leupaxin was tyrosine phosphorylated upon TCR engagement. The non-transformed CTL clone AB.1 were stimulated with the immobilized anti-CD3 antibodies for the indicated times, and the extent of total tyrosine phosphorylation from cell lysates was detected with anti-phosphotyrosine antibody 4G10 **(Figure 4.1A)**. As shown by 4G10 blot, CTL showed increased tyrosine phosphorylation after stimulation, with the overall phosphorylation reaching maximum level at 20 minutes after stimulation. Consistent with previous publication from our lab, robust tyrosine phosphorylated bands were detected at the positions around ~110 and 65 KDa [169]. These two bands are most likely Pyk2 and paxillin [168, 169], as both of the two proteins have been shown to be tyrosine phosphorylated and migrate in these positions on the SDS-PAGE gel.

Next, I immunoprecipitated the endogenous leupaxin from cell lysates which were stimulated with the immobilized anti-CD3 antibodies as above. 4G10 blot indicated that leupaxin underwent robust tyrosine phosphorylation after anti-CD3 stimulation **(Figure 4.1B)**. Although the total tyrosine phosphorylation started

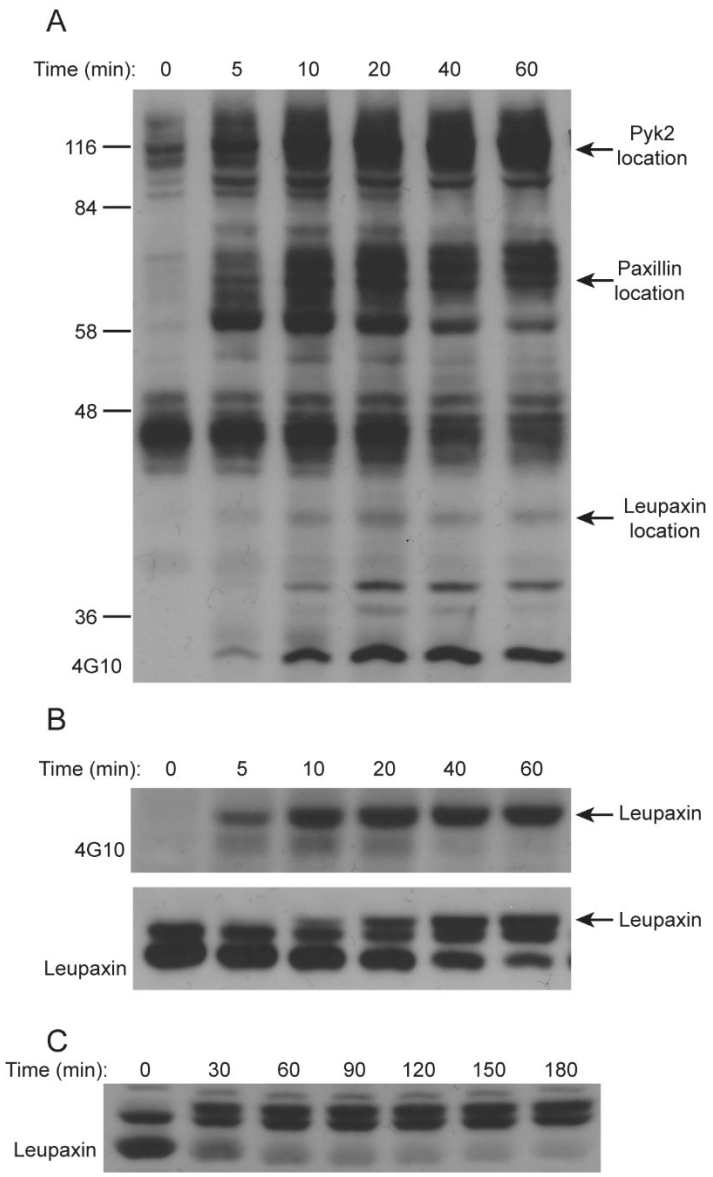

Figure 4.1. Leupaxin is tyrosine phosphorylated and undergoes a mobility shift upon TCR stimulation. (A) Clone AB.1 cells were stimulated with the immobilized anti-CD3 antibody for the indicated time points. Cells were lysed by 1% NP-40 lysis buffer. Cell lysates from 4×10^5 cells were separated by SDS-PAGE, followed by transferring to PVDF membrane. Phosphorylated proteins were detected with 4G10 antibody. (B) Clone AB.1 were stimulated as above for various times. Leupaxin was immunoprecipitated from cell lysates and proteins were separated by SDS-PAGE. Immunoblot was probed with clone 4G10 antibody followed by stripping and reprobed with anti-leupaxin antibody. (C) Experiment was performed similar as (B) except cell lysates were detected with anti-leupaxin antibody. All experiments were performed three times, and representative data are shown.

to decrease at 20 minutes after stimulation, the level of leupaxin tyrosine phosphorylation remained stable during the entire stimulation period. Determination of leupaxin phosphorylation in A20 cells were performed by stimulation with soluble anti-IgM antibodies [163], which showed that tyrosine phosphorylation of leupaxin reached the maximum level at 15 minutes after stimulation, and then quickly returned to the basal level along with the decrease of the BCR signaling. However, this is the first evidence showing that leupaxin is strongly tyrosine phosphorylated upon TCR engagement in non-transformed CTL clones.

In addition to the tyrosine phosphorylation, leupaxin exhibited a mobility shift upon TCR engagement as shown by leupaxin blot **(Figure 4.1B)**. A third leupaxin band began to appear at 10 minutes after stimulation concurrent with a gradual decrease of the two leupaxin basal bands. The mobility shift reached the maximal level at 60 minutes after stimulation. Even when I stimulated the CTL with immobilized anti-CD3 antibodies for up to three hours, the mobility shift remained stable **(Figure 4.1C)**. Interestingly, paxillin has been shown to exhibit mobility shift upon TCR engagement [169]. It has been demonstrated that the gel retardation of paxillin was caused by serine or threonine phosphorylation, as treatment of paxillin with alkaline phosphorylation removed the shift [211]. This rapid and sustained tyrosine phosphorylation followed by a gradual increase in mobility shift has not been shown in previous studies. This is the first examination of leupaxin phosphorylation in non-transformed cells. The possible reason why leupaxin mobility shift was not detected before was due to the use of different

leupaxin antibodies. Thus, my data showed the first time that leupaxin underwent tyrosine phosphorylation upon TCR engagement in CTL, and exhibited a mobility shift which has not been identified before.

4.2.2. Leupaxin tyrosine phosphorylation is dependent on Pyk2 and the mobility shift is dependent on Pyk2 and ERK

In the last chapter, I have shown that tyrosine phosphorylation of leupaxin upon LFA-1 stimulation was dependent on Pyk2 and Src family kinase activity. Similar to LFA-1 stimulation, leupaxin tyrosine phosphorylation upon anti-CD3 stimulation was also dependent on Pyk2 and Src family kinase. As shown in **Figure 4.2**, inhibition of Pyk2 and Src family kinase by the corresponding inhibitors prevented leupaxin tyrosine phosphorylation upon anti-CD3 antibody stimulation. It was possible that the anti-CD3 stimulated leupaxin phosphorylation was also a result of LFA-1 activation, and initiation of the Lck-Pyk2-leupaxin signaling in the 'outside-in' pathway. In addition to tyrosine phosphorylation, leupaxin mobility shift was also dependent on Pyk2 and Src family kinase, suggesting that the potential serine/threonine phosphorylation was mediated by the signaling events downstream of Pyk2 and Src family kinase activity. TCR stimulated signaling can be replaced by the treatment of T cells with PMA and ionomycin. PMA leads to activation of serine/threonine kinase protein kinase C (PKC) and the following RasGRP-ERK signaling cascade [225, 226], while bypassing the TCR induced PI3K activation. Ionomycin is a potent calcium ionophore and activates Ca^{2+} dependent pathway. As shown in **Figure 4.2C**, treatment of clone AB.1 cells with either PMA alone or PMA and ionomycin resulted in leupaxin mobility shift,

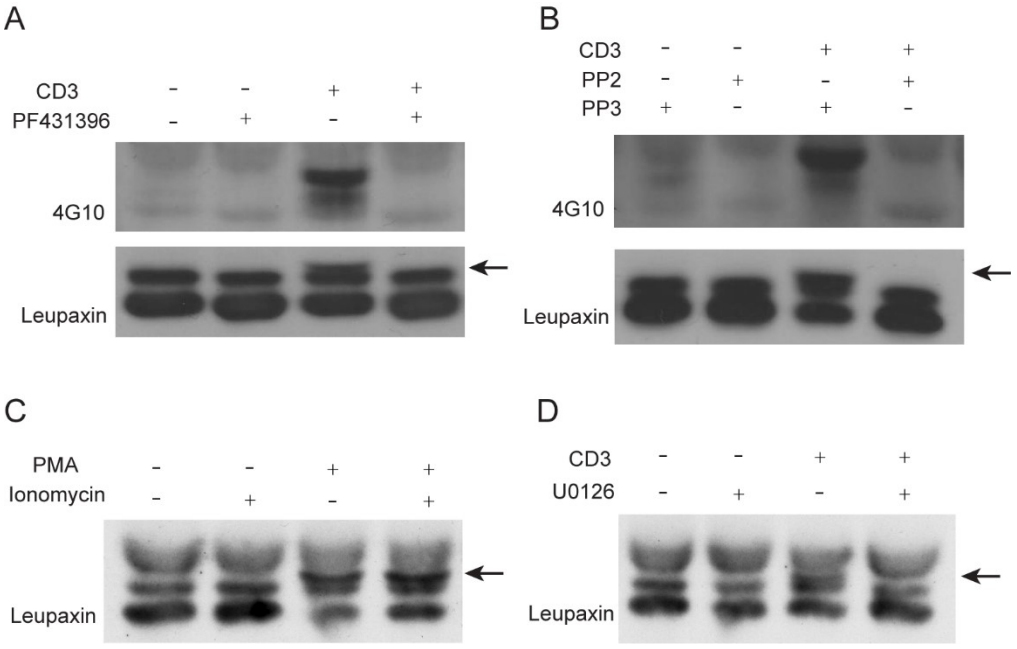

Figure 4.2. Leupaxin tyrosine phosphorylation is dependent on Pyk2 and the mobility shift is dependent on Pyk2 and ERK. (A) AB.1 were pre-treated with either carrier control or Pyk2 inhibitor PF431396 (5 μM) for 1 hour, followed by stimulation with plate-bound anti-CD3 antibody for 20 minutes. Lysates of 10 million cells were immunoprecipitated with anti-leupaxin antibody, followed by SDS-PAGE and transfer. Immunoblots were probed with 4G10 antibody, then stripped and re-probed with anti-leupaxin antibody. (B) AB.1 were pre-treated with either control PP3 or Src kinase inhibitor PP2 (10 μM) on ice for 15 minutes, followed by stimulation as above. Proteins were detected with clone 4G10 and anti-leupaxin antibodies. (C) AB.1 were stimulated with PMA (100 ng/ml) and ionomycin (2 μM) for 20 minutes. Cells were lysed by 1% NP-40 lysis buffer followed by leupaxin immunoprecipitation. The immunoblot was probed with anti-leupaxin antibody. (D) AB.1 were pre-treated with MEK inhibitor U0126 (10 μM) for 30 minutes, followed by stimulation with anti-CD3 antibody as above. Leupaxin was immunoprecipitated and probed as above. All experiments were performed three times, and representative data are shown.

implying that the leupaxin molecular weight shift was dependent on ERK activity. Previous investigations have demonstrated that paxillin mobility shift was dependent on the TCR-stimulated RasGRP-MEK-ERK pathway [188]. I treated clone AB.1 cells with MEK inhibitor U0126, followed by stimulation with anti-CD3 antibodies for 20 minutes. leupaxin mobility shift was no longer detected **(Figure 4.2D)**. Thus, similar to paxillin, leupaxin mobility shift was dependent on the RasGRP-MEK-ERK signaling pathway. Together, these data implied that leupaxin was both tyrosine and serine phosphorylated upon TCR engagement and both were dependent on Pyk2 and Src family kinase activity.

4.2.3. Leupaxin mobility shift is mediated by the serine phosphorylation at Ser54

Based on previous publications of paxillin [211], I hypothesized that the leupaxin mobility shift was a result of serine/threonine phosphorylation, a possibility I wanted to explore through mutational analysis. To focus on the relevant domain, I first transfected cells with leupaxin individual domains. As the CTL clones were difficult to obtain a high level of transfection, I used the A20 cell line for transfection with various leupaxin mutants. A20 cells were first transfected with GFP-leupaxin, GFP-leupaxin-NT LD domains (amino acids 1-151) or GFP-leupaxin-CT LIM domains (amino acids 147-386). Twenty-four hours after transfection, cells were stimulated with PMA for 20 minutes, and lysed in 1% NP-40 lysis buffer. Cell lysates were loaded to SDS-PAGE, followed by immunoblot with the anti-GFP antibody. As shown in **Figure 4.3A**, the full-length GFP-leupaxin and GFP-leupaxin-LD domain exhibited the mobility shift after PMA

stimulation, whereas the GFP-leupaxin-LIM domain did not show the mobility shift when LD domains were deleted from the full-length protein. This result implied that the potential serine/threonine phosphorylation sites were in the N-terminal LD domains. Next, I performed similar experiments by transfecting A20 cells with the following constructs: GFP-leupaxin-LD1Δ, GFP-leupaxin-LD2Δ, GFP-leupaxin-LD3Δ, GFP-leupaxin-LD4Δ. GFP blot showed that when LD1 or LD2 domain was deleted, the mobility shift was no longer detected, suggesting that the potential serine/threonine phosphorylation sites were in LD1-2 segment **(Figure 4.3B)**.

In order to map the serine/threonine phosphorylation sites, I predicted the ERK-dependent phosphorylation sites by two online tools: NetPhos 2.0 (http://www.cbs.dtu.dk/services/NetPhos/) and KinasePhos 2.0 (http://kinasephos2.mbc.nctu.edu.tw/). The prediction results suggested high values of phosphorylation at the following residues: Ser19, Ser34, Ser54 and Ser73. These residues were mutated into alanines and transfected into A20 cells, which were then stimulated with PMA to induce the mobility shift. The results demonstrated that leupaxin containing all the serine mutations exhibited a molecular weight shift except the Ser54 mutation **(Figure 3C)**. This suggested that the leupaxin mobility shift was mediated by a single phosphorylation at Ser54. In order to confirm that leupaxin molecular weight shift in non-transformed CTL was also caused by the phosphorylation at Ser54, this Ser54A mutant was transfected into CTL clone 11 by nucleofection, followed by immunoprecipitation with anti-GFP antibodies. As shown in **Figure 4.3D**, GFP blot confirmed that the mobility shift of leupaxin was also mediated by the Ser54 phosphorylation. Thus, my data demonstrated

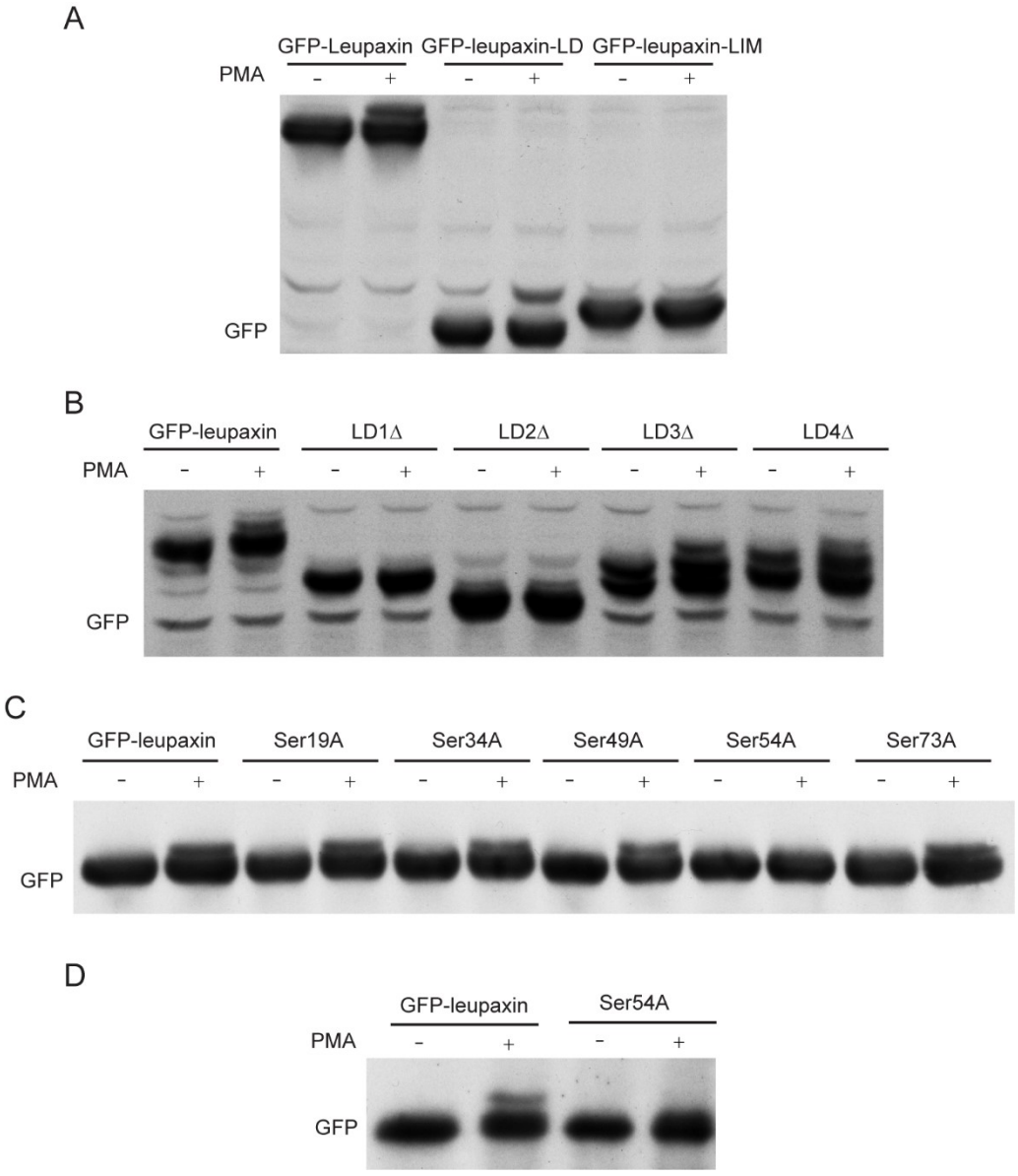

Figure 4.3. Leupaxin mobility shift is mediated by the serine phosphorylation at Ser54. (A) to (C) A20 cells were transfected with the indicated leupaxin constructs. At 24 hours post-transfection, cells were stimulated with PMA (100 ng/ml) for 20 minutes. Cell lysates from 4×10^5 cells were separated by SDS-PAGE. The membrane was probed with anti-GFP antibody to detect the mobility shift of leupaxin. (D) Clone 11 cells were transfected with the indicated constructs. Twenty-four hours after transfection, cells were stimulated with PMA for 20 minutes. Proteins were immunoprecipitated with anti-GFP antibody, followed by SDS-PAGE, transfer and immunoblot. All experiments were performed three times except (D), which was performed once, and representative data are shown.

that the mobility shift of leupaxin was mediated by a single serine phosphorylation at Ser54 in CTL. In addition, another possibility is that phosphorylation at Ser54 leads to the recruitment of a leupaxin binding partner that initiates the following leupaxin phosphorylation and the mobility shift. As leupaxin binding partners are largely unknown, this will be addressed in the future by mass spectrometry or yeast two-hybrid system to identify the potential binding partners.

4.2.4. Leupaxin is recruited to the immunological synapse in CTL when conjugated with the target cells

LFA-1 is not only involved in T cell adhesion and migration, but also participates in CTL function by forming the immunological synapse and providing costimulatory signals for TCR activation [84, 227]. In addition, the 'outside-in' signals provided by LFA-1 engagement with ICAM-1 lead to the cytoskeleton reorganization and lytic granule polarization during NK cell degranulation [107, 228]. Paxillin has been shown to function as a cytoskeletal adaptor protein in LFA-1 signaling and colocalize with the microtubule cytoskeleton and the immunological synapse in CTL [77, 188]. Next, I addressed the question of whether leupaxin was also recruited to the immunological synapse.

I performed the live cell imaging to characterize the distribution of leupaxin during CTL conjugation with the target cells for degranulation. Non-transformed clone 11 cells were transfected with either GFP, GFP-paxillin or GFP-leupaxin. Twenty-four hours later, the transfected CTL cells were collected and conjugated with the target cells L1210K^b/D^d, which were labeled with CellTracker blue. I only imaged the conjugates which demonstrated the MTOC reorientation, to make sure

that the cells I collected were real conjugates between CTL and the target cells. As shown in **Figure 4.4A**, both GFP-paxillin and GFP-leupaxin were accumulated at the interface between CTL and target cells. I have shown in the last chapter that paxillin exhibited strong colocalization with the MTOC, whereas leupaxin transfected cells showed variable colocalization with the MTOC **(Figure 3.6)**. When paxillin was recruited to the interface between CTL and target cells, it still demonstrated strong distribution at the MTOC. I could not detect the strong colocalization of leupaxin with the MTOC at the immunological synapse, consistent with the data in the previous chapter. In contrast, leupaxin was evenly distributed along the contact interface between CTL and target cell. It is already known that recruitment of paxillin to the immunological synapse is mediated by TCR signaling and the MTOC reorients only when TCR is activated [77]. The different distribution of leupaxin at the MTOC raised the question whether leupaxin recruitment to the immunological synapse was mediated by TCR signaling. This question will be addressed later **(Figure 4.5)**.

In addition to live cell imaging, I also confirmed the recruitment of leupaxin to the immunological synapse by fixed cell staining. Similar to above, clone 11 cells were transfected with either GFP, GFP-paxillin or GFP-leupaxin. Twenty-four hours later, the transfected CTL were conjugated with the target cells L1210K^b/D^d, which were labeled with CellTracker blue. Cells were fixed, permeabilized and stained for GFP and α-tubulin. The α-tubulin staining showed the reoriented MTOC, confirming the activation of 'outside-in' signaling. Both

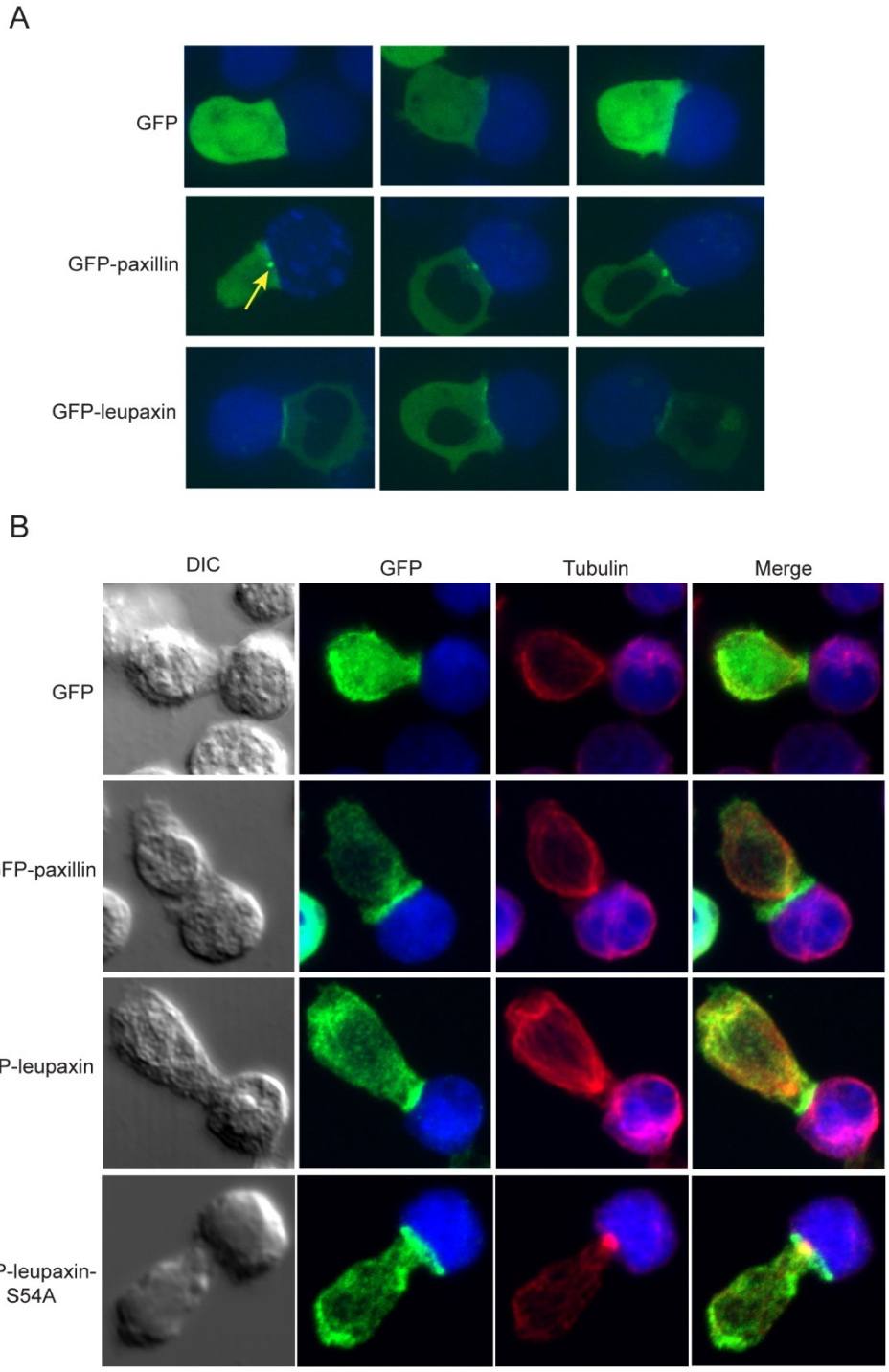
A
GFP
GFP-paxillin
GFP-leupaxin
B
DIC
GFP
Tubulin
Merge
GFP
GFP-paxillin
GFP-leupaxin
GFP-leupaxin-S54A

Figure 4.4. Leupaxin is recruited to the immunological synapse in CTL when conjugated with the target cell. (A) Clone 11 cells were transfected with either GFP, GFP-paxillin or GFP-leupaxin. Twenty-four hours after transfection, CTL were harvested and mixed with L1210K^b/D^d target cells which were labeled with CellTracker blue. Cells were then transferred to ICAM-1 coated chambered coverglass and live cell imaging was captured by spinning disk confocal microscopy. The yellow arrow pointed to the MTOC. Thirty images for each experiment were collected from three independent transfections, and representative images are shown. (B) Clone 11 which were transfected with the indicated plasmids were conjugated with the target cells L1210K^b/D^d which were labeled with CellTracker blue. Cells were fixed, permeabilized and then stained with anti-GFP antibody (detected by anti-mouse Alexa Fluor 488) and anti-α-tubulin (detected by anti-rabbit Alexa Fluor 594). Z stack was collected with an interval of 0.3 um between slices. At least 45 conjugates were collected from three independent transfections, and representative images are shown.

paxillin and leupaxin were accumulated at the interface between CTL and target cells **(Figure 4.4B)**.

As shown in **Figure 4.3**, I demonstrated that leupaxin was phosphorylated at Ser54 in response to anti-CD3 antibody stimulation. Next, I determined whether Ser54 phosphorylation was required for leupaxin recruitment to the immunological synapse. Clone 11 cells were transfected with the construct GFP-leupaxin-Ser54A. The transfected clone 11 cells were conjugated with the target cells L1210K^b/D^d. Cells were fixed, permeabilized and stained for GFP and α-tubulin. Similar to the full-length leupaxin, leupaxin Ser54A mutant was still recruited to the immunological synapse, implying that phosphorylation of Ser54 was not important for the recruitment. This was probably expected, as leupaxin was recruited to the synapse very quickly (within 5 minutes upon engagement with the target cells), whereas the Ser54 phosphorylation occurred at 10 minutes after anti-CD3 stimulation. It is possible that leupaxin is serine phosphorylated at the immunological synapse after recruitment.

4.2.5. Leupaxin is recruited to the synapse by LFA-1 engagement with ICAM-1

In NK cells, LFA-1 engagement with ICAM-1 alone initiated a signaling pathway centered on ILK-Pyk2-leupaxin which regulated NK cell function [107], although they did not further address whether leupaxin was tyrosine phosphorylated and recruited to the immunological synapse. As I have detected leupaxin tyrosine phosphorylation upon stimulation with anti-LFA-1 antibody **(Figure 3.3B)**, I asked

whether LFA-1 engagement with ICAM-1 alone would be enough to recruit leupaxin to the interface between CTL and target cells.

To study the LFA-1 signaling alone, I used the target cells which did not have antigen for T cell activation. First, *ex vivo* activated OT-1 cells were labeled with CellTracker green and mixed with L1210K^b/D^d cells in the absence of OVA peptide. Cells were mixed and centrifuged to facilitate the cell contact. Cells were fixed, permeabilized and stained for endogenous leupaxin by the polyclonal anti-leupaxin antibodies. Surprisingly, I detected robust accumulation of the endogenous leupaxin at the interface between OT-1 T cells and L1210K^b/D^d cells **(Figure 4.5A)**. In addition to the OT-1 T cells, I also used the CTL clone AB.1 cells which recognized the alloantigen H-$2K^b$ molecules. The L1210 target cells, which were H-$2K^b$ negative, were labeled with CellTracker blue and mixed with clone AB.1 as above. Staining of endogenous leupaxin suggested that leupaxin was also recruited to the synapse between CTL and target cells **(Figure 4.5B)**. These results both suggested that leupaxin can be recruited to the interface between CTL and target cells in the absence of TCR signaling.

The leupaxin recruitment to the synapse was independent of TCR signaling suggested that this might be mediated by LFA-1 engagement with the ligand ICAM-1. Next, I coated the latex beads with recombinant ICAM-1 and mixed the beads with the *ex vivo* activated OT-1 T cells which were labeled with CellTracker green. Staining of endogenous leupaxin showed that leupaxin was strongly recruited to the contact interface between the beads and OT-1 T cells **(Figure 4.5C)**. Thus, these results demonstrated that leupaxin was recruited to the synapse by the

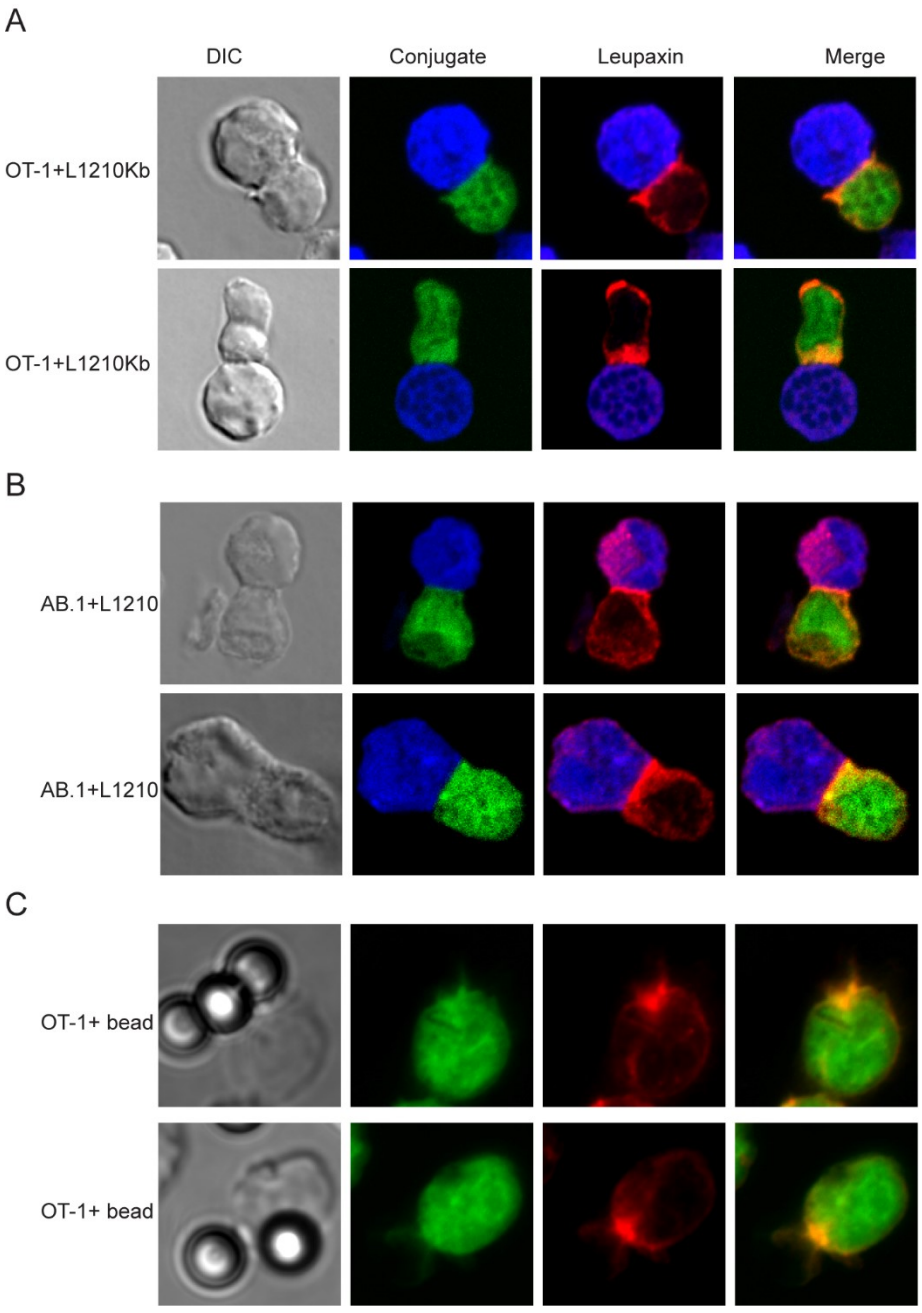

Figure 4.5. Leupaxin is recruited to the synapse by LFA-1 engagement with ICAM-1. (A) to (B) CTL OT-1 or AB.1 (labeled with CellTracker green) were mixed with the antigen-negative target cells (labeled with CellTracker blue) which did not have antigens for TCR activation. Cells were fixed, permeabilized and endogenous leupaxin was stained with anti-leupaxin antibody (detected by anti-rabbit Alexa Fluor 594). (C) OT-1 T cells (labeled with CellTracker green) were mixed with beads coated with ICAM-1. Cells were fixed, permeabilized and stained as above. Z stack was collected for (C) with an interval of 0.3 um between slices. At least 30 images were collected from three independent experiments, and representative images are shown.

LFA-1 mediated adhesion to ICAM-1 prior to TCR engagement. However, I could not rule out the possibility that TCR activation may further promote the recruitment of leupaxin to the immunological synapse as leupaxin colocalized with the MTOC and the microtubules, and the microtubules reoriented to the immunological synapse after TCR activation.

4.2.6. Leupaxin is recruited to the immunological synapse by the N-terminal LD domains

Paxillin has been shown to be recruited to the immunological synapse and the recruitment was mediated by the N-terminal LD domains [77]. In chapter 3, I have shown that leupaxin C-terminal LIM domains mediated the recruitment of leupaxin to the focal adhesion-like structures, which was also consistent with previous studies in adherent cells [148]. As both CTL migration on ICAM-1 and making contact with target cells were mediated by LFA-1, this made me wonder whether the LIM domains contributed to the recruitment to the synapse. To address this question, clone 11 cells were transfected with either GFP-leupaxin-LD mutant or GFP-leupaxin-LIM mutant. Twenty-four hours later, the transfected CTL were conjugated with the target cells L1210K^b/D^d, which were labeled with CellTracker blue. Cells were fixed, permeabilized and stained for GFP and α-tubulin as above. The MTOC was reoriented towards the target cells, as shown by α-tubulin staining. Surprisingly, leupaxin N-terminal LD domains were required for leupaxin recruitment to the immunological synapse, which was similar to paxillin **(Figure 4.6)**. Although both the focal adhesion-like structures and the immunological synapse are mediated by LFA-1, leupaxin utilizes distinct domains to be recruited

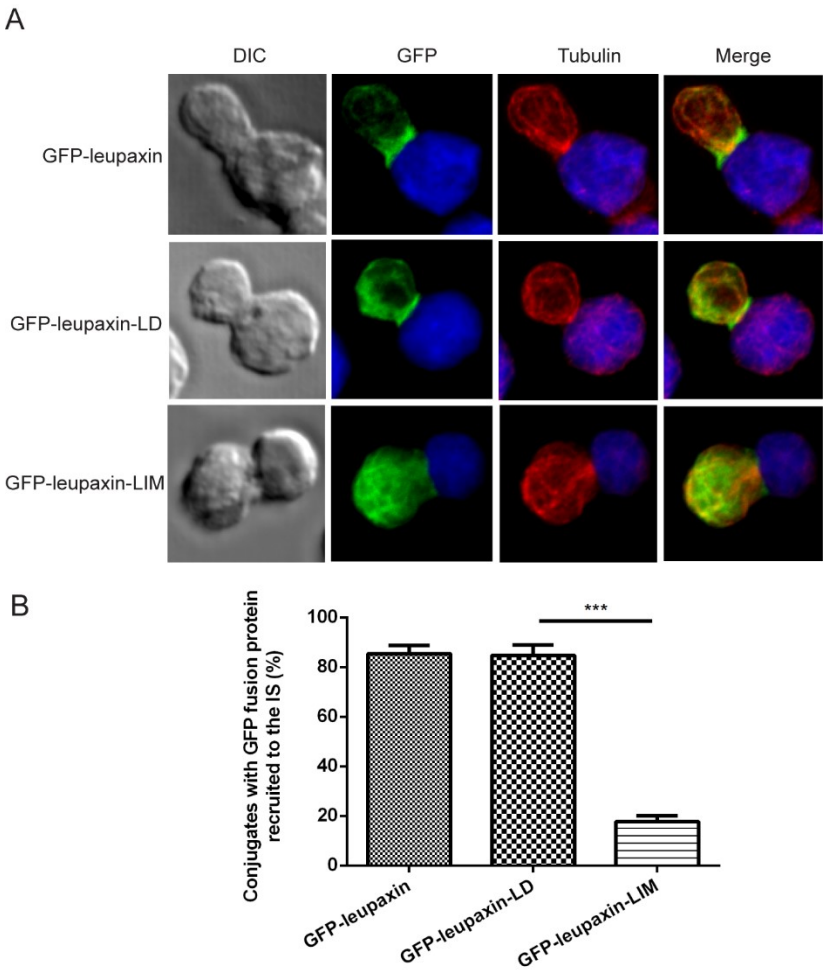

Figure 4.6. Leupaxin is recruited to the immunological synapse by the NT-LD domains. (A) Clone 11 were transfected with the indicated leupaxin mutants. At 24 hours post-transfection, CTL were conjugated with the target cells L1210K^{b}/D^{d} which were labeled with CellTracker blue. Cells were fixed, permeabilized and then stained for GFP (detected by anti-mouse Alexa Fluor 488) and α-tubulin (detected by anti-rabbit Alexa Fluor 594). Z stack was collected with an interval of 0.3 um between slices. (B) The conjugates that showed the recruited GFP fusion proteins to the immunological synapse were quantified. At least 45 conjugates were collected from three independent transfections. The unpaired student *t*-test was used with 95% confidence intervals. The error bar represents standard error of the mean. All experiments were performed three times, and representative images are shown.

to these sites, suggesting that leupaxin may be recruited to these sites by different binding partners. In addition, I found that the GFP-leupaxin-LD transfected clone 11 showed the absence of protein localization at the nucleus, whereas GFP-leupaxin-LIM proteins were present in both the nucleus and the cytoplasm, determined by fixed cell staining **(Figure 4.6)**. This was consistent with previous studies showing that the leupaxin LD domains contained nucleus exporting sequence [229].

4.2.7. Leupaxin LD domain shows redundancy in the recruitment of leupaxin to the immunological synapse

In order to determine which LD domains were required for leupaxin recruitment to the immunological synapse, I generated LD domain truncations by deleting each LD domain from the full-length leupaxin. These genes were inserted into the EGFP-C1 plasmids as above and the constructs were transfected into clone 11 cells. Twenty-four hours after transfection, I checked the transfection efficiency and protein expression by flow cytometry. Around 20% of cells expressed the GFP fusion proteins, which was in the normal range of transfection efficiency for CTL clones. The transfected CTL cells were collected and conjugated with the target cells L1210K^b/D^d and the conjugates were fixed, permeabilized and stained for GFP and α-tubulin as above.

As shown in **Figure 4.7**, when a single LD domain was deleted from the full-length leupaxin, all mutants were still recruited to the immunological synapse during conjugation with the target cells. This suggested that LD domains showed redundancy in recruiting leupaxin to the synapse. Similar to leupaxin, paxillin LD

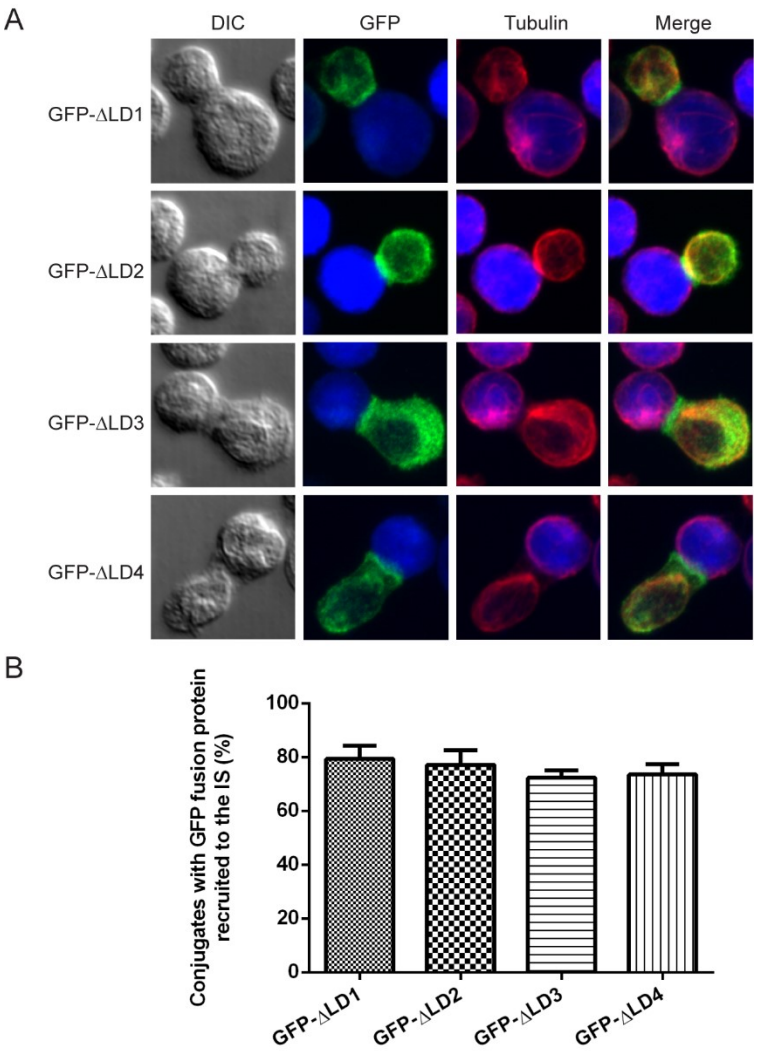

Figure 4.7. Leupaxin LD domain shows redundancy in the recruitment of leupaxin to the immunological synapse. (A) Clone 11 cells were transfected with various leupaxin LD domain mutants. At 24 hours post-transfection, CTL were collected and conjugated with the target cells L1210K^b/D^d which were labeled with CellTracker blue. Cells were fixed, permeabilized and then stained for GFP (detected by anti-mouse Alexa Fluor 488) and α-tubulin (detected by anti-rabbit Alexa Fluor 594). Z stack was collected with an interval of 0.3 um between slices. (B) The conjugates that showed the recruited GFP fusion proteins to the immunological synapse were quantified. The error bar represents standard error of the mean. At least 45 conjugates were collected from three independent transfections. All experiments were performed three times, and representative images are shown.

domains were also demonstrated to exhibit redundancy in recruiting paxillin to the synapse [77]. We still did not know how paxillin and leupaxin were recruited to the synapse, but these results suggested that the signaling proteins that recruit paxillin and leupaxin are capable of binding more than one LD domains. Indeed, it is not surprising that many paxillin binding partners, including FAK and Pyk2, can bind more than one LD domains [152, 153].

4.2.8. Leupaxin is recruited to the immunological synapse by the LD2-4 domains

As the LD domains showed redundancy in recruiting leupaxin to the synapse **(Figure 4.7)**, I deleted one or more LD domains from the full-length leupaxin and generated the following constructs: GFP-leupaxin-ΔLD4, GFP-leupaxin-ΔLD3-4, GFP-leupaxin-ΔLD2-3, and GFP-leupaxin-ΔLD2-4. The plasmids were transfected into clone 11 cells by nucleofection. Twenty-four hours later, clone 11 were conjugated with the target cells L1210K^b/D^d, followed by cell fixation, permeabilization and staining for GFP and α-tubulin as above.

The antigen-specific conjugation was confirmed by the reoriented MTOC. Deletion of the LD2-3 segment and the LD3-4 segment were still not enough to disrupt the recruitment, respectively **(Figure 4.8)**. However, when the LD2-4 segment was deleted from the full-length leupaxin, GFP staining showed the loss of proteins recruited to the immunological synapse. When the LD2-4 segment was deleted from the full-length paxillin, it functioned as a dominant negative mutant and impaired the MTOC reorientation when transfected into the CTL [77]. We did not detect impaired MTOC reorientation when the leupaxin LD2-4 segment was

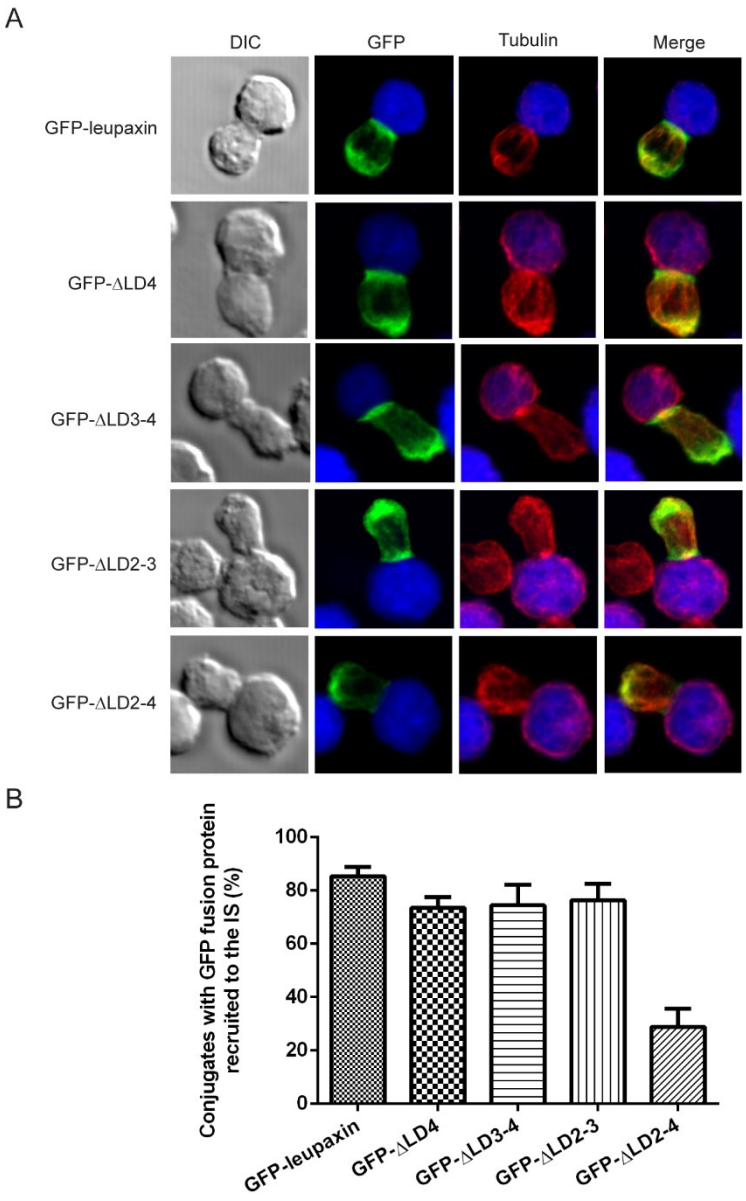

Figure 4.8. Leupaxin is recruited to the immunological synapse by the LD2-4 domains. (A) Clone 11 CTL were transfected with the indicated leupaxin mutants. CTL were collected 24 hours after transfection and conjugated with the target cells L1210K^{b}/D^{d} which were labeled with CellTracker blue. Cells were fixed, permeabilized and stained for GFP (detected by anti-mouse Alexa Fluor 488) and α-tubulin (detected by anti-rabbit Alexa Fluor 594). Z stack was collected with an interval of 0.3 um between slices. (B) The conjugates that showed the recruited GFP fusion proteins to the immunological synapse were quantified. The error bar represents standard error of the mean. At least 45 conjugates were collected from three independent transfections. All experiments were performed three times, and representative images are shown.

deleted and transfected into the CTL clone 11. However, clone 11 cells are alloreactive CTL and have much higher TCR signal strength than the CTL clone 3/4 which are specific for an influenza nucleoprotein (NP) and used for paxillin experiment. Thus, similar experiment needs to be repeated with CTL clone 3/4 to titrate down the TCR signals to determine whether GFP-leupaxin-ΔLD2-4 functions as a dominant negative mutant.

Since I made truncations within the leupaxin protein, one possibility was that it could disrupt protein structure and affect protein association. In order to confirm the role of LD2-4 domain in recruiting leupaxin to the immunological synapse, in future experiment the LD2-4 segment should be generated and to determine whether it is sufficient for recruitment.

4.2.9. Leupaxin is recruited to the peripheral SMAC

When CTL conjugated with either target cells or APCs, a cascade of signaling networks were activated and signaling proteins were recruited to the contact surface, forming the supramolecular activation complex (SMAC) [83, 230]. SMAC was divided into central SMAC, peripheral SMAC and distal SMAC, according to the spatial distribution of signaling proteins. Given that leupaxin was recruited to the focal-adhesion like structures and colocalized with talin and vinculin, I determined whether leupaxin was recruited to the peripheral SMAC. Clone 11 cells were mixed with the labeled target cells L1210K^b/D^d. Cells were allowed to conjugate by centrifugation, followed by cell fixation, permeabilization and staining for the endogenous leupaxin and β2 subunit of LFA-1.

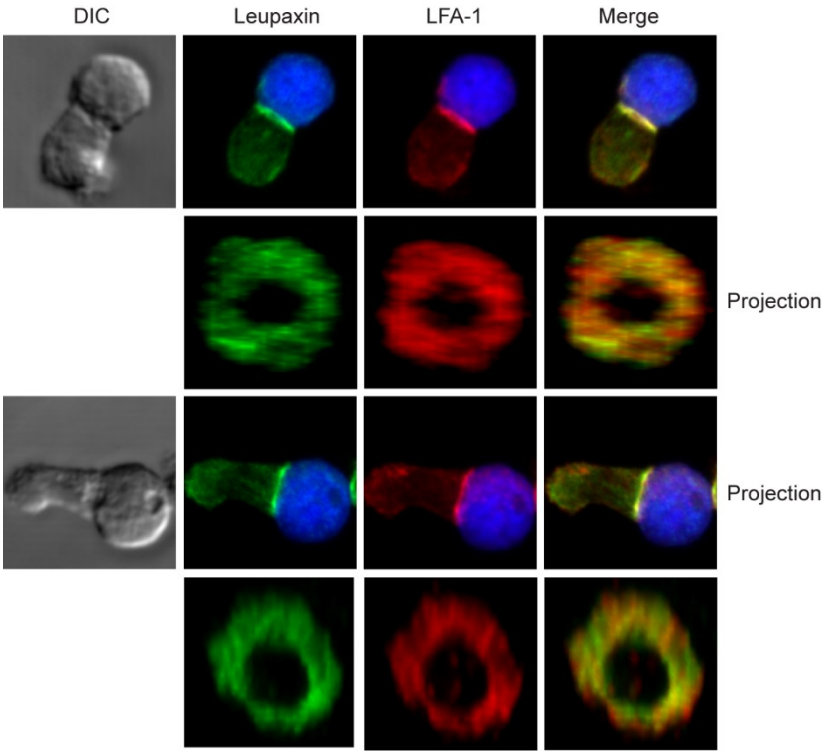

Figure 4.9. Leupaxin is recruited to the peripheral SMAC. Unlabeled clone11 were mixed with L1210K^b/D^d target cells which were labeled with CellTracker blue. Conjugates were fixed, permeabilized and stained for endogenous leupaxin (detected by anti-rabbit Alexa Fluor 488) and LFA-1 (detected by anti-rat Alexa Fluor 594). The three-dimensional projections of the pSMAC were generated by the software Imaris. The conjugates were captured with an interval of 0.3 um to reconstruct pSMAC. All experiments were performed three times, and representative images are shown.

For the conjugates, a number of images were collected with the interval of 0.3 um. The immunological synapse in three dimensions was reconstructed by Imaris. As shown in **Figure 4.9**, leupaxin demonstrated the localization at the peripheral SMAC. Although the colocalization between leupaxin and LFA-1 was not absolutely complete, this suggested that LFA-1 may not bind to leupaxin directly. Thus, this result indicated that leupaxin might participate in the 'outside-in' signaling downstream of the LFA-1.

4.3. Discussion

In this chapter, I have shown that leupaxin was both tyrosine and serine phosphorylated in response to TCR signaling. This unique serine phosphorylation occurred at Ser54, leading to the mobility shift. TCR mediated leupaxin phosphorylation was also dependent on the tyrosine kinase Pyk2. Unlike anti-LFA-1 mediated tyrosine phosphorylation, TCR signaling mediated leupaxin phosphorylation was more robust and prolonged. Staining of leupaxin indicated that leupaxin was recruited to the immunological synapse. However, LFA-1 engagement to ICAM-1 coated beads was sufficient to recruit leupaxin, even in the absence of TCR signaling. Similar to paxillin, leupaxin was also recruited to the immunological synapse by the N-terminal LD2-4 domains. At the immunological synapse, leupaxin was accumulated at the peripheral SMAC, and colocalized with the LFA-1 β2 subunit as has been shown with paxillin [77].

Although anti-LFA-1 stimulation can trigger leupaxin tyrosine phosphorylation, the phosphorylation was transient and started to decrease by about 20 minutes after stimulation **(Figure 3.3)**. This was consistent with the idea that the activation of high-affinity LFA-1 relies on the 'inside-out' signals from receptors such as TCR and chemokine receptors. Whereas when CTL were stimulated upon TCR engagement, leupaxin demonstrated robust tyrosine phosphorylation **(Figure 4.1)**. In addition to the kinetic difference, they also exhibited distinct phosphorylation patterns. LFA-1 stimulated leupaxin phosphorylation showed two tyrosine phosphorylated bands, corresponding to the two leupaxin bands. But TCR stimulated leupaxin phosphorylation only exhibited one highly phosphorylated

band **(Figure 4.1 B)**. This phosphorylated band overlapped with the upper leupaxin band. Different phosphorylation sites might explain the phosphorylation patterns. Previous studies showed that leupaxin was tyrosine phosphorylated at Tyr 22, Tyr 62 and Try72 in BALB/c fibroblasts and at Try72 in HEK 293T cells [162, 163]. I also mutated the leupaxin at Tyr 22, Tyr 62 and Try72 and transfected them into clone 11 cells. However, due to the low transfection efficiency, I was unable to determine which tyrosine residues were phosphorylated in CTL clones. Further experiments need to be performed to identify the phosphorylation sites by mass spectrometry.

In addition to tyrosine phosphorylation, I showed the unique leupaxin mobility shift upon TCR engagement, which has not been reported before. The mobility shift was mediated by a single serine phosphorylation at Ser54. Although leupaxin serine phosphorylation has not been reported, paxillin has been demonstrated to be phosphorylated at a number of serine residues. Serine phosphorylation at a number of sites in paxillin regulates paxillin turnover at focal adhesions, cytoskeletal rearrangement, protein degradation by proteasomes and protein shuttling between the nucleus and cytoplasm [135, 151, 231, 232]. Phosphorylation of Ser126 was dependent on MEK/ERK pathway and regulated the translocation of paxillin from focal adhesions to the cytosol [232]. Similarly, leupaxin Ser54 phosphorylation was dependent on the serine kinase ERK, as U0126 treatment prevented the mobility shift **(Figure 4.2)**. However, T cells do not form traditional focal adhesions and LFA-1 stimulation alone does not induce the serine phosphorylation. This implied that leupaxin Ser54 phosphorylation might play a

unique role in the TCR signaling. I determined whether Ser54 phosphorylation was important for leupaxin recruitment to the immunological synapse. The Ser54 mutation, however, did not disrupt leupaxin recruitment to the immunological synapse. The kinetics of serine phosphorylation occurred later than tyrosine phosphorylation, reaching maximal mobility shift at 60 minutes after stimulation. I hypothesized that leupaxin serine phosphorylation might be involved in the later stages of processes, such as CTL disassociation with the target cells. Further experiments are required to examine the consequences of leupaxin serine phosphorylation during CTL degranulation.

The Ser54 phosphorylation was dependent on both Pyk2 and ERK activity **(Figure 4.2)**. In addition, PMA treatment alone also led to the mobility shift, implying that the serine phosphorylation was independent of leupaxin tyrosine phosphorylation. Previous literature showed that paxillin was a substrate of ERK in EL4 cells [233]. Paxillin was also a target of the ERK signaling pathway in CTL upon TCR engagement [188]. An association between ERK and leupaxin was established in prostate cancer cells [140]. Our lab has previously reported that ERK could regulate Pyk2 activity in CTL [234], but how Pyk2 regulates ERK activity, and the downstream ERK-mediated leupaxin serine phosphorylation is unknown. Indeed, a recent study has demonstrated that Pyk2 could regulate ERK1/2 activation in pulmonary artery smooth muscle cells [235]. Similar studies are required to determine whether Pyk2 can affect ERK activity, thus regulate leupaxin serine phosphorylation in CTL.

I have shown that leupaxin was recruited to the immunological synapse during CTL conjugation with the target cells **(Figure 4.4)**. By separating the TCR signaling and LFA-1 signaling, I found that LFA-1 engagement with ICAM-1 alone can lead to leupaxin recruitment **(Figure 4.5)**. As leupaxin also associated with the microtubules and MTOC, TCR engagement would further recruit leupaxin to the synapse. I speculated that there were at least two pools of leupaxin in the cytosol. The first population of leupaxin associated with the microtubule cytoskeleton in CTL. This population of leupaxin was only recruited to the immunological synapse along with the MTOC reorientation upon TCR engagement. The second population of leupaxin did not colocalize with the microtubule and was recruited to the synapse upon the initial contact between CTL and target cell, even before TCR activation **(Figure 4.5)**. Further experiments will be required to determine the function of leupaxin in the initial adhesion between CTL and target cells.

I characterized the domains required for leupaxin recruitment to the synapse. Similar to paxillin, leupaxin LD2-4 domains were required for the recruitment **(Figure 4.8)**. I also observed redundancy in leupaxin recruitment to the synapse by LD domains. Despite the fact that leupaxin binding partners being largely unknown, paxillin was reported to associate with a number of proteins through LD domains. Pyk2 constitutively binds to both LD2 and LD4 domains [152]. Vinculin also associates with paxillin through LD1, LD2 and LD4 domains [236]. Some other reported proteins such as ILK and PAK only bound to a single LD domain [237, 238]. This suggests that the functions of LD domains are not identical in protein association. To identify the potential binding partners of leupaxin, I performed

leupaxin and paxillin immunoprecipitation in cell lysates of A20 cells, and the whole lanes of SDS-PAGE were analyzed by mass spectrometry. Pyk2 was used as a binding control as we have confirmed the association between leupaxin and Pyk2. However, I could only identify one potential binding partner, IQGAP1. Paxillin immunoprecipitation from cell lysates of CTL clones confirmed the association between IQGAP1 and paxillin. As leupaxin was recruited to the synapse in the absence of TCR signaling, I speculated that this recruitment was mediated by the low-affinity LFA-1 interaction. However, relatively little is known about the regulation of transient LFA-1 adhesion. In NK cells, it has been shown that LFA-1 signaling alone triggered a phosphorylated signaling complex centered on integrin-linked kinase (ILK)-Pyk2-leupaxin [107]. Furthermore, ILK associated with the β2 subunit of LFA-1 [107]. As Pyk2 constitutively associated with leupaxin, further experiments are required to determine whether ILK is responsible for recruiting Pyk2-leupaxin complex to the synapse.

Despite the fact that LFA-1 mediated both CTL migration and synapse formation, the LIM 2-3 domains were required for recruiting to the focal adhesion-like structures, instead of using LD domains **(Figure 3.8)**. Thus, leupaxin might be recruited to the synapse and focal adhesion-like complexes by distinct proteins. The fact that leupaxin used distinct domains for different subcellular localizations suggested that it might have distinct functions at each site. The role of paxillin family proteins in traditional focal adhesions is well established, which may apply to the focal adhesion-like structures in T cells. Although leupaxin has not been shown to be a substrate of calpain, paxillin cleavage at the trailing edge promotes

focal adhesion disassembly and cell migration [121]. Once having killed the target cells, CTL are detached from the target cells. Whether paxillin family proteins are involved in this process as that in focal adhesion disassembly is unknown. I showed the leupaxin Ser54 phosphorylation upon TCR engagement. Unlike the tyrosine phosphorylation which occurred very early, serine phosphorylation peaked at 60 minutes after stimulation. Further experiments are required to determine the role of serine phosphorylation in leupaxin cleavage and CTL disassociation with target cells.

CHAPTER 5: Leupaxin contributes to MTOC reorientation during CTL conjugation with the target cell

5.1. Introduction

Activated $CD8^+$ T cells play a critical role in adaptive immunity by destroying intracellular pathogen-infected cells. Before activation, the naïve $CD8^+$ T cells do not possess lytic granules and cytotoxic capability. Activation of naïve $CD8^+$ T cells is mediated by the professional antigen-presenting cells (APCs) at the peripheral lymphoid organs [239]. This cell-to-cell interaction triggers the formation of highly organized structures called the immunological synapse. The activation signals induce the proliferation and differentiation of naïve $CD8^+$ T cells and become the functional CTL.

CTL are serial killers and capable of destroying one target cells after another [240]. TCR recognition of MHC I/peptide complexes triggers the formation of the immunological synapse between CTL and target cells. This structure is similar to the immunological synapse formed between the naïve $CD8^+$ T cells and APCs. The early signaling events have been extensively investigated and discussed in the introduction. Once TCR signaling is activated, the antigen receptors cluster in the center of the immunological synapse [241]. This process is dependent on the activity of actin flow away from the center of the synapse [203].

A key feature of degranulation is the directional reorientation of MTOC and lytic granules. However, the molecular mechanism for controlling MTOC reorientation remains largely unknown. Many studies suggested an important role of the motor protein dynein in this process [76, 105]. Disruption of dynein function

significantly impaired the MTOC reorientation [105]. Dynein is recruited to the synapse within minutes of target cell engagement and the process is dependent on DAG and the cytoskeletal adaptor protein ADAP [76, 104, 105]. It was proposed that dynein pulled on the microtubules, allowing MTOC to move towads the synapse [75, 242].

As leupaxin is a cytoskeletal adaptor protein involved in integrin signaling [135], we propose that it may regulate the 'outside-in signaling' mediated cellular processes in CTL. The majority of leupaxin studies have been performed in adherent cells and tumor cells. Its function in leukocytes is largely unknown. The only solid evidence which supports a role for leupaxin in leukocytes is from studies in NK cells. Knockdown of leupaxin expression in NK cells impaired MTOC reorientation towards the target cells [107]. However, they did not further investigate the contribution of leupaxin in degranulation and NK cell cytotoxicity. Unlike NK cells which do not require the 'inside-out' signals for MTOC reorientation and lytic granule polarization [107], CTL degranulation is dependent on signals from the TCR for MTOC reorientation and degranulation [80]. Thus, whether leupaxin has the similar contribution in CTL is unknown.

In this chapter, I sought to investigate the role of leupaxin in TCR signaling, degranulation and cytotoxicity. We generated the leupaxin KO mice by breeding leupaxin floxed mice with the CMV-Cre mice. I am the first to use primary T cells and leupaxin deficient CTL to explore leupaxin function. Unlike previous studies which suggested that leupaxin was a negative regulator, I found that Pyk2 reduced activation during TCR signaling in the absence of leupaxin. Consistent with the role

of leupaxin in NK cells, I showed that leupaxin regulated the MTOC reorientation during CTL conjugation with the target cells. My results suggested for the first time that, leupaxin is required for optimal TCR signaling and MTOC reorientation in CTL.

5.2. Results

5.2.1. Generation of leupaxin$^{-/-}$ mice

To further investigate the role of leupaxin during T cell development and in T cell function, we generated the leupaxin floxed mice using sperm acquired from Sanger Institute, and generated the germline leupaxin$^{-/-}$ mice by breeding with CMV-Cre mice which contained the transgenic Cre gene under the control of human cytomegalovirus minimal promoter resulting in germline deletion. The leupaxin floxed mice contain two FRT sites and three loxp sites **(Figure 5.1A)**. In brief, to delete the floxed exon of leupaxin gene specifically, we first bred the mice with ROSA-FLP1 mice containing the FLP1 recombinase gene. Once the first loxp site was deleted, as confirmed by PCR, the mice were bred with the CMV-Cre mice to drive the deletion of the second leupaxin exon. The leupaxin$^{KO/WT}$-CMV-Cre mice were bred until the generation of homologous leupaxin$^{KO/KO}$ mice. In addition, we also bred the leupaxin$^{-/-}$ mice with OT-1 transgenic mice, thus allowing us to obtain the OT-1 transgenic leupaxin$^{-/-}$ mice. These breeding processes were performed by Dr. Samuel Cheung, the postdoctoral fellow in our lab.

In addition to the PCR screen of leupaxin gene performed by Dr. Cheung, I confirmed the absence of leupaxin protein by immunoblot. The spleen, thymus and lymph nodes isolated from WT and leupaxin$^{-/-}$ mice were homogenized and cells were lysed as before **(Figure 3.1)**. Leupaxin blot confirmed the absence of leupaxin in leupaxin$^{-/-}$ mice **(Figure 5.1B)**. I stripped and re-blotted with the anti-paxillin antibody. Deletion of leupaxin gene did not upregulate the expression of

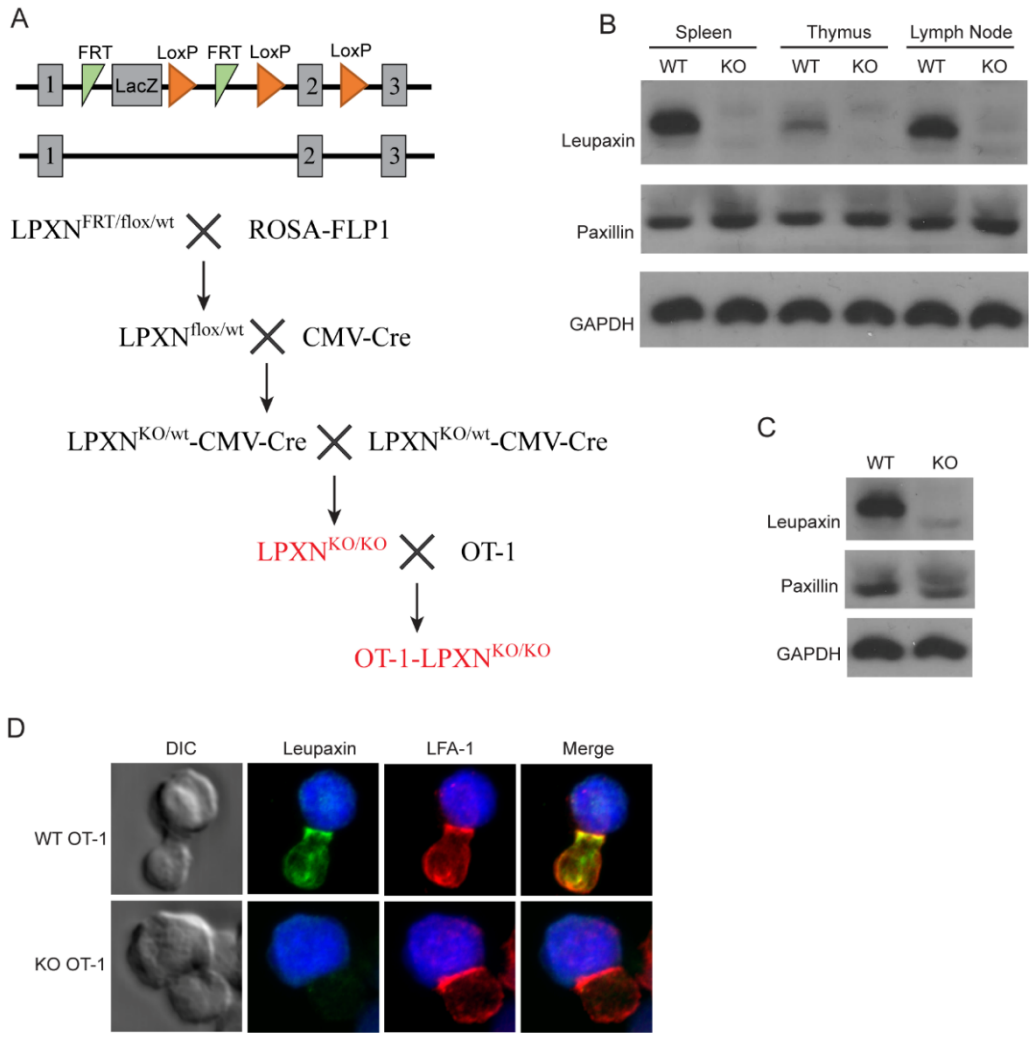

Figure 5.1. Generation of leupaxin knockout mice. (A) The leupaxin knockout mice were generated by breeding leupaxin floxed mice with CMV-Cre mice following the diagram. OT-1 leupaxin KO mice were generated by breeding OT-1 transgenic mice with the leupaxin KO mice. (B) Spleen, thymus and lymph nodes from WT and leupaxin KO mice were homogenized and the cell lysates of 4×10^5 cells were separated by SDS-PAGE. Immunoblots were probed with the indicated antibodies. (C) 4×10^5 splenocytes from OT-1 WT and leupaxin KO mice were lysed and proteins were separated by SDS-PAGE. Immunoblots were performed as above. (D) The WT and leupaxin KO OT-1 cells were conjugated with CellTracker blue labeled L1210K^b/D^d target cells which were pulsed with OVA N4 peptide (1 μM). Cells were fixed, permeabilized and then stained for the endogenous leupaxin (detected by anti-rabbit Alexa Fluor 488) and LFA-1 (detected by anti-rat Alexa Fluor 594). Z stack was collected for (D) with an interval of 0.3 um between slices.

paxillin. The absence of leupaxin in cells was also confirmed in OT-1 transgenic leupaxin$^{-/-}$ mice **(Figure 5.1C)**.

I also verified that leupaxin protein was absent in leupaxin deficient T cells by immune fluorescence staining. The endogenous leupaxin was stained with anti-leupaxin antibody and detected by anti-rabbit Alexa Fluor 488. In WT OT-1 T cells, leupaxin was accumulated at the interface between T cells and the target cells L1210K^{b}/D^{d} (labeled by CellTrace blue). Whereas the endogenous leupaxin was not detected in leupaxin deficient OT-1 T cells **(Figure 5.1D)**. This result further confirmed that the polyclonal anti-leupaxin serum I generated did not cross-react with paxillin.

5.2.2. Thymocytes development is normal in leupaxin$^{-/-}$ mice

Thomas's group has tried to develop the paxillin deficient mice more than a decade ago [136]. Compare to the WT mice, no embryos were detected in paxillin$^{-/-}$ mice after E9.5 stage [136]. In contrast to the paxillin$^{-/-}$ mice which were early embryo lethal, the leupaxin$^{-/-}$ mice are healthy and viable. Similar to leupaxin, loss of Hic-5, another paxillin family protein, did not affect embryonic development and mice growth [139]. It is possible that paxillin may compensate for part of Hic-5 and leupaxin function.

The thymocyte development and peripheral T cells were analyzed in leupaxin$^{-/-}$ mice. The thymocytes were stained for CD4 and CD8. The cell number and percentage of double negative (DN), double positive (DP), and single positive (SP) T cells were not affected in the absence of leupaxin **(Figure 5.2A)**. In addition, I also quantified the percentage of CD4^{+} and CD8^{+} T cells in the spleen and lymph

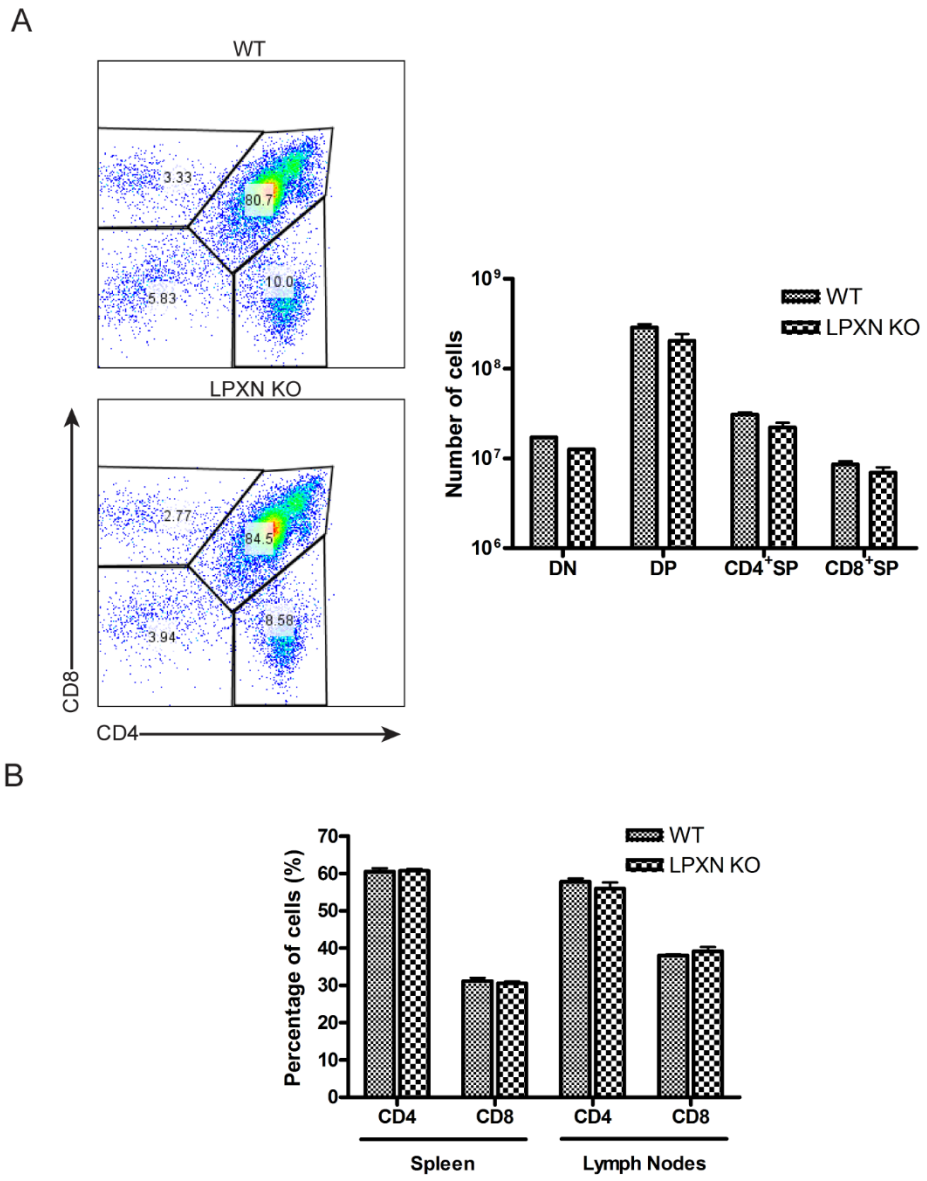

Figure 5.2. Thymocytes development is normal in leupaxin$^{-/-}$ mice. (A) Thymus from WT and leupaxin KO mice were homogenized and thymocytes were stained for CD4 and CD8. Cells were analyzed by flow cytometry and the cell number was shown. (B) Spleen and lymph nodes from WT and leupaxin KO mice were homogenized. The percentage of $CD4^+$ and $CD8^+$ cells were counted. Three mice between 4-6 weeks old were used. The error bar represents standard error of the mean.

nodes. There was no difference in the percentage of $CD4^+$ and $CD8^+$ T cells in the periphery **(Figure 5.2B)**. Indeed, leupaxin gene expression profile from the Immunological Genome Project **(Figure 1.3)** and western blot analysis **(Figure 5.1B)** both suggest that thymocytes express much lower level of leupaxin than the $CD4^+$ and $CD8^+$ T cells. In contrast, DN and DP thymocytes express a higher level of paxillin than the naïve $CD4^+$ and $CD8^+$ T cells **(Figure 1.3)**. This may suggest that paxillin, instead of leupaxin, plays an important role in T cell development in the thymus. Overall, these data implied that loss of leupaxin did not affect T cell development.

5.2.3. Leupaxin deficient CTL reduces tyrosine phosphorylation at specific phosphorylated band upon anti-CD3 stimulation

Leupaxin was demonstrated as a negative regulator of BCR signaling [163]. Overexpression of leupaxin in A20 cells suppressed the tyrosine phosphorylation of JNK, p38 MAPK and Akt [163]. Thus, I explored whether leupaxin negatively regulated TCR signaling as in B cells. Naïve $CD8^+$ T cells were purified from splenocytes of WT and leupaxin$^{-/-}$ mice. T cells were then stimulated with immobilized anti-CD3 and anti-CD28 antibodies for 48 hours. Cells were further cultured in the presence of IL-2. I stimulated the activated CTL with immobilized anti-CD3 antibody for the indicated times. As shown in **Figure 5.3**, CTL showed increased tyrosine phosphorylation upon anti-CD3 stimulation. Compared to the WT CTL, leupaxin deficient CTL showed a similar phosphorylation pattern, except one specific tyrosine phosphorylated band which was indicated by the arrow. The

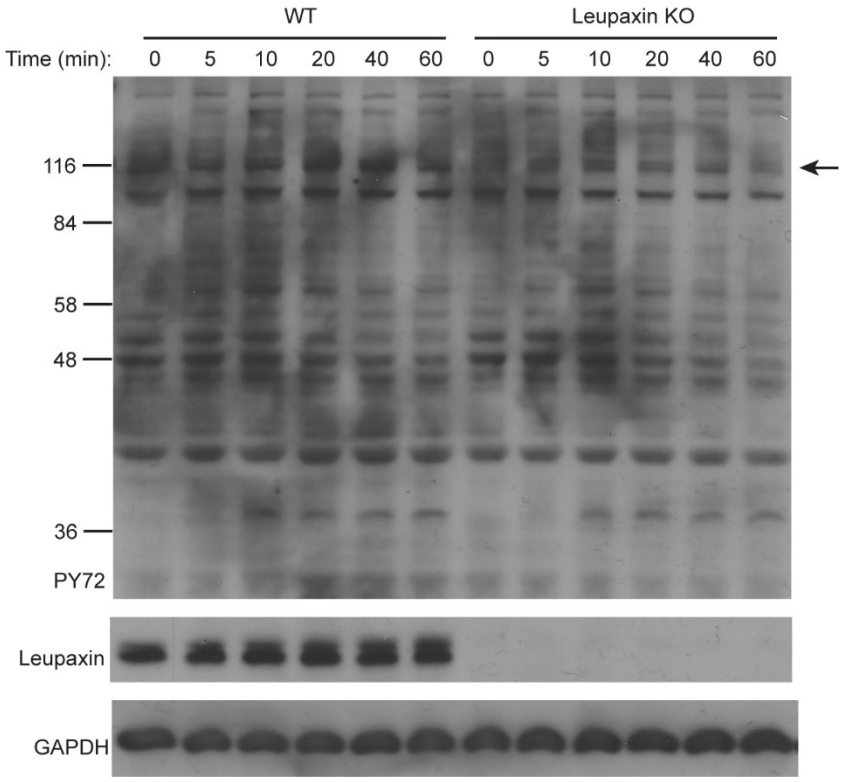

Figure 5.3. Leupaxin deficient CTL reduces tyrosine phosphorylation at specific phosphorylated band upon anti-CD3 stimulation. The naïve $CD8^+$ T cells were purified from splenocytes of WT and leupaxin KO mice. Cells were stimulated with anti-CD3 (10 μg/ml) and anti-CD28 (3 μg/ml) antibodies for activation. At day six post-stimulation, cells were stimulated with the anti-CD3 antibody (10 μg/ml) at various time points. Cell lysates corresponding to 4×10^5 cells were separated by SDS-PAGE. Immunoblots were probed with the indicated antibodies. The arrow pointed to the specific tyrosine phosphorylated band which showed a reduction in leupaxin deficient CTL. Experiments were performed three times, and representative immunoblots are shown.

position of this phosphorylated band was very close to the Pyk2 band. Thus, Pyk2 phosphorylation and activation will be further determined in the next section.

5.2.4. Pyk2 reduces tyrosine phosphorylation at Tyr579 and Tyr580 in leupaxin deficient CTL upon anti-CD3 stimulation

To verify whether the reduced phosphorylated band in the above experiment **(Figure 5.3)** was Pyk2, I immunoprecipitated Pyk2 from cell lysates of anti-CD3 stimulated CTL generated from WT, heterozygous and leupaxin KO mice, and probed with anti-phosphotyrosine antibody 4G10. As shown in **Figure 5.4**, Pyk2 exhibited increased tyrosine phosphorylation, upon CD3 stimulation. However, Pyk2 immunoprecipitated from leupaxin deficient CTL reduced tyrosine phosphorylation, compared to the WT and heterozygous CTL. This confirmed my speculation that the reduced phosphorylated band was most likely Pyk2.

The current model for Pyk2 activation is based on studies of FAK that the autophosphorylation at Tyr402 recruits a Src family kinase, which in turn phosphorylates Pyk2 at Tyr578 and Tyr580, leading to Pyk2 activation [193]. Next, I stripped and re-probed with various phospho-Pyk2 antibodies. I detected reduced phosphorylation at Tyr578 and Tyr580, but not Tyr402, after leupaxin deletion. This implied that leupaxin may facilitate Pyk2 activation upon TCR engagement. As leupaxin constitutively associated with Pyk2, I hypothesized that leupaxin promoted Pyk2 activation via association with Src-family kinases. In addition, I also examined paxillin in Pyk2 immunoprecipitates. It was found that paxillin increased association with Pyk2 after leupaxin deletion **(Figure 5.4)**. Although

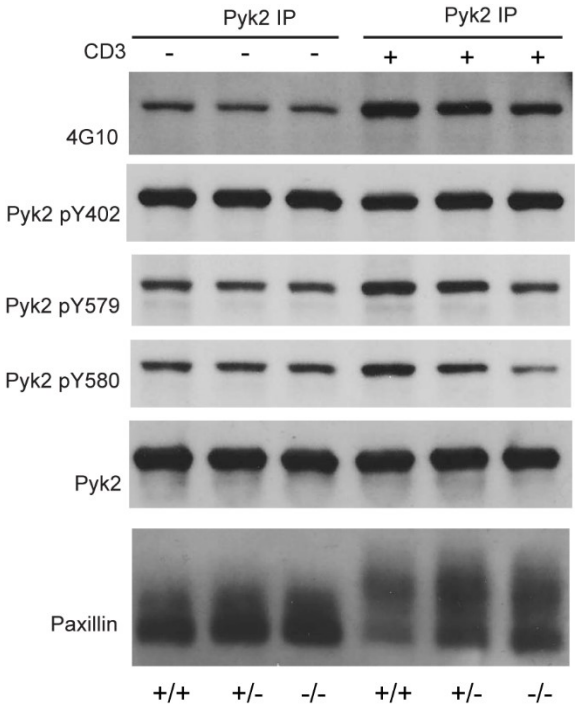

Figure 5.4. Pyk2 reduces tyrosine phosphorylation at Tyr579 and Tyr580 in leupaxin deficient CTL upon anti-CD3 stimulation. The naïve $CD8^+$ T cells were purified from splenocytes of WT, heterozygous and leupaxin KO mice. Cells were stimulated with anti-CD3 (10 μg/ml) and anti-CD28 (3 μg/ml) antibodies for activation. At day six post-stimulation, cells were stimulated with anti-CD3 antibody for 25 minutes. Pyk2 was immunoprecipitated from lysates corresponding to 10 million cells with Pyk2 F245 antibodies. Proteins were separated by SDS-PAGE, followed by transferring to PVDF membrane. Immunoblots were probed with the indicated antibodies. Experiments were performed two times, and representative immunoblots are shown.

paxillin and leupaxin formed distinct complex with Pyk2, this result suggested that they may still compete with each other for binding to Pyk2.

5.2.5. Leupaxin deletion does not affect MTOC reorientation, degranulation and killing when pulsed with the OVA N4 peptide

Both NK cells and CTL utilize a similar mechanism for degranulation, which is characterized by the reorientation of MTOC and directional release of lytic granules [243]. The Long group has found a novel signaling network centered on integrin-linked kinase (ILK)-Pyk2-leupaxin which was required for MTOC reorientation and granule retention in NK cells [244]. To address whether leupaxin regulated these process in CTL, I used *ex vivo* activated OT-1 CTL to investigate leupaxin function. The splenocytes separated from OT-1 transgenic mice were stimulated with $OVA_{257-264}$ N4 peptide (SIINFEKL), the ligand for the OT-1 receptor in the presence of IL-2. Six days after stimulation, cells were collected to perform various functional assays.

I first analyzed the MTOC reorientation during CTL degranulation. As shown in **Figure 5.5A**, the target cells L1210K^b/D^d were labeled with CellTrace blue and pulsed with OVA N4 peptide (10 nM). I detected no difference between WT and leupaxin deficient OT-1 transgenic CTL. They both exhibited a high percentage of the MTOC reorientation. In addition, I also measured the CTL degranulation by flow analysis of externalized CD107a. The *ex vivo* activated OT-1 T cells were mixed with $OVA_{257-264}$ N4 peptide-pulsed target cells at the ratio of 1:2. Cells were centrifuged at 4 ^oC for 3 minutes to facilitate the conjugation. At each time point, cells were fixed and stained for CD107a. However, there was no

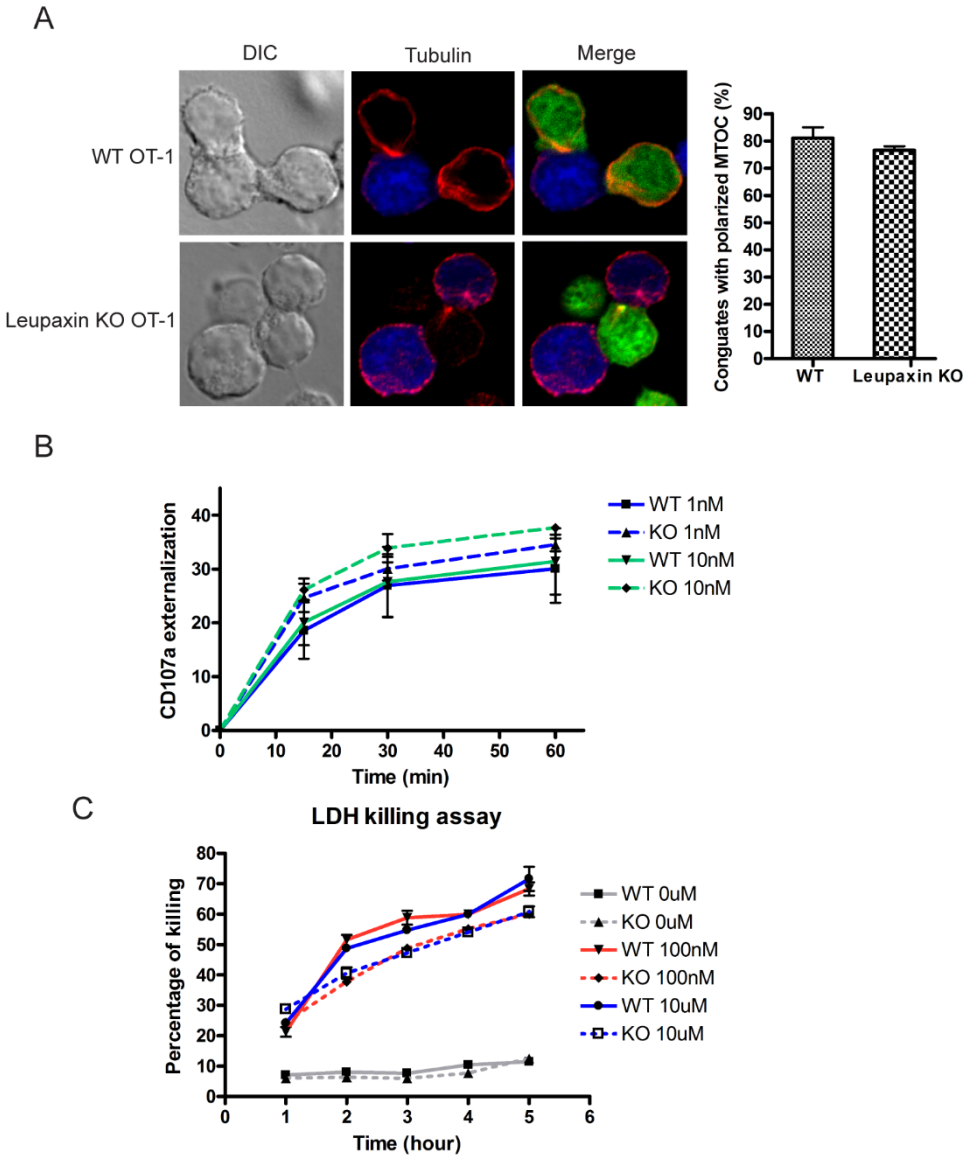
A
DIC
Tubulin
Merge
WT OT-1
Leupaxin KO OT-1
Conguates with polarized MTOC (%)
WT
Leupaxin KO
B
CD107a externalization
Time (min)
WT 1nM
KO 1nM
WT 10nM
KO 10nM
C
LDH killing assay
Percentage of killing
Time (hour)
WT 0uM
KO 0uM
WT 100nM
KO 100nM
WT 10uM
KO 10uM

Figure 5.5. Leupaxin deletion does not affect MTOC reorientation, degranulation and killing when pulsed with OVA N4 peptide. (A) Splenocytes were separated from WT or leupaxin KO OT-1 mice and then stimulated with OVA N4 peptides in the presence of IL-2 for T cell activation. At day 6 post-stimulation, OT-1 CTL were collected and labeled with CellTracker green. L1210K^b/D^d target cells were labeled with CellTracker blue and pulsed with OVA N4 (10 nM) peptide. T cells were mixed with target cells and centrifuged for 3 minutes at 37 ^oC to facilitate conjugation. After incubation for 5 minutes at 37 ^oC, cells were fixed, permeabilized and stained for α-tubulin (detected by anti-rabbit Alexa Fluor 594) to determine the MTOC reorientation. At least 60 conjugates were captured for each group and repeated for 3 times. (B) L1210K^b/D^d target cells were labeled with CellTracker blue, followed by pulsing with OVA N4 peptide for various concentrations. OT-1 T cells were labeled with CellTracker green, followed by mixing with target cells at a 2:1 ratio. Cells were centrifuged for 3 minutes at 100g in 4 ^oC centrifuge to facilitate the conjugation. Cells were incubated at 37 ^oC in the presence of APC-conjugated anti-CD107a antibody for the indicated time points. After each time point, cells were fixed, washed and analyzed by flow cytometry. Experiments were repeated three times. (C) L1210K^b/D^d target cells were pulsed with OVA N4 peptide for various concentrations as above. OT-1 T cells were mixed with the target cells at a 5:1 ratio in V-bottom 96-well plates. Cells were centrifuged for 3 minutes at 100 g in a 4 ^oC centrifuge, followed by incubation at 37 ^oC for the indicated times. After each time, 50 μl of the sample medium were transferred to new 96-well plates and mixed with 50 μl reaction medium, followed by incubation for 10 minutes at room temperature. The reaction was stopped by adding 50 μl stopping reagent. Plates were read for the absorbance at 490 nm. All experiments were repeated three times. The error bar represents standard error of the mean.

difference detected between WT and leupaxin deficient T cells in degranulation. Even though I diluted the OVA N4 peptide concentration from 10 nM to 1 nM, there was no decrease in CTL degranulation. This result suggested that I should further dilute the OVA N4 peptide concentration, as the TCR signaling strength was still very strong.

In addition to degranulation assay, I also determined the level of CTL killing by LDH (lactate dehydrogenase) assay. LDH is a cytosolic enzyme which is present in the cells. When the cell membrane is damaged, LDH is released from cell and detected by the enzymatic reaction [245]. The target cells were pulsed with $OVA_{257-264}$ N4 peptide at various concentrations and mixed with T cells at a ratio of 1:5. I detected a slight decrease in CTL killing in the absence of leupaxin **(Figure 5.5C)**, however it was not statistically significant.

5.2.6. Leupaxin deficient OT-1 CTL shows impaired MTOC reorientation when pulsed with OVA T4 peptide

It was previously shown that the strength of TCR signaling controls the polarization of MTOC and lytic granules in CTL [246]. The OVA N4 peptide is a strong agonist with high affinity for the transgenic OT-1 TCR. Even when I diluted the concentration of N4 antigen to 1 nM, CTL degranulation was not affected **(Figure 5.5B)**. I wondered if it was due to the cognate H-$2K^b$/ OVA N4 peptide complex was such a strong agonist that I was unable to detect the functional difference between WT and leupaxin deficient CTL. Indeed, it has been shown that OVA N4 peptide alone was enough to activate the naïve $CD8^+$ T cells, whereas the

low-affinity OVA N4 variant peptide T4 required the provision of IL-2 and costimulatory molecules [247].

In order to titrate down the stimulation strength OT-1 transgenic CTL received, I tested the other two OVA N4 variant T4 peptide (SIITFEKL) and G4 peptide (SIIGFEKL). The target cells L1210K^b/D^d were pulsed with OVA N4, T4 and G4 peptides at various concentrations. Target cells were mixed with the WT OT-1 CTL at the ratio of 2:1 and the level of CTL degranulation was measured as above. Even diluted from 1 μM to 1 nM, the strong agonist OVA N4 peptide still stimulated high CTL degranulation **(Figure 5.6A)**. When OVA T4 peptide was titrated from 1 μM to 1 nM, I was able to titrate down the TCR signaling and the level of CTL degranulation. Whereas OVA G4 peptide was a very weak agonist with low-affinity to the TCR. It only stimulated CTL for a low level of degranulation. As the OVA T4 peptide gave me a broad range to titrate down the antigen for CTL degranulation, I used the OVA T4 peptide to investigate the role of leupaxin in the following functional experiments.

First I measured the degree of MTOC reorientation by pulsing target cells with various concentrations of T4 peptide. The conjugates were prepared, fixed and permeabilized as above. The MTOC was stained with anti-α-tubulin antibody and detected with Alexa Fluor 594. As shown in **Figure 5.6B&C**, I detected a significant decrease of the MTOC reorientation in leupaxin deficient OT-1 CTL. The degree of the MTOC reorientation depends on OVA T4 peptide concentration. I detected almost 50% decrease at the concentration of 100 nM. Thus, consistent with the role of leupaxin in NK cells, leupaxin also regulated the MTOC

reorientation during CTL degranulation. It was noted that there was still around 50% of CTL conjugates showing normal MTOC reorientation. As our lab has previously shown that paxillin also regulated MTOC reorientation during CTL conjugation [77], it was possible that paxillin may compensate for the function after leupaxin deletion.

I also rescued the MTOC reorientation by transfecting leupaxin back into the leupaxin deficient T cells. First, the naïve OT-1 transgenic leupaxin deficient T cells were activated with OVA N4 peptide for 48 hours as above. Three days after activation, the leupaxin deficient CTL were nucleofected with either GFP or GFP-leupaxin constructs. Twenty-four hours after transfection, cell staining was prepared as above. Leupaxin transfection led to approximately 30% increase in MTOC reorientation **(Figure 5.6D)**. This further confirmed that leupaxin regulated the MTOC reorientation during CTL degranulation.

In chapter 4, I have demonstrated that leupaxin is serine phosphorylated at Ser54 upon TCR engagement, but the function of this serine phosphorylation is unknown. To determine if it regulated the MTOC reorientation, I transfected leupaxin Ser54A mutant back into the leupaxin deficient T cells as above. Similarly, the mutant transfection led to approximately 30% increase in MTOC reorientation. I concluded that leupaxin phosphorylation at Ser54 did not impact MTOC reorientation. As the MTOC reorients towards the target cells as early as 3 minutes after the TCR is activated, the serine phosphorylation is probably involved in later stages of CTL function [74].

A

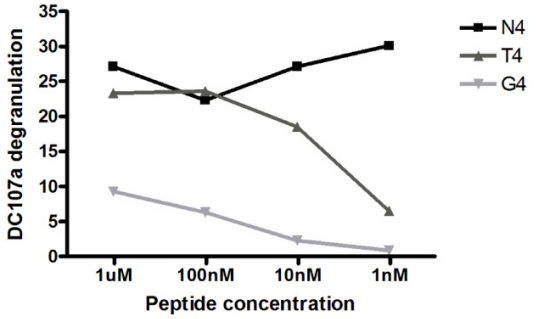
DC107a degranulation
35
30
25
20
15
10
5
0
1uM
100nM
10nM
1nM
Peptide concentration
N4
T4
G4

B

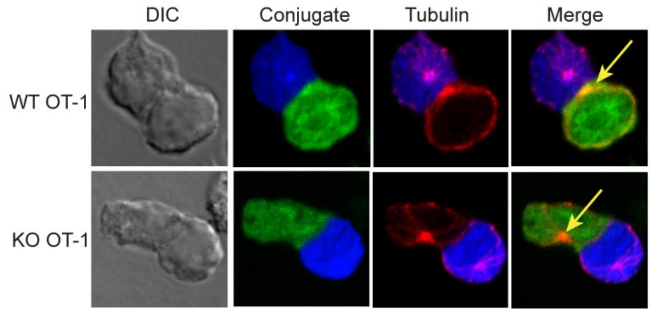
DIC
Conjugate
Tubulin
Merge
WT OT-1
KO OT-1

C

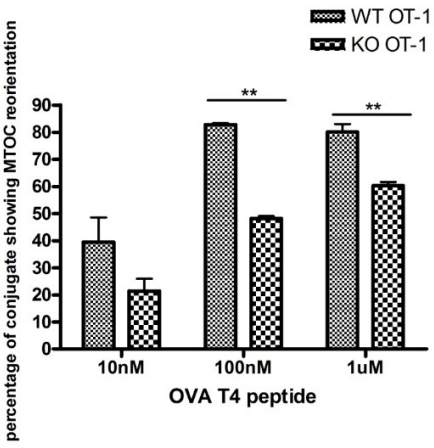
WT OT-1
KO OT-1
percentage of conjugate showing MTOC reorientation
90
80
70
60
50
40
30
20
10
0
**
**
10nM
100nM
1uM
OVA T4 peptide

D

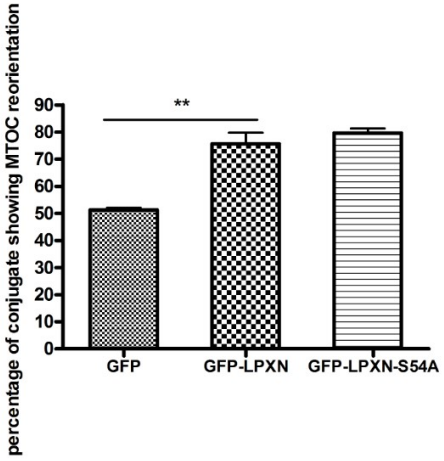
percentage of conjugate showing MTOC reorientation
90
80
70
60
50
40
30
20
10
0
**
GFP
GFP-LPXN
GFP-LPXN-S54A

Figure 5.6. Leupaxin deficient OT-1 CTL shows impaired MTOC reorientation when pulsed with OVA T4 peptide. (A) L1210K^b/D^d target cells were labeled with CellTracker blue and pulsed with various OVA peptides for the indicated concentration. T cells were mixed with the target cells for conjugation. Degranulation assay was performed as in Figure 5.5. The experiment was performed once. (B) OT-1 CTL were labeled with CellTracker green and then mixed with L1210K^b/D^d target cells which were labeled with CellTracker blue and pulsed with OVA T4 peptide. Cell staining of MTOC was performed as above. Images were collected by confocal microscopy. The yellow arrow pointed to the MTOC. (C) The conjugates that showed clearly MTOC staining was quantified for the MTOC reorientation. At least 60 conjugates were captured from repeated experiments of 3 times. (D) OT-1 transgenic leupaxin KO T cells were transfected with the indicated plasmids at day 4 post-stimulation. Twenty-four hours after transfection. T cells were collected, labeled with CellTracker green and mixed with T4 (100 nM) pulsed L1210K^b/D^d target cells which were pre-labeled with CellTracker blue. Cells were fixed, permeabilized and stained for α-tubulin as above. The conjugates were quantified for the MTOC reorientation. At least 60 conjugates were captured from repeated experiments of 3 times. The unpaired student *t*-test was used for statistical analysis. ** represents $p < 0.01$. The error bar represents standard error of the mean.

5.2.7. Leupaxin deletion does not affect CTL degranulation and killing when pulsed with OVA T4 peptide

Next, I measured the CTL degranulation and killing by pulsing target cells with OVA T4 peptide. The WT and leupaxin deficient OT-1 T cells were activated by OVA N4 peptide as above. The CD107a based degranulation assay suggested no difference between WT and leupaxin deficient OT-1 T cells **(Figure 5.7A)**. One possibility is that the degree of degranulation is not affected, but the granules are not released specifically towards the target cells. Thus, I attempted to stain for the lytic granules with anti-perforin antibody to determine whether granules were reoriented towards the target cells. However, I was unable to detect the lytic granules, due to the fact that the cytotoxic granules in *ex vivo* activated OT-1 T cells were barely detectable using this method. To solve this problem, live cell imaging will need to be performed with the lytic granules labeled with Lysotracker. The dynamics of granule reorientation will then need to be imaged by time-lapse confocal microscopy.

In addition to degranulation, CTL cytotoxicity was measured by LDH assay as before. I detected no difference in CTL cytotoxicity between WT and leupaxin deficient CTL **(Figure 5.7B)**. When I pulsed L1210K^b/D^d target cells with T4 peptide, the degree of killing was much lower than the N4 peptide, suggesting a decreased TCR signaling received by CTL. I only obtained 30% of target cell death at 5 hour after incubation. This was in contrast to the high level of killing when pulsed with N4 peptide, in which I detected more than 40% of killing at 2 hour after incubation. One explanation for the result is that such low degree of killing may not

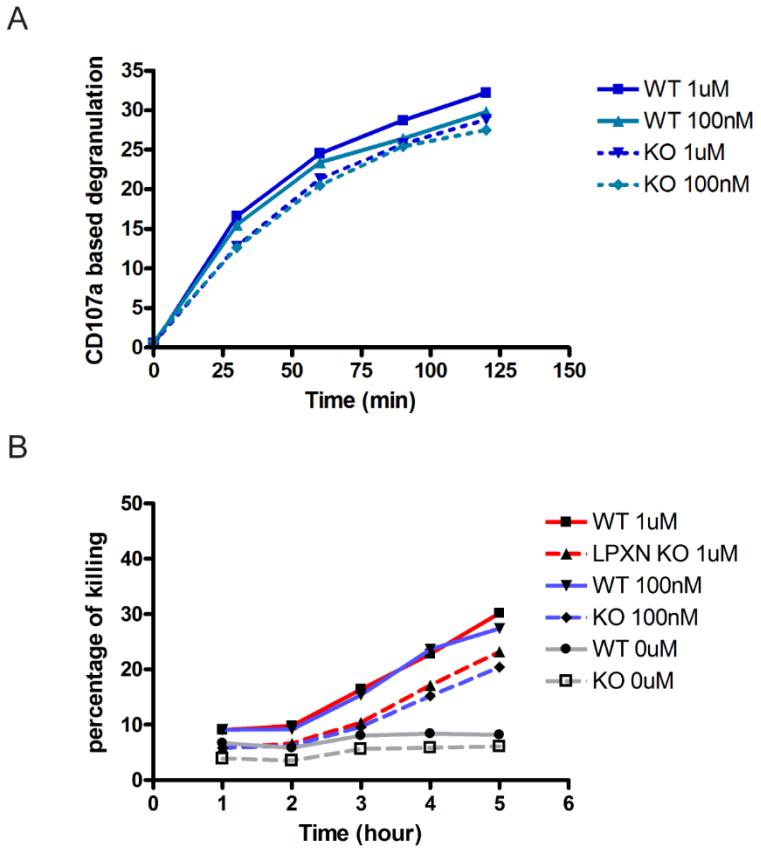

Figure 5.7. Leupaxin deletion does not affect CTL degranulation and killing when pulsed with OVA T4 peptide. (A) L1210K^{b}/D^{d} target cells were labeled with CellTracker blue and pulsed with OVA T4 peptide for the indicated concentration. OT-1 T cells were labeled with CellTracker green and mixed with target cell for degranulation assay, as in Figure 5.5. After each time point, cells were fixed, washed and analyzed by flow cytometry. (B) L1210K^{b}/D^{d} target cells were pulsed with OVA T4 peptide for various concentrations. LDH killing assay was performed as that in Figure 5.5. Plates were read for the absorbance at 490nm. Both degranulation and LDH killing assay were performed once.

allow us to distinguish the difference between WT and leupaxin deficient CTL. Further experiments should be performed by using more sensitive killing assays, such as the chromium-release assay. In addition, bystander killing assay will be carried out to determine whether loss of leupaxin leads to the non-directional release of cytotoxic granules and non-specific killing of target cells.

5.2.8. Leupaxin deletion does not affect CTL migration velocity on ICAM-1

In chapter 3, I have shown that overexpression of leupaxin in CTL clone 11 decreased the migration velocity on ICAM-1 **(Figure 3.9)**. This led me to determine the migration of leupaxin deficient CTL on ICAM-1. I purified the naïve $CD8^+$ T cells from splenocytes and activated them by anti-CD3 and anti-CD28 antibodies as above. The cell migration velocity was measured by time-lapse confocal microscopy. However, there was no difference in migration velocity between WT and leupaxin deficient CTL **(Figure 5.8)**. As our results showed that both paxillin and leupaxin had similar functions in CTL adhesion and spreading, one possible explanation was that paxillin might compensate for leupaxin function when leupaxin is absent.

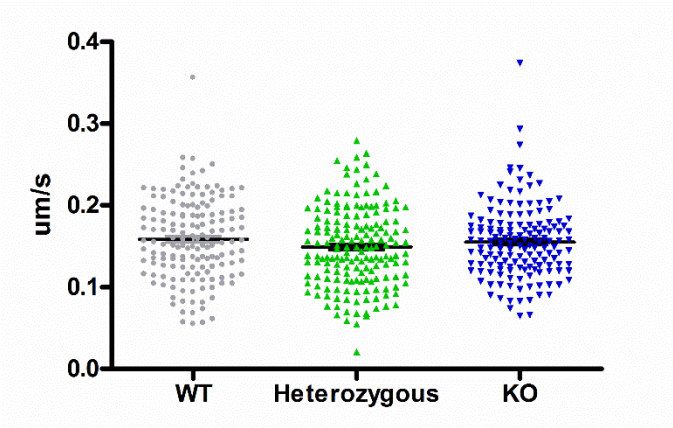

Figure 5.8. Leupaxin deletion does not affect the CTL migration velocity on ICAM-1. The naïve $CD8^+$ T cells were purified from splenocytes of WT, heterozygous and leupaxin KO mice. Cells were stimulated with anti-CD3 (10 μg/ml) and anti-CD28 (3 μg/ml) antibodies for activation. After activation, cells were transferred to chamber coverglass coated with ICAM-1. After incubation at 37ºC for 45 minutes, cell migration was tracked by spinning disk confocal microscopy for 10 minutes. The average migration velocity was measured by imageJ. At least 150 cells were analyzed for each group from 3 repeated experiments. The error bar represents standard error of the mean.

5.3. Discussion

In this chapter, we generated the germline leupaxin knockout mice and evaluated the role of leupaxin in TCR signaling and degranulation. To our knowledge, this is the first leupaxin knockout mice generated and the first evidence showing the contribution of leupaxin in primary CTL. Previous studies carried out in several cell lines suggested a negative regulatory role of leupaxin [148, 162, 163]. However, our results of leupaxin deficient CTL have demonstrated that leupaxin is required for optimal TCR signaling. Furthermore, our data is consistent with studies of leupaxin in NK cells, supporting the regulation of leupaxin in MTOC reorientation during conjugation with the target cells.

Paxillin, Hic-5 and leupaxin knockout mice have now all been generated, however paxillin knockout mice is the only one that is embryo lethal [136]. The reason is that loss of paxillin prevents the development of mesodermally derived structures [136]. Compared with paxillin which is ubiquitously expressed, Hic-5 and leupaxin exhibit restricted expression. Both Hic-5 and leupaxin deficient mice are viable and breed normally. As leupaxin is preferentially expressed in leukocytes, we expected that there might be a defect in T cell development in the thymus, as thymocytes need to interact with other cells for positive and negative selection. However, the T cell development in the thymus is normal. It is still possible that paxillin may compensate for leupaxin after deletion, even though we did not detect an obvious upregulation of paxillin expression. Based on the expression profile of paxillin and leupaxin in thymocytes **(Figure 1.4)**, it is also possible that paxillin

plays more important roles in T cell development. Conditional knockout mice may be developed to determine the role of paxillin and leupaxin in T cell development.

Leupaxin has gained a lot of interest due to previous studies showing that it may function as a negative regulator. However, these experiments were mainly performed by overexpression of leupaxin in transformed cell lines [148, 163]. Many tumor cells have been shown to have aberrant expression of paxillin family proteins and abnormal integrin signaling [143], thus these studies may not represent the role of leupaxin in physiological conditions. Structural analysis of leupaxin-Pyk2 complex has demonstrated that leupaxin has higher affinity with Pyk2 than paxillin, thus may function as a native binding partner of Pyk2 and compete with paxillin [152]. However, these results do not support directly that leupaxin can compete with paxillin for binding to Pyk2 in cells. To explore the role of leupaxin in TCR signaling, we first determined the overall tyrosine phosphorylation upon TCR stimulation. The majority of phosphorylated bands from leupaxin deficient CTL was similar to that from WT CTL, except for one band at the Pyk2 position. Indeed, further experiment indicated that Pyk2 reduced the tyrosine phosphorylation at Tyr579/Tyr580. Pyk2 is tyrosine phosphorylated by Src kinase during TCR signaling [248]. It has been shown that Pyk2 is required for optimal T cell activation, proliferation and $CD8^+$ T cell response *in vivo* [249]. In the A20 cell, leupaxin negatively regulated BCR signaling by suppressing JNK, p38 and Akt phosphorylation [163]. If leupaxin functions as a negative regulator, I thought I would detect increased overall tyrosine phosphorylation in leupaxin deficient CTL. However, the biochemistry result did not support my initial hypothesis. Thus,

instead of supporting leupaxin as a negative regulator, our data suggested that leupaxin is required for optical Pyk2 activation and TCR signaling. Although I am comparing different cell types, my data may represent the real leupaxin function in the physiological situation as we used the *ex vivo* activated $CD8^+$ T cells whereas previous studies were carried out in transformed cell lines.

The majority of previous studies focused on the role of leupaxin in integrin-mediated spreading and migration. T cells and NK cells not only utilize LFA-1 for migration, but also for the formation of the immunological synapse before degranulation. Dr. Long's group has shown that knockdown of leupaxin expression in primary NK cells impaired MTOC reorientation during conjugation with the target cells. Similarly, I found that leupaxin regulated MTOC reorientation during CTL degranulation. This phenotype was only detected when I used the OVA T4 peptide, but not the N4 peptide. Similar to leupaxin, our lab has previously demonstrated that paxillin also contributed to MTOC reorientation in CTL. Again this result suggested that paxillin and leupaxin have similar roles in regulating CTL function. But whether paxillin and leupaxin are redundant in CTL is unknown. I speculate that although paxillin and leupaxin have many similarities in CTL, leupaxin may have a unique role in specific cellular processes.

Dr. Long's group also showed that leupaxin regulated the granule convergence and retention at the MTOC in NK cells, although they used a NK cell line in which the lytic granules constitutively colocalized with the MTOC which does not happen in *ex vivo* CTL [107]. As the granules polarize towards the target cells along the microtubules after MTOC reorientation, it is expected that loss of

leupaxin will reduce directional movement of granules. I addressed this question in CTL by staining lytic granules with the anti-perforin antibody. However, due to the fact that the lytic granules were far too small in *ex vivo* T cells, I was unable to detect the localization of the granules. So I cannot determine the role of leupaxin in granule reorientation using this approach. One possible solution is to visualize the granule reorientation process by live cell imaging. This will be addressed in future experiments.

In the proposed degranulation model, MTOC reorientation allows the directional release of cytotoxic granules specific to target cells. I determined whether reduced MTOC reorientation would impair degranulation in leupaxin deficient CTL. No difference was detected between WT and leupaxin deficient CTL. One possibility is that granules are released but not directionally towards the target cells. Indeed, some study has suggested that the granule release can still occur in the absence of MTOC reorientation [250]. The non-directional release of granules may kill target cells non-specifically. This will be tested by the bystander killing assays. Another possibility is that paxillin may compensate for leupaxin function in degranulation. Knockdown of paxillin in leupaxin deficient CTL will be performed to address this question.

I have demonstrated a role of paxillin and leupaxin in CTL migration on ICAM-1. Our results suggested that both paxillin and leupaxin promoted LFA-1 mediated adhesion. In order to confirm the role of leupaxin in CTL migration, I measured the migration velocity of activated OT-1 CTL on ICAM-1. However, I did not detect a difference between WT and leupaxin deficient CTL. One possibility

is that paxillin has similar roles with leupaxin in LFA-1 mediated adhesion and compensates for leupaxin function. I detected a reduced migration velocity on ICAM-1 by overexpression. However, it would be difficult to detect an increase in CTL migration on ICAM-1 in the absence of leupaxin, since CTL already moves very fast. Future experiments can be performed by using the endothelial cell layer model or *in vivo* model to study the role of leupaxin in CTL migration.

CHAPTER 6: General discussion

6.1. Summary of results

6.1.1. Leupaxin promotes TCR-stimulated Pyk2 activation

Leupaxin has been demonstrated to be tyrosine phosphorylated in response to cell stimuli in several cell types [162, 163, 187], but these studies are mainly performed in transformed cell lines. To explore the role of leupaxin in CTL signaling, we first generated a high-affinity anti-leupaxin serum. With this serum, we showed that leupaxin underwent robust tyrosine phosphorylation when TCR signaling was activated with anti-CD3 antibody stimulation. This suggests that leupaxin is involved in the TCR signaling cascade. But whether leupaxin is in the 'inside-out' signaling that activates LFA-1 or in the 'outside-in' signaling that controls effector function is unknown, however it is difficult to separate these two signaling pathways. Based on studies of leupaxin in NK cells in which a signaling pathway of ILK-Pyk2-leupaxin controls NK cell effector function, I speculate that leupaxin functions as an adaptor protein mainly in the 'outside-in' signaling pathway. I found that this tyrosine phosphorylation was dependent on Lck and Pyk2 kinase activity. Consistent with previous publications [152], I found that leupaxin constitutively associated with Pyk2. As Lck is required for Pyk2 activation, I proposed a signaling pathway of Lck-Pyk2-leupaxin that led to leupaxin phosphorylation upon TCR engagement.

In addition to tyrosine phosphorylation, I detected the unique leupaxin mobility shift upon TCR stimulation, which I later identified to be mediated by a single phosphorylation at Ser54. The kinetics showed that this serine

phosphorylation occurred later than the tyrosine phosphorylation. Inhibition of Lck, Pyk2 and ERK activity all prevented the leupaxin mobility shift, suggesting that these kinases were in the same signaling pathway in leupaxin serine phosphorylation. Together, I proposed a signaling pathway, Lck-Pyk2-ERK, leading to leupaxin serine phosphorylation **(Figure 6.1)**.

To determine whether leupaxin negatively regulated TCR signaling, I compared the overall tyrosine phosphorylation between WT and leupaxin deficient CTL upon TCR stimulation. I found that Pyk2 exhibited reduced tyrosine phosphorylation at the two activation sites in leupaxin deficient CTL. As leupaxin constitutively associates with Pyk2, I propose the model that leupaxin facilitates Pyk2 activation by recruiting Pyk2 to Lck at the membrane for phosphorylation. Thus, instead of being a negative regulator, my data is consistent with leupaxin being required for optimal TCR signaling by promoting Pyk2 activation. Reciprocally, activation of Pyk2 by Lck is required for the subsequent leupaxin tyrosine and serine phosphorylation.

6.1.2. Leupaxin regulates LFA-1 mediated CTL migration on ICAM-1

As paxillin family proteins are cytoskeletal adaptor proteins in integrin signaling, the majority of leupaxin studies are carried out in adherent cells to determine its role in adhesion and migration. Different from adherent cells, leukocytes do not have stress fibers and classical focal adhesions. I found that both paxillin and leupaxin were recruited to the contact zone during CTL migration on ICAM-1, and formed the dynamic focal adhesion-like structures. This was

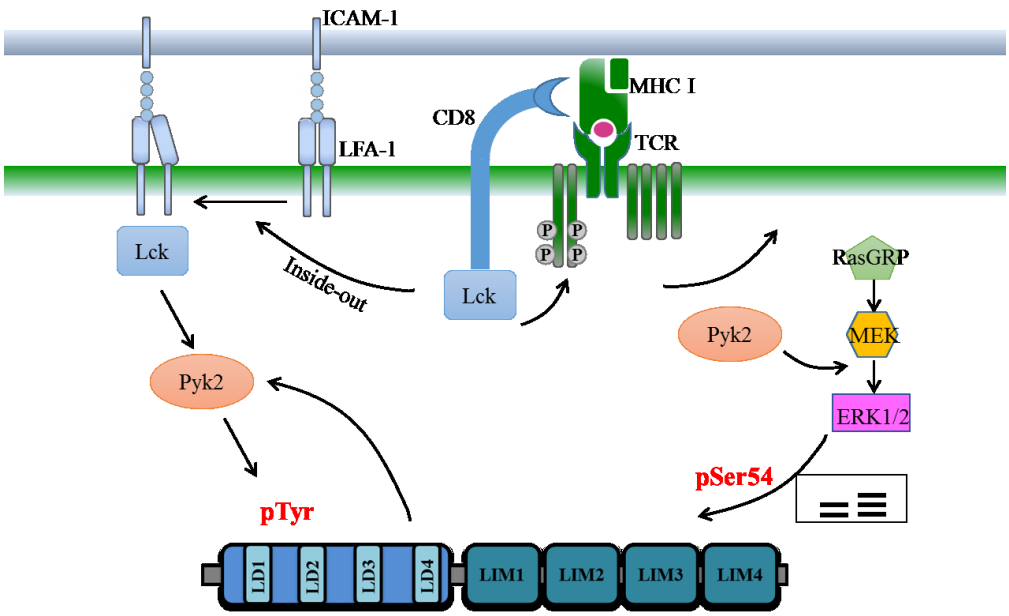

Figure 6.1. Proposed model for leupaxin function in the TCR signaling. TCR stimulation initiates the 'inside-out' signaling and activation of the kinases Lck and Pyk2. Pyk2 phosphorylates its binding partner leupaxin. Leupaxin in turn regulates Pyk2 activation probably by recruiting Pyk2 to the kinase Lck. Additionally, TCR engagement results in ERK activation and the following serine phosphorylation of leupaxin at Ser54, leading to leupaxin mobility shift.

consistent with a recently published paper showing that the focal adhesion proteins paxillin, vinculin and talin were recruited to the focal adhesion-like complexes during T cell spreading on ICAM-1 [203]. We showed that the focal adhesion-like structures which contained paxillin, leupaxin, vinculin and talin were assembled at the leading edge, but absent at the focal zone **(Figure 6.2A)**. The Hogg group has demonstrated that the leading edge mainly contained the intermediate-affinity LFA-1, whereas the focal zone contained the high-affinity LFA-1 [132, 133]. This is in contrast to the classical focal adhesions in adherent cells, where these focal adhesion proteins connected to the high-affinity integrin [198, 216]. T cells may form less adhesive complexes to maintain high motility for migration.

Previous studies showed that leupaxin suppressed integrin-mediated cell spreading in NIH 3T3 cells and breast cancer cells [148, 162]. I repeated the NIH 3T3 cell spreading experiment by leupaxin overexpression. Surprisingly, instead of suppressing cell spreading, leupaxin promoted cell spreading on fibronectin. I cannot explain why the result we obtained was completely opposite with previous publication. In addition, Dr. Samuel Cheung also overexpressed leupaxin in *ex vivo* activated OT-1 T cells, and found that leupaxin promoted CTL spreading on ICAM-1 (S. Cheung and H. Ostergaard, unpublished observation). Thus, I concluded that leupaxin was recruited to the adhesive complexes and promoted cell adhesion and spreading at the protrusion of CTL. I also tracked the CTL migration after overexpression of leupaxin, and found that CTL reduced the migration velocity. I speculated that overexpression of leupaxin enabled the adhesive complex to be more stable and disassembled less frequently, thus slowing cell migration.

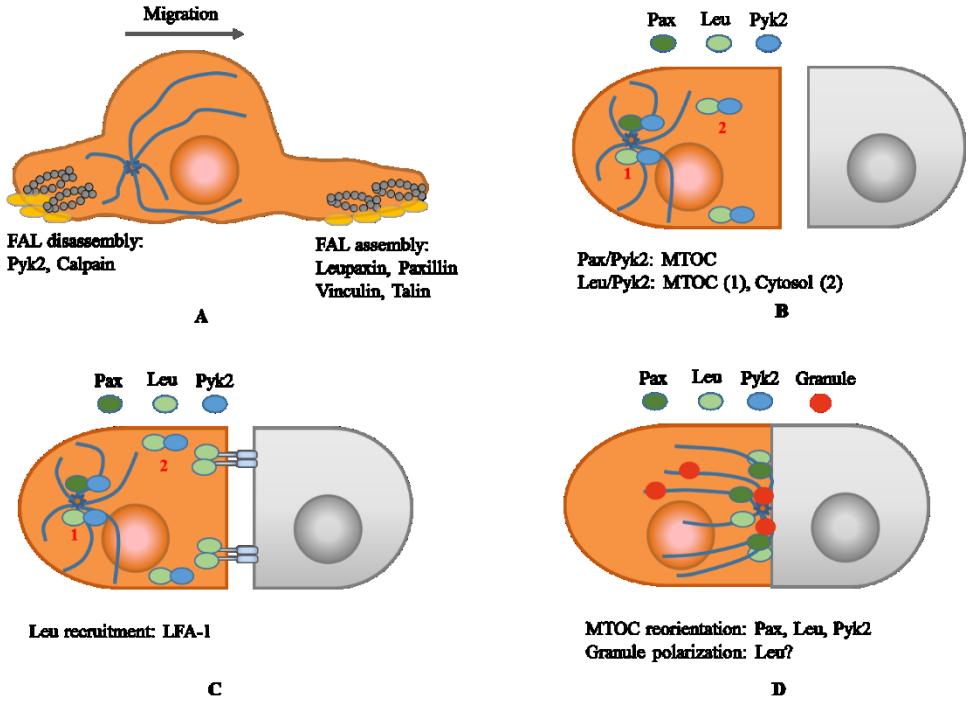

Figure 6.2. Proposed model for leupaxin localization and function in CTL. (A) Leupaxin is recruited to the focal adhesion-like structures at the leading edge during CTL migration. Paxillin, vinculin and talin also go to the focal adhesion-like structures. At the trailing edge, the focal adhesion-like structures are disassembled for turnover, which is dependent on Pyk2 and calpain. (B) In CTL, paxillin mainly associates with the F245 recognized Pyk2 and localizes at the MTOC, whereas leupaxin associates with both F245 and F298 recognized Pyk2 populations and localizes at both MTOC and the cytosol. (C). Leupaxin is recruited to the synapse by LFA-1 signaling when CTL contacts the target cell. This leupaxin population is very likely from the cytosol, as the MTOC is not reoriented yet. (D) Leupaxin regulates MTOC during CTL conjugation with the target cell. Other proteins that have been identified to regulate this process include paxillin and Pyk2.

6.1.3. Leupaxin regulates MTOC reorientation during CTL conjugation with the target cell

Although leupaxin is predominately expressed in leukocytes compared to the other two paxillin family members, its role in CTL has not been explored. I first showed that leupaxin was recruited to the immunological synapse. LFA-1 engagement with ICAM-1 is sufficient for the recruitment, suggesting a fast recruiting pattern after conjugation. We have found two populations of leupaxin-Pyk2 complexes in CTL, it is possible that this early recruiting leupaxin population is from the cytosol, as the MTOC has not reoriented in the absence of TCR signaling. Paxillin family proteins serve as cytoskeletal adaptor proteins that connect actin and microtubules [109], it is possible that leupaxin serves as the adaptor proteins between the two cytoskeletons, similar to IQGAP1. Indeed, I detected IQGAP1 in mass spectrometry analysis of leupaxin and paxillin immunoprecipitation. I also detected the association between paxillin and IQGAP1 by immunoprecipitation, but did not include this data in the thesis as I was unable to confirm the association between IQGAP1 and leupaxin. I propose a model that leupaxin is first recruited to the synapse by LFA-1 signaling when CTL initially contacts the target cell. Once TCR signaling is activated, the actin cytoskeleton is cleared away from the center of the synapse. Leupaxin functions as an adaptor protein that binds to the microtubule and actin cytoskeleton. The mechanical forces generated by actin reorganization pulls the MTOC towards the membrane **(Figure 6.3)**.

6.2. Conclusions

6.2.1. Leupaxin is not a negative regulator of CTL activation

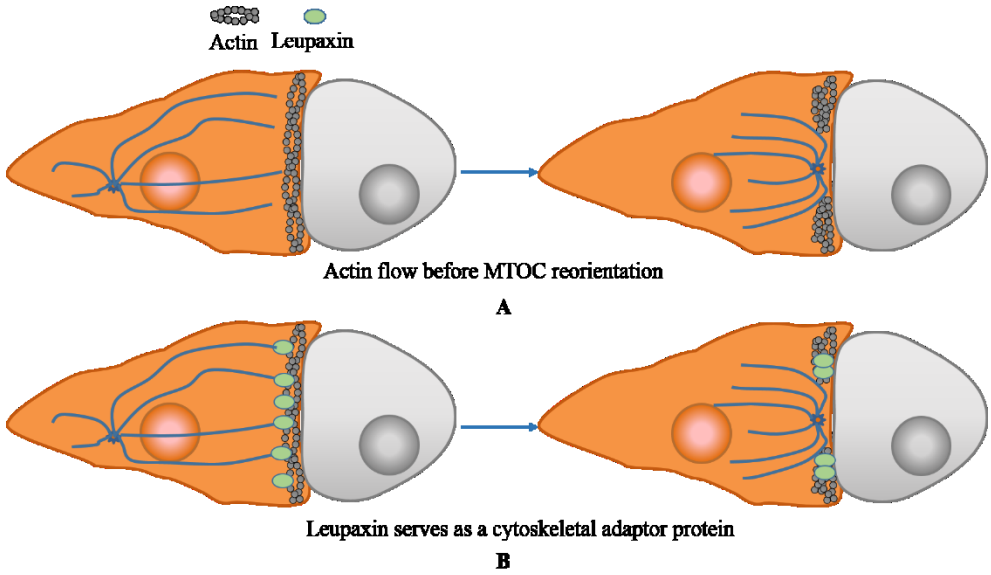

Figure 6.3. Proposed model of leupaxin in regulating MTOC reorientation. (A) Actin depletion has been proposed to drive MTOC reorientation in CTL. Before MTOC reorientation, the actin cytoskeleton first reorganizes at the immunological synapse and actin clears away from the center of the synapse. The generated forces from actin reorganization pull the MTOC towards the synapse. (B) Both paxillin and leupaxin function as cytoskeletal adaptor proteins and have been shown to associate with cytoskeletal proteins including tubulin, actomyosin and caldesmon. Thus, leupaxin may serve as bridge that connects both microtubules and actin cytoskeleton. During actin depletion, leupaxin supports the link between actin and microtubules and facilitates MTOC reorientation.

The direct evidence that supported leupaxin as a negative regulator came from literature studying the role of leupaxin in B cells. They showed that overexpression of leupaxin suppressed the phosphorylation of JNK, p38 and Akt upon BCR engagement [163]. Furthermore, overexpression of leupaxin reduced IL-2 secretion in A20 cells [163]. The problem is that all of the experiments were performed in transformed B lymphoma cell line upon overexpression of leupaxin, raising whether it can represent leupaxin function in primary B cells. Even if leupaxin could suppress IL-2 production in non-transformed B cells, it is not enough to support that leupaxin is a negative regulator of BCR signaling and B cell function. In addition to this, another study suggested leupaxin as a negative regulator because overexpression of leupaxin suppressed paxillin phosphorylation [148]. But one possibility is that leupaxin overexpression decreased paxillin-Pyk2 association and the following phosphorylation.

We generated the leupaxin KO mice and I first determined the TCR stimulated tyrosine phosphorylation. The leupaxin deficient CTL showed reduced Pyk2 tyrosine phosphorylation and activation. Dr. Samuel Cheung also examined the cytokine production including IFN-γ and TNF-α from *ex vivo* stimulated CTL but no difference was detected between WT and leupaxin deficient CTL. In $CD8^+$ T cells, Pyk2 is required for normal CTL adhesion, $CD8^+$ T activation and *in vivo* T cell response [154, 249]. Thus, I propose that instead of being a negative regulator, leupaxin is required for optimal TCR signaling and MTOC reorientation during CTL degranulation.

6.2.2. Leupaxin has similar functions to paxillin in CTL

It has been discussed extensively whether leupaxin has similar roles with paxillin and is redundant in regulating adhesion and migration, or antagonizes paxillin and has opposite roles [140, 148, 162, 163]. Two publications suggested that leupaxin inhibited cell adhesion and spreading in contrast to the role of paxillin which promotes adhesion [148, 162]. One publication showed that leupaxin has similar roles with paxillin and promoted cell adhesion and cell spreading on collagen and fibronectin [140]. However, all of these studies were performed in distinct cell lines, raising the question whether these phenotypes were cell-type specific. In addition, structural studies show that leupaxin has higher affinity for, and more stable conformation with Pyk2 [152], and assumed to be the preferred binding partner of Pyk2.

I repeated previously published results by overexpression of leupaxin in NIH 3T3 cells [148]. Surprisingly, I got completely contradictory results and paxillin and leupaxin both promoted cell spreading. Dr. Samuel Cheung obtained similar results when he overexpressed either paxillin or leupaxin in *ex vivo* OT-1 cells. In addition, overexpression of either paxillin or leupaxin in clone 11 reduced cell motility on ICAM-1, which could have been the result of increased adhesion, although this was not specifically addressed. Thus, all of my results supported that leupaxin and paxillin have similar roles adhesion and migration.

However, this does not mean leupaxin and paxillin are completely redundant in CTL. I have studied the distribution of leupaxin in CTL, and found that leupaxin formed two distinct complexes with Pyk2 F245 and F298 species, and this two Pyk2 complexes have been shown to have different localization in CTL

[196]. This is in contrast to paxillin which forms one major complex with Pyk2. Furthermore, I found that leupaxin was more dynamic than paxillin at the MTOC. Taken together, my results suggested that leupaxin has its unique role and participates in unique cellular processes compared to paxillin.

6.3. Future directions

I showed that leupaxin was a component of the focal adhesion-like structures in CTL and regulated CTL spreading and migration. How leupaxin is disassembled at the trailing edge is unknown. The majority of focal adhesion proteins including paxillin, talin, vinculin, integrin are substrates of calpain and the cleavage is necessary for focal adhesion turnover. I predicted with the online tool (GPS-CCD 1.0) that leupaxin was a potential substrate of calpain. Thus, future experiment will be performed to determine whether leupaxin is a substrate of calpain. If so, the cleavage sites could be identified and the importance of leupaxin cleavage by calpain in CTL migration will be explored.

Although I showed that leupaxin was tyrosine phosphorylated upon TCR engagement, I was unable to identify which tyrosine residue(s) are phosphorylated in CTL, due to the low transfection efficiency. Previous studies showed three tyrosine residues that were phosphorylated, Tyr22, Tyr62 and Tyr72. Future experiments can be performed by alanine substitution followed by Phos-tag-SDS-PAGE or mass spectrometry to locate the phosphorylated residues. In addition, the Phos-tag-SDS-PAGE will also tell us whether the initial leupaxin mobility shift is caused by phosphorylation. Once the phosphorylation sites are identified, the

importance of these phosphorylation sites in leupaxin localization and function will be determined by transfection back into the leupaxin deficient CTL.

Although I have demonstrated that leupaxin regulates the MTOC reorientation, we still do not know whether it is also important for the directional granule polarization. As a CD107a based degranulation assay did not detect a difference between WT and leupaxin deficient CTL, one possibility is that the granules were released non-directionally towards the target cells, which could cause non-specific killing of non-antigen bearing cells. This will be addressed by live cell imaging and bystander killing assays in future experiments.

The *in vivo* CTL response requires both CTL migration and CTL function. My *in vitro* results suggested that leupaxin regulated both CTL migration and MTOC reorientation during degranulation. Since we have generated the leupaxin KO mice, the role of leupaxin to CTL function *in vivo* will be determined. In collaboration with Dr. Gang in Dr. Kane's lab, Dr. Cheung has used the influenza virus infection model to investigate the role of leupaxin *in vivo*. Interestingly, they found that the leupaxin KO mice have a higher survival rate than the WT mice after infection. Preliminary analysis of $CD8^+$ T cell response in the lung showed that the leupaxin KO mice only had half the numbers of $CD8^+$ T cell in the lung at day 5 after infection, suggesting a defective CTL response. This might be due to a migration problem or activation and proliferation at the secondary lymphoid organs. Further experiments will be performed to identify the underlying mechanisms.

References

1. Brubaker, S.W., K.S. Bonham, I. Zanoni, and J.C. Kagan, *Innate immune pattern recognition: a cell biological perspective.* Annu Rev Immunol, 2015. **33**: p. 257-90.
2. Iwasaki, A. and R. Medzhitov, *Regulation of adaptive immunity by the innate immune system.* Science, 2010. **327**(5963): p. 291-5.
3. Iwasaki, A. and R. Medzhitov, *Control of adaptive immunity by the innate immune system.* Nat Immunol, 2015. **16**(4): p. 343-53.
4. Janeway, C.A., Jr., *Approaching the asymptote? Evolution and revolution in immunology.* Cold Spring Harb Symp Quant Biol, 1989. **54 Pt 1**: p. 1-13.
5. Lamkanfi, M. and V.M. Dixit, *Mechanisms and functions of inflammasomes.* Cell, 2014. **157**(5): p. 1013-22.
6. Deretic, V., T. Saitoh, and S. Akira, *Autophagy in infection, inflammation and immunity.* Nat Rev Immunol, 2013. **13**(10): p. 722-37.
7. Inaba, K. and R.M. Steinman, *Protein-specific helper T-lymphocyte formation initiated by dendritic cells.* Science, 1985. **229**(4712): p. 475-9.
8. Inaba, K., J.P. Metlay, M.T. Crowley, and R.M. Steinman, *Dendritic cells pulsed with protein antigens in vitro can prime antigen-specific, MHC-restricted T cells in situ.* J Exp Med, 1990. **172**(2): p. 631-40.
9. Chaplin, D.D., *Overview of the immune response.* J Allergy Clin Immunol, 2010. **125**(2 Suppl 2): p. S3-23.
10. Carsetti, R., *The development of B cells in the bone marrow is controlled by the balance between cell-autonomous mechanisms and signals from the microenvironment.* J Exp Med, 2000. **191**(1): p. 5-8.
11. Blackwell, T.K. and F.W. Alt, *Mechanism and developmental program of immunoglobulin gene rearrangement in mammals.* Annu Rev Genet, 1989. **23**: p. 605-36.
12. Batista, F.D. and N.E. Harwood, *The who, how and where of antigen presentation to B cells.* Nat Rev Immunol, 2009. **9**(1): p. 15-27.
13. Pape, K.A., D.M. Catron, A.A. Itano, and M.K. Jenkins, *The humoral immune response is initiated in lymph nodes by B cells that acquire soluble antigen directly in the follicles.* Immunity, 2007. **26**(4): p. 491-502.
14. Junt, T., E.A. Moseman, M. Iannacone, S. Massberg, P.A. Lang, M. Boes, K. Fink, S.E. Henrickson, D.M. Shayakhmetov, N.C. Di Paolo, N. van Rooijen, T.R. Mempel, S.P. Whelan, and U.H. von Andrian, *Subcapsular sinus macrophages in lymph nodes clear lymph-borne viruses and present them to antiviral B cells.* Nature, 2007. **450**(7166): p. 110-4.
15. Carrasco, Y.R. and F.D. Batista, *B cells acquire particulate antigen in a macrophage-rich area at the boundary between the follicle and the subcapsular sinus of the lymph node.* Immunity, 2007. **27**(1): p. 160-71.
16. Raphael, I., S. Nalawade, T.N. Eagar, and T.G. Forsthuber, *T cell subsets and their signature cytokines in autoimmune and inflammatory diseases.* Cytokine, 2015. **74**(1): p. 5-17.
17. Golubovskaya, V. and L. Wu, *Different Subsets of T Cells, Memory, Effector Functions, and CAR-T Immunotherapy.* Cancers (Basel), 2016. **8**(3).

18. Ciofani, M. and J.C. Zuniga-Pflucker, *The thymus as an inductive site for T lymphopoiesis.* Annu Rev Cell Dev Biol, 2007. **23**: p. 463-93.
19. Koch, U. and F. Radtke, *Mechanisms of T cell development and transformation.* Annu Rev Cell Dev Biol, 2011. **27**: p. 539-62.
20. Matloubian, M., C.G. Lo, G. Cinamon, M.J. Lesneski, Y. Xu, V. Brinkmann, M.L. Allende, R.L. Proia, and J.G. Cyster, *Lymphocyte egress from thymus and peripheral lymphoid organs is dependent on S1P receptor 1.* Nature, 2004. **427**(6972): p. 355-60.
21. von Boehmer, H., *Unique features of the pre-T-cell receptor alpha-chain: not just a surrogate.* Nat Rev Immunol, 2005. **5**(7): p. 571-7.
22. Shah, D.K. and J.C. Zuniga-Pflucker, *An overview of the intrathymic intricacies of T cell development.* J Immunol, 2014. **192**(9): p. 4017-23.
23. Anderson, G. and E.J. Jenkinson, *Lymphostromal interactions in thymic development and function.* Nat Rev Immunol, 2001. **1**(1): p. 31-40.
24. Kappes, D.J., X. He, and X. He, *CD4-CD8 lineage commitment: an inside view.* Nat Immunol, 2005. **6**(8): p. 761-6.
25. Hogquist, K.A., T.A. Baldwin, and S.C. Jameson, *Central tolerance: learning self-control in the thymus.* Nat Rev Immunol, 2005. **5**(10): p. 772-82.
26. Miyasaka, M. and T. Tanaka, *Lymphocyte trafficking across high endothelial venules: dogmas and enigmas.* Nat Rev Immunol, 2004. **4**(5): p. 360-70.
27. Bromley, S.K., T.R. Mempel, and A.D. Luster, *Orchestrating the orchestrators: chemokines in control of T cell traffic.* Nat Immunol, 2008. **9**(9): p. 970-80.
28. Nandi, A., P. Estess, and M. Siegelman, *Bimolecular complex between rolling and firm adhesion receptors required for cell arrest; CD44 association with VLA-4 in T cell extravasation.* Immunity, 2004. **20**(4): p. 455-65.
29. Evans, R., I. Patzak, L. Svensson, K. De Filippo, K. Jones, A. McDowall, and N. Hogg, *Integrins in immunity.* J Cell Sci, 2009. **122**(Pt 2): p. 215-25.
30. Shiow, L.R., D.B. Rosen, N. Brdickova, Y. Xu, J. An, L.L. Lanier, J.G. Cyster, and M. Matloubian, *CD69 acts downstream of interferon-alpha/beta to inhibit S1P1 and lymphocyte egress from lymphoid organs.* Nature, 2006. **440**(7083): p. 540-4.
31. Baeyens, A., V. Fang, C. Chen, and S.R. Schwab, *Exit Strategies: S1P Signaling and T Cell Migration.* Trends Immunol, 2015. **36**(12): p. 778-787.
32. Curtsinger, J.M. and M.F. Mescher, *Inflammatory cytokines as a third signal for T cell activation.* Curr Opin Immunol, 2010. **22**(3): p. 333-40.
33. Courtney, A.H., W.L. Lo, and A. Weiss, *TCR Signaling: Mechanisms of Initiation and Propagation.* Trends Biochem Sci, 2018. **43**(2): p. 108-123.
34. Chen, L. and D.B. Flies, *Molecular mechanisms of T cell co-stimulation and co-inhibition.* Nat Rev Immunol, 2013. **13**(4): p. 227-42.
35. Sharpe, A.H. and A.K. Abbas, *T-cell costimulation--biology, therapeutic potential, and challenges.* N Engl J Med, 2006. **355**(10): p. 973-5.

36. Rudd, C.E., A. Taylor, and H. Schneider, *CD28 and CTLA-4 coreceptor expression and signal transduction.* Immunol Rev, 2009. **229**(1): p. 12-26.
37. Snanoudj, R., C. Frangie, B. Deroure, H. Francois, C. Creput, S. Beaudreuil, A. Durrbach, and B. Charpentier, *The blockade of T-cell co-stimulation as a therapeutic stratagem for immunosuppression: Focus on belatacept.* Biologics, 2007. **1**(3): p. 203-13.
38. Rentenaar, R.J., J.L. Vosters, F.N. van Diepen, E.B. Remmerswaal, R.A. van Lier, and I.J. ten Berge, *Differentiation of human alloreactive CD8(+) T cells in vitro.* Immunology, 2002. **105**(3): p. 278-85.
39. Lindahl, K.F. and D.B. Wilson, *Histocompatibility antigen-activated cytotoxic T lymphocytes. II. Estimates of the frequency and specificity of precursors.* J Exp Med, 1977. **145**(3): p. 508-22.
40. Ngoenkam, J., W.W. Schamel, and S. Pongcharoen, *Selected signalling proteins recruited to the T-cell receptor-CD3 complex.* Immunology, 2018. **153**(1): p. 42-50.
41. Smith-Garvin, J.E., G.A. Koretzky, and M.S. Jordan, *T cell activation.* Annu Rev Immunol, 2009. **27**: p. 591-619.
42. Harder, T., *Lipid raft domains and protein networks in T-cell receptor signal transduction.* Curr Opin Immunol, 2004. **16**(3): p. 353-9.
43. Horejsi, V., *The roles of membrane microdomains (rafts) in T cell activation.* Immunol Rev, 2003. **191**: p. 148-64.
44. Kabouridis, P.S., *Lipid rafts in T cell receptor signalling.* Mol Membr Biol, 2006. **23**(1): p. 49-57.
45. Shaw, A.S., J. Chalupny, J.A. Whitney, C. Hammond, K.E. Amrein, P. Kavathas, B.M. Sefton, and J.K. Rose, *Short related sequences in the cytoplasmic domains of CD4 and CD8 mediate binding to the amino-terminal domain of the p56lck tyrosine protein kinase.* Mol Cell Biol, 1990. **10**(5): p. 1853-62.
46. Huang, Y. and R.L. Wange, *T cell receptor signaling: beyond complex complexes.* J Biol Chem, 2004. **279**(28): p. 28827-30.
47. Zhang, W., C.L. Sommers, D.N. Burshtyn, C.C. Stebbins, J.B. DeJarnette, R.P. Trible, A. Grinberg, H.C. Tsay, H.M. Jacobs, C.M. Kessler, E.O. Long, P.E. Love, and L.E. Samelson, *Essential role of LAT in T cell development.* Immunity, 1999. **10**(3): p. 323-32.
48. Koretzky, G.A., F. Abtahian, and M.A. Silverman, *SLP76 and SLP65: complex regulation of signalling in lymphocytes and beyond.* Nat Rev Immunol, 2006. **6**(1): p. 67-78.
49. Balagopalan, L., R.L. Kortum, N.P. Coussens, V.A. Barr, and L.E. Samelson, *The linker for activation of T cells (LAT) signaling hub: from signaling complexes to microclusters.* J Biol Chem, 2015. **290**(44): p. 26422-9.
50. Liu, S.K., N. Fang, G.A. Koretzky, and C.J. McGlade, *The hematopoietic-specific adaptor protein gads functions in T-cell signaling via interactions with the SLP-76 and LAT adaptors.* Curr Biol, 1999. **9**(2): p. 67-75.
51. Roncagalli, R., S. Hauri, F. Fiore, Y. Liang, Z. Chen, A. Sansoni, K. Kanduri, R. Joly, A. Malzac, H. Lahdesmaki, R. Lahesmaa, S. Yamasaki,

T. Saito, M. Malissen, R. Aebersold, M. Gstaiger, and B. Malissen, *Quantitative proteomics analysis of signalosome dynamics in primary T cells identifies the surface receptor CD6 as a Lat adaptor-independent TCR signaling hub.* Nat Immunol, 2014. **15**(4): p. 384-392.
52. Reynolds, L.F., L.A. Smyth, T. Norton, N. Freshney, J. Downward, D. Kioussis, and V.L. Tybulewicz, *Vav1 transduces T cell receptor signals to the activation of phospholipase C-gamma1 via phosphoinositide 3-kinase-dependent and -independent pathways.* J Exp Med, 2002. **195**(9): p. 1103-14.
53. Berg, L.J., L.D. Finkelstein, J.A. Lucas, and P.L. Schwartzberg, *Tec family kinases in T lymphocyte development and function.* Annu Rev Immunol, 2005. **23**: p. 549-600.
54. Rhee, S.G. and Y.S. Bae, *Regulation of phosphoinositide-specific phospholipase C isozymes.* J Biol Chem, 1997. **272**(24): p. 15045-8.
55. Carrasco, S. and I. Merida, *Diacylglycerol-dependent binding recruits PKCtheta and RasGRP1 C1 domains to specific subcellular localizations in living T lymphocytes.* Mol Biol Cell, 2004. **15**(6): p. 2932-42.
56. Genot, E. and D.A. Cantrell, *Ras regulation and function in lymphocytes.* Curr Opin Immunol, 2000. **12**(3): p. 289-94.
57. Schulze-Luehrmann, J. and S. Ghosh, *Antigen-receptor signaling to nuclear factor kappa B.* Immunity, 2006. **25**(5): p. 701-15.
58. Lewis, R.S., *Calcium signaling mechanisms in T lymphocytes.* Annu Rev Immunol, 2001. **19**: p. 497-521.
59. Stinchcombe, J.C., G. Bossi, S. Booth, and G.M. Griffiths, *The immunological synapse of CTL contains a secretory domain and membrane bridges.* Immunity, 2001. **15**(5): p. 751-61.
60. Anthony, D.A., D.M. Andrews, S.V. Watt, J.A. Trapani, and M.J. Smyth, *Functional dissection of the granzyme family: cell death and inflammation.* Immunol Rev, 2010. **235**(1): p. 73-92.
61. Smyth, M.J., K.Y. Thia, E. Cretney, J.M. Kelly, M.B. Snook, C.A. Forbes, and A.A. Scalzo, *Perforin is a major contributor to NK cell control of tumor metastasis.* J Immunol, 1999. **162**(11): p. 6658-62.
62. Kagi, D., B. Ledermann, K. Burki, P. Seiler, B. Odermatt, K.J. Olsen, E.R. Podack, R.M. Zinkernagel, and H. Hengartner, *Cytotoxicity mediated by T cells and natural killer cells is greatly impaired in perforin-deficient mice.* Nature, 1994. **369**(6475): p. 31-7.
63. Podack, E.R., J.D. Young, and Z.A. Cohn, *Isolation and biochemical and functional characterization of perforin 1 from cytolytic T-cell granules.* Proc Natl Acad Sci U S A, 1985. **82**(24): p. 8629-33.
64. Barry, M. and R.C. Bleackley, *Cytotoxic T lymphocytes: all roads lead to death.* Nat Rev Immunol, 2002. **2**(6): p. 401-9.
65. Shi, L., S. Mai, S. Israels, K. Browne, J.A. Trapani, and A.H. Greenberg, *Granzyme B (GraB) autonomously crosses the cell membrane and perforin initiates apoptosis and GraB nuclear localization.* J Exp Med, 1997. **185**(5): p. 855-66.

66. Thiery, J., D. Keefe, S. Boulant, E. Boucrot, M. Walch, D. Martinvalet, I.S. Goping, R.C. Bleackley, T. Kirchhausen, and J. Lieberman, *Perforin pores in the endosomal membrane trigger the release of endocytosed granzyme B into the cytosol of target cells.* Nat Immunol, 2011. **12**(8): p. 770-7.
67. Voskoboinik, I., J.C. Whisstock, and J.A. Trapani, *Perforin and granzymes: function, dysfunction and human pathology.* Nat Rev Immunol, 2015. **15**(6): p. 388-400.
68. MacDonald, G., L. Shi, C. Vande Velde, J. Lieberman, and A.H. Greenberg, *Mitochondria-dependent and -independent regulation of Granzyme B-induced apoptosis.* J Exp Med, 1999. **189**(1): p. 131-44.
69. Kroemer, G. and J.C. Reed, *Mitochondrial control of cell death.* Nat Med, 2000. **6**(5): p. 513-9.
70. Volpe, E., M. Sambucci, L. Battistini, and G. Borsellino, *Fas-Fas Ligand: Checkpoint of T Cell Functions in Multiple Sclerosis.* Front Immunol, 2016. **7**: p. 382.
71. Rouvier, E., M.F. Luciani, and P. Golstein, *Fas involvement in Ca(2+)-independent T cell-mediated cytotoxicity.* J Exp Med, 1993. **177**(1): p. 195-200.
72. He, J.S. and H.L. Ostergaard, *CTLs contain and use intracellular stores of FasL distinct from cytolytic granules.* J Immunol, 2007. **179**(4): p. 2339-48.
73. Krammer, P.H., *CD95's deadly mission in the immune system.* Nature, 2000. **407**(6805): p. 789-95.
74. Ritter, A.T., Y. Asano, J.C. Stinchcombe, N.M. Dieckmann, B.C. Chen, C. Gawden-Bone, S. van Engelenburg, W. Legant, L. Gao, M.W. Davidson, E. Betzig, J. Lippincott-Schwartz, and G.M. Griffiths, *Actin depletion initiates events leading to granule secretion at the immunological synapse.* Immunity, 2015. **42**(5): p. 864-76.
75. Stinchcombe, J.C. and G.M. Griffiths, *Secretory mechanisms in cell-mediated cytotoxicity.* Annu Rev Cell Dev Biol, 2007. **23**: p. 495-517.
76. Combs, J., S.J. Kim, S. Tan, L.A. Ligon, E.L. Holzbaur, J. Kuhn, and M. Poenie, *Recruitment of dynein to the Jurkat immunological synapse.* Proc Natl Acad Sci U S A, 2006. **103**(40): p. 14883-8.
77. Robertson, L.K. and H.L. Ostergaard, *Paxillin associates with the microtubule cytoskeleton and the immunological synapse of CTL through its leucine-aspartic acid domains and contributes to microtubule organizing center reorientation.* J Immunol, 2011. **187**(11): p. 5824-33.
78. Dennert, G. and E.R. Podack, *Cytolysis by H-2-specific T killer cells. Assembly of tubular complexes on target membranes.* J Exp Med, 1983. **157**(5): p. 1483-95.
79. Monks, C.R., B.A. Freiberg, H. Kupfer, N. Sciaky, and A. Kupfer, *Three-dimensional segregation of supramolecular activation clusters in T cells.* Nature, 1998. **395**(6697): p. 82-6.
80. Kabanova, A., V. Zurli, and C.T. Baldari, *Signals Controlling Lytic Granule Polarization at the Cytotoxic Immune Synapse.* Front Immunol, 2018. **9**: p. 307.

81. Varma, R., G. Campi, T. Yokosuka, T. Saito, and M.L. Dustin, *T cell receptor-proximal signals are sustained in peripheral microclusters and terminated in the central supramolecular activation cluster.* Immunity, 2006. **25**(1): p. 117-27.
82. Lee, K.H., A.R. Dinner, C. Tu, G. Campi, S. Raychaudhuri, R. Varma, T.N. Sims, W.R. Burack, H. Wu, J. Wang, O. Kanagawa, M. Markiewicz, P.M. Allen, M.L. Dustin, A.K. Chakraborty, and A.S. Shaw, *The immunological synapse balances T cell receptor signaling and degradation.* Science, 2003. **302**(5648): p. 1218-22.
83. Jenkins, M.R. and G.M. Griffiths, *The synapse and cytolytic machinery of cytotoxic T cells.* Curr Opin Immunol, 2010. **22**(3): p. 308-13.
84. Van Seventer, G.A., Y. Shimizu, K.J. Horgan, and S. Shaw, *The LFA-1 ligand ICAM-1 provides an important costimulatory signal for T cell receptor-mediated activation of resting T cells.* J Immunol, 1990. **144**(12): p. 4579-86.
85. Le Floc'h, A., Y. Tanaka, N.S. Bantilan, G. Voisinne, G. Altan-Bonnet, Y. Fukui, and M. Huse, *Annular PIP3 accumulation controls actin architecture and modulates cytotoxicity at the immunological synapse.* J Exp Med, 2013. **210**(12): p. 2721-37.
86. Abram, C.L. and C.A. Lowell, *The ins and outs of leukocyte integrin signaling.* Annu Rev Immunol, 2009. **27**: p. 339-62.
87. Hogg, N., I. Patzak, and F. Willenbrock, *The insider's guide to leukocyte integrin signalling and function.* Nat Rev Immunol, 2011. **11**(6): p. 416-26.
88. Burbach, B.J., R.B. Medeiros, K.L. Mueller, and Y. Shimizu, *T-cell receptor signaling to integrins.* Immunol Rev, 2007. **218**: p. 65-81.
89. Kim, C., F. Ye, X. Hu, and M.H. Ginsberg, *Talin activates integrins by altering the topology of the beta transmembrane domain.* J Cell Biol, 2012. **197**(5): p. 605-11.
90. Tadokoro, S., S.J. Shattil, K. Eto, V. Tai, R.C. Liddington, J.M. de Pereda, M.H. Ginsberg, and D.A. Calderwood, *Talin binding to integrin beta tails: a final common step in integrin activation.* Science, 2003. **302**(5642): p. 103-6.
91. Das, M., S. Ithychanda, J. Qin, and E.F. Plow, *Mechanisms of talin-dependent integrin signaling and crosstalk.* Biochim Biophys Acta, 2014. **1838**(2): p. 579-88.
92. Wang, J.H., *Pull and push: talin activation for integrin signaling.* Cell Res, 2012. **22**(11): p. 1512-4.
93. Garcia-Alvarez, B., J.M. de Pereda, D.A. Calderwood, T.S. Ulmer, D. Critchley, I.D. Campbell, M.H. Ginsberg, and R.C. Liddington, *Structural determinants of integrin recognition by talin.* Mol Cell, 2003. **11**(1): p. 49-58.
94. Notarangelo, L.D., C.H. Miao, and H.D. Ochs, *Wiskott-Aldrich syndrome.* Curr Opin Hematol, 2008. **15**(1): p. 30-6.
95. Tsun, A., I. Qureshi, J.C. Stinchcombe, M.R. Jenkins, M. de la Roche, J. Kleczkowska, R. Zamoyska, and G.M. Griffiths, *Centrosome docking at the*

immunological synapse is controlled by Lck signaling. J Cell Biol, 2011. **192**(4): p. 663-74.
96. Stinchcombe, J.C., E. Majorovits, G. Bossi, S. Fuller, and G.M. Griffiths, *Centrosome polarization delivers secretory granules to the immunological synapse.* Nature, 2006. **443**(7110): p. 462-5.
97. Kuhn, J.R. and M. Poenie, *Dynamic polarization of the microtubule cytoskeleton during CTL-mediated killing.* Immunity, 2002. **16**(1): p. 111-21.
98. Yi, J., X. Wu, A.H. Chung, J.K. Chen, T.M. Kapoor, and J.A. Hammer, *Centrosome repositioning in T cells is biphasic and driven by microtubule end-on capture-shrinkage.* J Cell Biol, 2013. **202**(5): p. 779-92.
99. Kanwar, N. and J.A. Wilkins, *IQGAP1 involvement in MTOC and granule polarization in NK-cell cytotoxicity.* Eur J Immunol, 2011. **41**(9): p. 2763-73.
100. Fukata, M., S. Kuroda, K. Fujii, T. Nakamura, I. Shoji, Y. Matsuura, K. Okawa, A. Iwamatsu, A. Kikuchi, and K. Kaibuchi, *Regulation of cross-linking of actin filament by IQGAP1, a target for Cdc42.* J Biol Chem, 1997. **272**(47): p. 29579-83.
101. Fukata, M., T. Watanabe, J. Noritake, M. Nakagawa, M. Yamaga, S. Kuroda, Y. Matsuura, A. Iwamatsu, F. Perez, and K. Kaibuchi, *Rac1 and Cdc42 capture microtubules through IQGAP1 and CLIP-170.* Cell, 2002. **109**(7): p. 873-85.
102. Watanabe, T., S. Wang, J. Noritake, K. Sato, M. Fukata, M. Takefuji, M. Nakagawa, N. Izumi, T. Akiyama, and K. Kaibuchi, *Interaction with IQGAP1 links APC to Rac1, Cdc42, and actin filaments during cell polarization and migration.* Dev Cell, 2004. **7**(6): p. 871-83.
103. Malarkannan, S., A. Awasthi, K. Rajasekaran, P. Kumar, K.M. Schuldt, A. Bartoszek, N. Manoharan, N.K. Goldner, C.M. Umhoefer, and M.S. Thakar, *IQGAP1: a regulator of intracellular spacetime relativity.* J Immunol, 2012. **188**(5): p. 2057-63.
104. Quann, E.J., E. Merino, T. Furuta, and M. Huse, *Localized diacylglycerol drives the polarization of the microtubule-organizing center in T cells.* Nat Immunol, 2009. **10**(6): p. 627-35.
105. Martin-Cofreces, N.B., J. Robles-Valero, J.R. Cabrero, M. Mittelbrunn, M. Gordon-Alonso, C.H. Sung, B. Alarcon, J. Vazquez, and F. Sanchez-Madrid, *MTOC translocation modulates IS formation and controls sustained T cell signaling.* J Cell Biol, 2008. **182**(5): p. 951-62.
106. March, M.E. and E.O. Long, *beta2 integrin induces TCRzeta-Syk-phospholipase C-gamma phosphorylation and paxillin-dependent granule polarization in human NK cells.* J Immunol, 2011. **186**(5): p. 2998-3005.
107. Zhang, M., M.E. March, W.S. Lane, and E.O. Long, *A signaling network stimulated by beta2 integrin promotes the polarization of lytic granules in cytotoxic cells*, in *Sci Signal*. 2014. p. ra96.
108. Deakin, N.O. and C.E. Turner, *Paxillin comes of age.* J Cell Sci, 2008. **121**(Pt 15): p. 2435-44.

109. Brown, M.C. and C.E. Turner, *Roles for the tubulin- and PTP-PEST-binding paxillin LIM domains in cell adhesion and motility.* Int J Biochem Cell Biol, 2002. **34**(7): p. 855-63.
110. Hogg, N., M. Laschinger, K. Giles, and A. McDowall, *T-cell integrins: more than just sticking points.* J Cell Sci, 2003. **116**(Pt 23): p. 4695-705.
111. Geiger, B., J.P. Spatz, and A.D. Bershadsky, *Environmental sensing through focal adhesions.* Nat Rev Mol Cell Biol, 2009. **10**(1): p. 21-33.
112. Wozniak, M.A., K. Modzelewska, L. Kwong, and P.J. Keely, *Focal adhesion regulation of cell behavior.* Biochim Biophys Acta, 2004. **1692**(2-3): p. 103-19.
113. Nobes, C.D. and A. Hall, *Rho, rac, and cdc42 GTPases regulate the assembly of multimolecular focal complexes associated with actin stress fibers, lamellipodia, and filopodia.* Cell, 1995. **81**(1): p. 53-62.
114. Ridley, A.J. and A. Hall, *The small GTP-binding protein rho regulates the assembly of focal adhesions and actin stress fibers in response to growth factors.* Cell, 1992. **70**(3): p. 389-99.
115. Arthur, W.T. and K. Burridge, *RhoA inactivation by p190RhoGAP regulates cell spreading and migration by promoting membrane protrusion and polarity.* Mol Biol Cell, 2001. **12**(9): p. 2711-20.
116. Dubash, A.D., M.M. Menold, T. Samson, E. Boulter, R. Garcia-Mata, R. Doughman, and K. Burridge, *Chapter 1. Focal adhesions: new angles on an old structure.* Int Rev Cell Mol Biol, 2009. **277**: p. 1-65.
117. Webb, D.J., K. Donais, L.A. Whitmore, S.M. Thomas, C.E. Turner, J.T. Parsons, and A.F. Horwitz, *FAK-Src signalling through paxillin, ERK and MLCK regulates adhesion disassembly.* Nat Cell Biol, 2004. **6**(2): p. 154-61.
118. Nagano, M., D. Hoshino, N. Koshikawa, T. Akizawa, and M. Seiki, *Turnover of focal adhesions and cancer cell migration.* Int J Cell Biol, 2012. **2012**: p. 310616.
119. Dourdin, N., A.K. Bhatt, P. Dutt, P.A. Greer, J.S. Arthur, J.S. Elce, and A. Huttenlocher, *Reduced cell migration and disruption of the actin cytoskeleton in calpain-deficient embryonic fibroblasts.* J Biol Chem, 2001. **276**(51): p. 48382-8.
120. Palecek, S.P., A. Huttenlocher, A.F. Horwitz, and D.A. Lauffenburger, *Physical and biochemical regulation of integrin release during rear detachment of migrating cells.* J Cell Sci, 1998. **111 (Pt 7)**: p. 929-40.
121. Cortesio, C.L., L.R. Boateng, T.M. Piazza, D.A. Bennin, and A. Huttenlocher, *Calpain-mediated proteolysis of paxillin negatively regulates focal adhesion dynamics and cell migration.* J Biol Chem, 2011. **286**(12): p. 9998-10006.
122. Franco, S.J., M.A. Rodgers, B.J. Perrin, J. Han, D.A. Bennin, D.R. Critchley, and A. Huttenlocher, *Calpain-mediated proteolysis of talin regulates adhesion dynamics.* Nat Cell Biol, 2004. **6**(10): p. 977-83.
123. Svensson, L., A. McDowall, K.M. Giles, P. Stanley, S. Feske, and N. Hogg, *Calpain 2 controls turnover of LFA-1 adhesions on migrating T lymphocytes.* PLoS One, 2010. **5**(11): p. e15090.

124. Beningo, K.A., M. Dembo, and Y.L. Wang, *Responses of fibroblasts to anchorage of dorsal extracellular matrix receptors.* Proc Natl Acad Sci U S A, 2004. **101**(52): p. 18024-9.
125. Cukierman, E., R. Pankov, D.R. Stevens, and K.M. Yamada, *Taking cell-matrix adhesions to the third dimension.* Science, 2001. **294**(5547): p. 1708-12.
126. Henson, M.M., K. Burridge, D. Fitzpatrick, D.B. Jenkins, H.C. Pillsbury, and O.W. Henson, Jr., *Immunocytochemical localization of contractile and contraction associated proteins in the spiral ligament of the cochlea.* Hear Res, 1985. **20**(3): p. 207-14.
127. Wong, A.J., T.D. Pollard, and I.M. Herman, *Actin filament stress fibers in vascular endothelial cells in vivo.* Science, 1983. **219**(4586): p. 867-9.
128. Mempel, T.R., S.E. Henrickson, and U.H. Von Andrian, *T-cell priming by dendritic cells in lymph nodes occurs in three distinct phases.* Nature, 2004. **427**(6970): p. 154-9.
129. Shimonaka, M., K. Katagiri, T. Nakayama, N. Fujita, T. Tsuruo, O. Yoshie, and T. Kinashi, *Rap1 translates chemokine signals to integrin activation, cell polarization, and motility across vascular endothelium under flow.* J Cell Biol, 2003. **161**(2): p. 417-27.
130. Friedl, P. and B. Weigelin, *Interstitial leukocyte migration and immune function.* Nat Immunol, 2008. **9**(9): p. 960-9.
131. Wei, X., B.J. Tromberg, and M.D. Cahalan, *Mapping the sensitivity of T cells with an optical trap: polarity and minimal number of receptors for Ca(2+) signaling.* Proc Natl Acad Sci U S A, 1999. **96**(15): p. 8471-6.
132. Smith, A., Y.R. Carrasco, P. Stanley, N. Kieffer, F.D. Batista, and N. Hogg, *A talin-dependent LFA-1 focal zone is formed by rapidly migrating T lymphocytes.* J Cell Biol, 2005. **170**(1): p. 141-51.
133. Stanley, P., A. Smith, A. McDowall, A. Nicol, D. Zicha, and N. Hogg, *Intermediate-affinity LFA-1 binds alpha-actinin-1 to control migration at the leading edge of the T cell.* EMBO J, 2008. **27**(1): p. 62-75.
134. Stanley, P., S. Tooze, and N. Hogg, *A role for Rap2 in recycling the extended conformation of LFA-1 during T cell migration.* Biol Open, 2012. **1**(11): p. 1161-8.
135. Lopez-Colome, A.M., I. Lee-Rivera, R. Benavides-Hidalgo, and E. Lopez, *Paxillin: a crossroad in pathological cell migration.* J Hematol Oncol, 2017. **10**(1): p. 50.
136. Hagel, M., E.L. George, A. Kim, R. Tamimi, S.L. Opitz, C.E. Turner, A. Imamoto, and S.M. Thomas, *The adaptor protein paxillin is essential for normal development in the mouse and is a critical transducer of fibronectin signaling.* Mol Cell Biol, 2002. **22**(3): p. 901-15.
137. Brown, M.C. and C.E. Turner, *Paxillin: adapting to change.* Physiol Rev, 2004. **84**(4): p. 1315-39.
138. Kim-Kaneyama, J.R., W. Suzuki, K. Ichikawa, T. Ohki, Y. Kohno, M. Sata, K. Nose, and M. Shibanuma, *Uni-axial stretching regulates intracellular localization of Hic-5 expressed in smooth-muscle cells in vivo.* J Cell Sci, 2005. **118**(Pt 5): p. 937-49.

139. Goreczny, G.J., J.L. Ouderkirk-Pecone, E.C. Olson, M. Krendel, and C.E. Turner, *Hic-5 remodeling of the stromal matrix promotes breast tumor progression.* Oncogene, 2017. **36**(19): p. 2693-2703.
140. Dierks, S., S. von Hardenberg, T. Schmidt, F. Bremmer, P. Burfeind, and S. Kaulfuss, *Leupaxin stimulates adhesion and migration of prostate cancer cells through modulation of the phosphorylation status of the actin-binding protein caldesmon.* Oncotarget, 2015. **6**(15): p. 13591-606.
141. Sundberg-Smith, L.J., L.A. DiMichele, R.L. Sayers, C.P. Mack, and J.M. Taylor, *The LIM protein leupaxin is enriched in smooth muscle and functions as an serum response factor cofactor to induce smooth muscle cell gene transcription.* Circ Res, 2008. **102**(12): p. 1502-11.
142. Gulvady, A.C., F. Dubois, N.O. Deakin, G.J. Goreczny, and C.E. Turner, *Hic-5 Expression is a Major Indicator of Cancer Cell Morphology, Migration and Plasticity in Three-Dimensional Matrices.* Mol Biol Cell, 2018: p. mbcE18020092.
143. Deakin, N.O., J. Pignatelli, and C.E. Turner, *Diverse roles for the paxillin family of proteins in cancer.* Genes Cancer, 2012. **3**(5-6): p. 362-70.
144. Brown, M.C., M.S. Curtis, and C.E. Turner, *Paxillin LD motifs may define a new family of protein recognition domains.* Nat Struct Biol, 1998. **5**(8): p. 677-8.
145. Schmeichel, K.L. and M.C. Beckerle, *The LIM domain is a modular protein-binding interface.* Cell, 1994. **79**(2): p. 211-9.
146. Perez-Alvarado, G.C., C. Miles, J.W. Michelsen, H.A. Louis, D.R. Winge, M.C. Beckerle, and M.F. Summers, *Structure of the carboxy-terminal LIM domain from the cysteine rich protein CRP.* Nat Struct Biol, 1994. **1**(6): p. 388-98.
147. Brown, M.C., J.A. Perrotta, and C.E. Turner, *Identification of LIM3 as the principal determinant of paxillin focal adhesion localization and characterization of a novel motif on paxillin directing vinculin and focal adhesion kinase binding.* J Cell Biol, 1996. **135**(4): p. 1109-23.
148. Tanaka, T., K. Moriwaki, S. Murata, and M. Miyasaka, *LIM domain-containing adaptor, leupaxin, localizes in focal adhesion and suppresses the integrin-induced tyrosine phosphorylation of paxillin.* Cancer Sci, 2010. **101**(2): p. 363-8.
149. Bellis, S.L., J.T. Miller, and C.E. Turner, *Characterization of tyrosine phosphorylation of paxillin in vitro by focal adhesion kinase.* J Biol Chem, 1995. **270**(29): p. 17437-41.
150. Schaller, M.D. and J.T. Parsons, *pp125FAK-dependent tyrosine phosphorylation of paxillin creates a high-affinity binding site for Crk.* Mol Cell Biol, 1995. **15**(5): p. 2635-45.
151. Abou Zeid, N., A.M. Valles, and B. Boyer, *Serine phosphorylation regulates paxillin turnover during cell migration.* Cell Commun Signal, 2006. **4**: p. 8.
152. Vanarotti, M.S., D.B. Finkelstein, C.D. Guibao, A. Nourse, D.J. Miller, and J.J. Zheng, *Structural Basis for the Interaction between Pyk2-FAT Domain and Leupaxin LD Repeats.* Biochemistry, 2016. **55**(9): p. 1332-45.

153. Vanarotti, M.S., D.J. Miller, C.D. Guibao, A. Nourse, and J.J. Zheng, *Structural and mechanistic insights into the interaction between Pyk2 and paxillin LD motifs.* J Mol Biol, 2014. **426**(24): p. 3985-4001.
154. Cheung, S.M. and H.L. Ostergaard, *Pyk2 Controls Integrin-Dependent CTL Migration through Regulation of De-Adhesion.* J Immunol, 2016. **197**(5): p. 1945-56.
155. Huang, Z., D.P. Yan, and B.X. Ge, *JNK regulates cell migration through promotion of tyrosine phosphorylation of paxillin.* Cell Signal, 2008. **20**(11): p. 2002-12.
156. Ishibe, S., D. Joly, X. Zhu, and L.G. Cantley, *Phosphorylation-dependent paxillin-ERK association mediates hepatocyte growth factor-stimulated epithelial morphogenesis.* Mol Cell, 2003. **12**(5): p. 1275-85.
157. Schlaepfer, D.D., C.R. Hauck, and D.J. Sieg, *Signaling through focal adhesion kinase.* Prog Biophys Mol Biol, 1999. **71**(3-4): p. 435-78.
158. Cote, J.F., C.E. Turner, and M.L. Tremblay, *Intact LIM 3 and LIM 4 domains of paxillin are required for the association to a novel polyproline region (Pro 2) of protein-tyrosine phosphatase-PEST.* J Biol Chem, 1999. **274**(29): p. 20550-60.
159. Sahu, S.N., S. Nunez, G. Bai, and A. Gupta, *Interaction of Pyk2 and PTP-PEST with leupaxin in prostate cancer cells.* Am J Physiol Cell Physiol, 2007. **292**(6): p. C2288-96.
160. Rhee, I., D. Davidson, C.M. Souza, J. Vacher, and A. Veillette, *Macrophage fusion is controlled by the cytoplasmic protein tyrosine phosphatase PTP-PEST/PTPN12.* Mol Cell Biol, 2013. **33**(12): p. 2458-69.
161. Jamieson, J.S., D.A. Tumbarello, M. Halle, M.C. Brown, M.L. Tremblay, and C.E. Turner, *Paxillin is essential for PTP-PEST-dependent regulation of cell spreading and motility: a role for paxillin kinase linker.* J Cell Sci, 2005. **118**(Pt 24): p. 5835-47.
162. Chen, P.W. and G.S. Kroog, *Leupaxin is similar to paxillin in focal adhesion targeting and tyrosine phosphorylation but has distinct roles in cell adhesion and spreading.* Cell Adh Migr, 2010. **4**(4): p. 527-40.
163. Chew, V. and K.P. Lam, *Leupaxin negatively regulates B cell receptor signaling.* J Biol Chem, 2007. **282**(37): p. 27181-91.
164. Blakely, A., K. Gorman, H. Ostergaard, K. Svoboda, C.C. Liu, J.D. Young, and W.R. Clark, *Resistance of cloned cytotoxic T lymphocytes to cell-mediated cytotoxicity.* J Exp Med, 1987. **166**(4): p. 1070-83.
165. Kane, K.P., L.A. Sherman, and M.F. Mescher, *Molecular interactions required for triggering alloantigen-specific cytolytic T lymphocytes.* J Immunol, 1989. **142**(12): p. 4153-60.
166. Kane, K.P. and M.F. Mescher, *Activation of CD8-dependent cytotoxic T lymphocyte adhesion and degranulation by peptide class I antigen complexes.* J Immunol, 1993. **150**(11): p. 4788-97.
167. Durairaj, M., R. Sharma, J.C. Varghese, and K.P. Kane, *Requirement for Q226, but not multiple charged residues, in the class I MHC CD loop/D strand for TCR-activated CD8 accessory function.* Eur J Immunol, 2003. **33**(3): p. 676-84.

168. Berg, N.N. and H.L. Ostergaard, *T cell receptor engagement induces tyrosine phosphorylation of FAK and Pyk2 and their association with Lck.* J Immunol, 1997. **159**(4): p. 1753-7.
169. Ostergaard, H.L., O. Lou, C.W. Arendt, and N.N. Berg, *Paxillin phosphorylation and association with Lck and Pyk2 in anti-CD3- or anti-CD45-stimulated T cells.* J Biol Chem, 1998. **273**(10): p. 5692-6.
170. Berg, N.N. and H.L. Ostergaard, *Characterization of intercellular adhesion molecule-1 (ICAM-1)-augmented degranulation by cytotoxic T cells. ICAM-1 and anti-CD3 must be co-localized for optimal adhesion and stimulation.* J Immunol, 1995. **155**(4): p. 1694-702.
171. Laukaitis, C.M., D.J. Webb, K. Donais, and A.F. Horwitz, *Differential dynamics of alpha 5 integrin, paxillin, and alpha-actinin during formation and disassembly of adhesions in migrating cells.* J Cell Biol, 2001. **153**(7): p. 1427-40.
172. Hu, Y.L., S. Lu, K.W. Szeto, J. Sun, Y. Wang, J.C. Lasheras, and S. Chien, *FAK and paxillin dynamics at focal adhesions in the protrusions of migrating cells.* Sci Rep, 2014. **4**: p. 6024.
173. Devreotes, P. and A.R. Horwitz, *Signaling networks that regulate cell migration.* Cold Spring Harb Perspect Biol, 2015. **7**(8): p. a005959.
174. Wehrle-Haller, B., *Assembly and disassembly of cell matrix adhesions.* Curr Opin Cell Biol, 2012. **24**(5): p. 569-81.
175. Anthis, N.J., K.L. Wegener, F. Ye, C. Kim, B.T. Goult, E.D. Lowe, I. Vakonakis, N. Bate, D.R. Critchley, M.H. Ginsberg, and I.D. Campbell, *The structure of an integrin/talin complex reveals the basis of inside-out signal transduction.* EMBO J, 2009. **28**(22): p. 3623-32.
176. Li, S.Y., D.D. Mruk, and C.Y. Cheng, *Focal adhesion kinase is a regulator of F-actin dynamics: New insights from studies in the testis.* Spermatogenesis, 2013. **3**(3): p. e25385.
177. Schwartz, M.A., M.D. Schaller, and M.H. Ginsberg, *Integrins: emerging paradigms of signal transduction.* Annu Rev Cell Dev Biol, 1995. **11**: p. 549-99.
178. Choi, C.K., M. Vicente-Manzanares, J. Zareno, L.A. Whitmore, A. Mogilner, and A.R. Horwitz, *Actin and alpha-actinin orchestrate the assembly and maturation of nascent adhesions in a myosin II motor-independent manner.* Nat Cell Biol, 2008. **10**(9): p. 1039-50.
179. Shibanuma, M., J.R. Kim-Kaneyama, K. Ishino, N. Sakamoto, T. Hishiki, K. Yamaguchi, K. Mori, J. Mashimo, and K. Nose, *Hic-5 communicates between focal adhesions and the nucleus through oxidant-sensitive nuclear export signal.* Mol Biol Cell, 2003. **14**(3): p. 1158-71.
180. Franco, S.J. and A. Huttenlocher, *Regulating cell migration: calpains make the cut.* J Cell Sci, 2005. **118**(Pt 17): p. 3829-38.
181. Pfaff, M., X. Du, and M.H. Ginsberg, *Calpain cleavage of integrin beta cytoplasmic domains.* FEBS Lett, 1999. **460**(1): p. 17-22.
182. Chan, K.T., D.A. Bennin, and A. Huttenlocher, *Regulation of adhesion dynamics by calpain-mediated proteolysis of focal adhesion kinase (FAK).* J Biol Chem, 2010. **285**(15): p. 11418-26.

183. Scharffetter-Kochanek, K., H. Lu, K. Norman, N. van Nood, F. Munoz, S. Grabbe, M. McArthur, I. Lorenzo, S. Kaplan, K. Ley, C.W. Smith, C.A. Montgomery, S. Rich, and A.L. Beaudet, *Spontaneous skin ulceration and defective T cell function in CD18 null mice.* J Exp Med, 1998. **188**(1): p. 119-31.
184. Etzioni, A., *Genetic etiologies of leukocyte adhesion defects.* Curr Opin Immunol, 2009. **21**(5): p. 481-6.
185. Smith, A., P. Stanley, K. Jones, L. Svensson, A. McDowall, and N. Hogg, *The role of the integrin LFA-1 in T-lymphocyte migration.* Immunol Rev, 2007. **218**: p. 135-46.
186. Kaulfuss, S., M. Grzmil, B. Hemmerlein, P. Thelen, S. Schweyer, J. Neesen, L. Bubendorf, A.G. Glass, H. Jarry, B. Auber, and P. Burfeind, *Leupaxin, a novel coactivator of the androgen receptor, is expressed in prostate cancer and plays a role in adhesion and invasion of prostate carcinoma cells.* Mol Endocrinol, 2008. **22**(7): p. 1606-21.
187. Lipsky, B.P., C.R. Beals, and D.E. Staunton, *Leupaxin is a novel LIM domain protein that forms a complex with PYK2.* J Biol Chem, 1998. **273**(19): p. 11709-13.
188. Robertson, L.K., L.R. Mireau, and H.L. Ostergaard, *A role for phosphatidylinositol 3-kinase in TCR-stimulated ERK activation leading to paxillin phosphorylation and CTL degranulation.* J Immunol, 2005. **175**(12): p. 8138-45.
189. Rodriguez-Fernandez, J.L., L. Sanchez-Martin, C.A. de Frutos, D. Sancho, M. Robinson, F. Sanchez-Madrid, and C. Cabanas, *LFA-1 integrin and the microtubular cytoskeleton are involved in the Ca(2)(+)-mediated regulation of the activity of the tyrosine kinase PYK2 in T cells.* J Leukoc Biol, 2002. **71**(3): p. 520-30.
190. Gupta, A., B.S. Lee, M.A. Khadeer, Z. Tang, M. Chellaiah, Y. Abu-Amer, J. Goldknopf, and K.A. Hruska, *Leupaxin is a critical adaptor protein in the adhesion zone of the osteoclast.* J Bone Miner Res, 2003. **18**(4): p. 669-85.
191. Feller, S.M., G. Posern, J. Voss, C. Kardinal, D. Sakkab, J. Zheng, and B.S. Knudsen, *Physiological signals and oncogenesis mediated through Crk family adapter proteins.* J Cell Physiol, 1998. **177**(4): p. 535-52.
192. Turner, C.E., *Paxillin and focal adhesion signalling.* Nat Cell Biol, 2000. **2**(12): p. E231-6.
193. Park, S.Y., H.K. Avraham, and S. Avraham, *RAFTK/Pyk2 activation is mediated by trans-acting autophosphorylation in a Src-independent manner.* J Biol Chem, 2004. **279**(32): p. 33315-22.
194. Zhao, M., D. Finlay, I. Zharkikh, and K. Vuori, *Novel Role of Src in Priming Pyk2 Phosphorylation.* PLoS One, 2016. **11**(2): p. e0149231.
195. Sahu, S.N., M.A. Khadeer, B.W. Robertson, S.M. Nunez, G. Bai, and A. Gupta, *Association of leupaxin with Src in osteoclasts.* Am J Physiol Cell Physiol, 2007. **292**(1): p. C581-90.

196. St-Pierre, J., T.L. Lysechko, and H.L. Ostergaard, *Hypophosphorylated and inactive Pyk2 associates with paxillin at the microtubule organizing center in hematopoietic cells.* Cell Signal, 2011. **23**(4): p. 718-30.
197. Brown, M.C., J.A. Perrotta, and C.E. Turner, *Serine and threonine phosphorylation of the paxillin LIM domains regulates paxillin focal adhesion localization and cell adhesion to fibronectin.* Mol Biol Cell, 1998. **9**(7): p. 1803-16.
198. Wehrle-Haller, B., *Structure and function of focal adhesions.* Curr Opin Cell Biol, 2012. **24**(1): p. 116-24.
199. Ma, E.A., O. Lou, N.N. Berg, and H.L. Ostergaard, *Cytotoxic T lymphocytes express a beta3 integrin which can induce the phosphorylation of focal adhesion kinase and the related PYK-2.* Eur J Immunol, 1997. **27**(1): p. 329-35.
200. Calderwood, D.A. and M.H. Ginsberg, *Talin forges the links between integrins and actin.* Nat Cell Biol, 2003. **5**(8): p. 694-7.
201. Nayal, A., D.J. Webb, and A.F. Horwitz, *Talin: an emerging focal point of adhesion dynamics.* Curr Opin Cell Biol, 2004. **16**(1): p. 94-8.
202. Tremuth, L., S. Kreis, C. Melchior, J. Hoebeke, P. Ronde, S. Plancon, K. Takeda, and N. Kieffer, *A fluorescence cell biology approach to map the second integrin-binding site of talin to a 130-amino acid sequence within the rod domain.* J Biol Chem, 2004. **279**(21): p. 22258-66.
203. Jankowska, K.I., E.K. Williamson, N.H. Roy, D. Blumenthal, V. Chandra, T. Baumgart, and J.K. Burkhardt, *Integrins Modulate T Cell Receptor Signaling by Constraining Actin Flow at the Immunological Synapse.* Front Immunol, 2018. **9**: p. 25.
204. Zhao, H., A. Langerod, Y. Ji, K.W. Nowels, J.M. Nesland, R. Tibshirani, I.K. Bukholm, R. Karesen, D. Botstein, A.L. Borresen-Dale, and S.S. Jeffrey, *Different gene expression patterns in invasive lobular and ductal carcinomas of the breast.* Mol Biol Cell, 2004. **15**(6): p. 2523-36.
205. Turashvili, G., J. Bouchal, K. Baumforth, W. Wei, M. Dziechciarkova, J. Ehrmann, J. Klein, E. Fridman, J. Skarda, J. Srovnal, M. Hajduch, P. Murray, and Z. Kolar, *Novel markers for differentiation of lobular and ductal invasive breast carcinomas by laser microdissection and microarray analysis.* BMC Cancer, 2007. **7**: p. 55.
206. Salgia, R., J.L. Li, D.S. Ewaniuk, Y.B. Wang, M. Sattler, W.C. Chen, W. Richards, E. Pisick, G.I. Shapiro, B.J. Rollins, L.B. Chen, J.D. Griffin, and D.J. Sugarbaker, *Expression of the focal adhesion protein paxillin in lung cancer and its relation to cell motility.* Oncogene, 1999. **18**(1): p. 67-77.
207. Cui, W., X. Wang, Y.C. Liu, Y.L. Wan, H.J. Guo, and J. Zhu, *[Expression of HIC-5/ARA55 in colonrectal cancer and its mechanisms of action]*. Beijing Da Xue Xue Bao Yi Xue Ban, 2006. **38**(3): p. 280-3.
208. Mestayer, C., M. Blanchere, F. Jaubert, B. Dufour, and I. Mowszowicz, *Expression of androgen receptor coactivators in normal and cancer prostate tissues and cultured cell lines.* Prostate, 2003. **56**(3): p. 192-200.
209. Kaulfuss, S., S. von Hardenberg, S. Schweyer, A.M. Herr, F. Laccone, S. Wolf, and P. Burfeind, *Leupaxin acts as a mediator in prostate carcinoma*

progression through deregulation of p120catenin expression. Oncogene, 2009. **28**(45): p. 3971-82.
210. Zhao, Q., Y. Xie, Y. Zheng, S. Jiang, W. Liu, W. Mu, Z. Liu, Y. Zhao, Y. Xue, and J. Ren, *GPS-SUMO: a tool for the prediction of sumoylation sites and SUMO-interaction motifs.* Nucleic Acids Res, 2014. **42**(Web Server issue): p. W325-30.
211. Ito, A., T.R. Kataoka, M. Watanabe, K. Nishiyama, Y. Mazaki, H. Sabe, Y. Kitamura, and H. Nojima, *A truncated isoform of the PP2A B56 subunit promotes cell motility through paxillin phosphorylation.* EMBO J, 2000. **19**(4): p. 562-71.
212. Terfera, D.R., M.C. Brown, and C.E. Turner, *Epidermal growth factor stimulates serine/threonine phosphorylation of the focal adhesion protein paxillin in a MEK-dependent manner in normal rat kidney cells.* J Cell Physiol, 2002. **191**(1): p. 82-94.
213. Rape, A.D., W.H. Guo, and Y.L. Wang, *The regulation of traction force in relation to cell shape and focal adhesions.* Biomaterials, 2011. **32**(8): p. 2043-51.
214. Burridge, K., K. Fath, T. Kelly, G. Nuckolls, and C. Turner, *Focal adhesions: transmembrane junctions between the extracellular matrix and the cytoskeleton.* Annu Rev Cell Biol, 1988. **4**: p. 487-525.
215. Kanchanawong, P., G. Shtengel, A.M. Pasapera, E.B. Ramko, M.W. Davidson, H.F. Hess, and C.M. Waterman, *Nanoscale architecture of integrin-based cell adhesions.* Nature, 2010. **468**(7323): p. 580-4.
216. Kiosses, W.B., S.J. Shattil, N. Pampori, and M.A. Schwartz, *Rac recruits high-affinity integrin alphavbeta3 to lamellipodia in endothelial cell migration.* Nat Cell Biol, 2001. **3**(3): p. 316-20.
217. Iiizumi, M., S. Bandyopadhyay, S.K. Pai, M. Watabe, S. Hirota, S. Hosobe, T. Tsukada, K. Miura, K. Saito, E. Furuta, W. Liu, F. Xing, H. Okuda, A. Kobayashi, and K. Watabe, *RhoC promotes metastasis via activation of the Pyk2 pathway in prostate cancer.* Cancer Res, 2008. **68**(18): p. 7613-20.
218. Sen, A., I. De Castro, D.B. Defranco, F.M. Deng, J. Melamed, P. Kapur, G.V. Raj, R. Rossi, and S.R. Hammes, *Paxillin mediates extranuclear and intranuclear signaling in prostate cancer proliferation.* J Clin Invest, 2012. **122**(7): p. 2469-81.
219. Wang, Y., D. Becker, T. Vass, J. White, P. Marrack, and J.W. Kappler, *A conserved CXXC motif in CD3epsilon is critical for T cell development and TCR signaling.* PLoS Biol, 2009. **7**(12): p. e1000253.
220. Wang, H., T.A. Kadlecek, B.B. Au-Yeung, H.E. Goodfellow, L.Y. Hsu, T.S. Freedman, and A. Weiss, *ZAP-70: an essential kinase in T-cell signaling.* Cold Spring Harb Perspect Biol, 2010. **2**(5): p. a002279.
221. Neumeister, E.N., Y. Zhu, S. Richard, C. Terhorst, A.C. Chan, and A.S. Shaw, *Binding of ZAP-70 to phosphorylated T-cell receptor zeta and eta enhances its autophosphorylation and generates specific binding sites for SH2 domain-containing proteins.* Mol Cell Biol, 1995. **15**(6): p. 3171-8.
222. Kane, L.P., J. Lin, and A. Weiss, *Signal transduction by the TCR for antigen.* Curr Opin Immunol, 2000. **12**(3): p. 242-9.

223. Wilkinson, B., H. Wang, and C.E. Rudd, *Positive and negative adaptors in T-cell signalling.* Immunology, 2004. **111**(4): p. 368-74.
224. Zhang, W., R.P. Trible, M. Zhu, S.K. Liu, C.J. McGlade, and L.E. Samelson, *Association of Grb2, Gads, and phospholipase C-gamma 1 with phosphorylated LAT tyrosine residues. Effect of LAT tyrosine mutations on T cell angigen receptor-mediated signaling.* J Biol Chem, 2000. **275**(30): p. 23355-61.
225. Roose, J.P., M. Mollenauer, V.A. Gupta, J. Stone, and A. Weiss, *A diacylglycerol-protein kinase C-RasGRP1 pathway directs Ras activation upon antigen receptor stimulation of T cells.* Mol Cell Biol, 2005. **25**(11): p. 4426-41.
226. Robinson, P.J., *Differential stimulation of protein kinase C activity by phorbol ester or calcium/phosphatidylserine in vitro and in intact synaptosomes.* J Biol Chem, 1992. **267**(30): p. 21637-44.
227. Marwali, M.R., M.A. MacLeod, D.N. Muzia, and F. Takei, *Lipid rafts mediate association of LFA-1 and CD3 and formation of the immunological synapse of CTL.* J Immunol, 2004. **173**(5): p. 2960-7.
228. Barber, D.F., M. Faure, and E.O. Long, *LFA-1 contributes an early signal for NK cell cytotoxicity.* J Immunol, 2004. **173**(6): p. 3653-9.
229. Kaulfuss, S., A.M. Herr, A. Buchner, B. Hemmerlein, A.R. Gunthert, and P. Burfeind, *Leupaxin is expressed in mammary carcinoma and acts as a transcriptional activator of the estrogen receptor alpha.* Int J Oncol, 2015. **47**(1): p. 106-14.
230. Dustin, M.L., *T-cell activation through immunological synapses and kinapses.* Immunol Rev, 2008. **221**: p. 77-89.
231. Cai, X., M. Li, J. Vrana, and M.D. Schaller, *Glycogen synthase kinase 3- and extracellular signal-regulated kinase-dependent phosphorylation of paxillin regulates cytoskeletal rearrangement.* Mol Cell Biol, 2006. **26**(7): p. 2857-68.
232. Woodrow, M.A., D. Woods, H.M. Cherwinski, D. Stokoe, and M. McMahon, *Ras-induced serine phosphorylation of the focal adhesion protein paxillin is mediated by the Raf-->MEK-->ERK pathway.* Exp Cell Res, 2003. **287**(2): p. 325-38.
233. Ku, H. and K.E. Meier, *Phosphorylation of paxillin via the ERK mitogen-activated protein kinase cascade in EL4 thymoma cells.* J Biol Chem, 2000. **275**(15): p. 11333-40.
234. Lysechko, T.L., S.M. Cheung, and H.L. Ostergaard, *Regulation of the tyrosine kinase Pyk2 by calcium is through production of reactive oxygen species in cytotoxic T lymphocytes.* J Biol Chem, 2010. **285**(41): p. 31174-84.
235. Bijli, K.M., B.Y. Kang, R.L. Sutliff, and C.M. Hart, *Proline-rich tyrosine kinase 2 downregulates peroxisome proliferator-activated receptor gamma to promote hypoxia-induced pulmonary artery smooth muscle cell proliferation.* Pulm Circ, 2016. **6**(2): p. 202-10.
236. Tumbarello, D.A., M.C. Brown, and C.E. Turner, *The paxillin LD motifs.* FEBS Lett, 2002. **513**(1): p. 114-8.

237. Nikolopoulos, S.N. and C.E. Turner, *Integrin-linked kinase (ILK) binding to paxillin LD1 motif regulates ILK localization to focal adhesions.* J Biol Chem, 2001. **276**(26): p. 23499-505.
238. Turner, C.E., M.C. Brown, J.A. Perrotta, M.C. Riedy, S.N. Nikolopoulos, A.R. McDonald, S. Bagrodia, S. Thomas, and P.S. Leventhal, *Paxillin LD4 motif binds PAK and PIX through a novel 95-kD ankyrin repeat, ARF-GAP protein: A role in cytoskeletal remodeling.* J Cell Biol, 1999. **145**(4): p. 851-63.
239. Gasteiger, G., M. Ataide, and W. Kastenmuller, *Lymph node - an organ for T-cell activation and pathogen defense.* Immunol Rev, 2016. **271**(1): p. 200-20.
240. Bossi, G., C. Trambas, S. Booth, R. Clark, J. Stinchcombe, and G.M. Griffiths, *The secretory synapse: the secrets of a serial killer.* Immunol Rev, 2002. **189**: p. 152-60.
241. Purtic, B., L.A. Pitcher, N.S. van Oers, and C. Wulfing, *T cell receptor (TCR) clustering in the immunological synapse integrates TCR and costimulatory signaling in selected T cells.* Proc Natl Acad Sci U S A, 2005. **102**(8): p. 2904-9.
242. Huse, M., A. Le Floc'h, and X. Liu, *From lipid second messengers to molecular motors: microtubule-organizing center reorientation in T cells.* Immunol Rev, 2013. **256**(1): p. 95-106.
243. Chavez-Galan, L., M.C. Arenas-Del Angel, E. Zenteno, R. Chavez, and R. Lascurain, *Cell death mechanisms induced by cytotoxic lymphocytes.* Cell Mol Immunol, 2009. **6**(1): p. 15-25.
244. Zhang, M., M.E. March, W.S. Lane, and E.O. Long, *A signaling network stimulated by beta2 integrin promotes the polarization of lytic granules in cytotoxic cells.* Sci Signal, 2014. **7**(346): p. ra96.
245. Chan, F.K., K. Moriwaki, and M.J. De Rosa, *Detection of necrosis by release of lactate dehydrogenase activity.* Methods Mol Biol, 2013. **979**: p. 65-70.
246. Jenkins, M.R., A. Tsun, J.C. Stinchcombe, and G.M. Griffiths, *The strength of T cell receptor signal controls the polarization of cytotoxic machinery to the immunological synapse.* Immunity, 2009. **31**(4): p. 621-31.
247. Denton, A.E., R. Wesselingh, S. Gras, C. Guillonneau, M.R. Olson, J.D. Mintern, W. Zeng, D.C. Jackson, J. Rossjohn, P.D. Hodgkin, P.C. Doherty, and S.J. Turner, *Affinity thresholds for naive CD8+ CTL activation by peptides and engineered influenza A viruses.* J Immunol, 2011. **187**(11): p. 5733-44.
248. Qian, D., S. Lev, N.S. van Oers, I. Dikic, J. Schlessinger, and A. Weiss, *Tyrosine phosphorylation of Pyk2 is selectively regulated by Fyn during TCR signaling.* J Exp Med, 1997. **185**(7): p. 1253-9.
249. Beinke, S., H. Phee, J.M. Clingan, J. Schlessinger, M. Matloubian, and A. Weiss, *Proline-rich tyrosine kinase-2 is critical for CD8 T-cell short-lived effector fate.* Proc Natl Acad Sci U S A, 2010. **107**(37): p. 16234-9.
250. Bertrand, F., S. Muller, K.H. Roh, C. Laurent, L. Dupre, and S. Valitutti, *An initial and rapid step of lytic granule secretion precedes microtubule*

organizing center polarization at the cytotoxic T lymphocyte/target cell synapse. Proc Natl Acad Sci U S A, 2013. **110**(15): p. 6073-8.